



**HAL**  
open science

## **Materials-Mediated In Situ Physical Cues for Bone Regeneration**

Shuo Liu, Liguang Zhang, Zhao Li, Fei Gao, Qun Zhang, Alberto Bianco, Hong Liu, Shaohua Ge, Baojin Ma

► **To cite this version:**

Shuo Liu, Liguang Zhang, Zhao Li, Fei Gao, Qun Zhang, et al.. Materials-Mediated In Situ Physical Cues for Bone Regeneration. *Advanced Functional Materials*, 2023, 34 (1), <10.1002/adfm.202306534>. <hal-04659511>

**HAL Id: hal-04659511**

**<https://hal.science/hal-04659511v1>**

Submitted on 23 Jul 2024

**HAL** is a multi-disciplinary open access archive for the deposit and dissemination of scientific research documents, whether they are published or not. The documents may come from teaching and research institutions in France or abroad, or from public or private research centers.

L'archive ouverte pluridisciplinaire **HAL**, est destinée au dépôt et à la diffusion de documents scientifiques de niveau recherche, publiés ou non, émanant des établissements d'enseignement et de recherche français ou étrangers, des laboratoires publics ou privés.



HAL Authorization

# Materials-mediated in situ physical cues for bone regeneration

*Shuo Liu, Liguozhang, Zhao Li, Fei Gao, Qun Zhang, Alberto Bianco\*, Hong Liu\*, Shaohua Ge\*,  
Baojin Ma\**

**Shuo Liu, Liguozhang, Zhao Li, Fei Gao, Qun Zhang, Shaohua Ge** – Department of Periodontology & Tissue Engineering and Regeneration, School and Hospital of Stomatology, Cheeloo College of Medicine, Shandong University & Shandong Key Laboratory of Oral Tissue Regeneration & Shandong Engineering Laboratory for Dental Materials and Oral Tissue Regeneration & Shandong Provincial Clinical Research Center for Oral Diseases, Jinan, Shandong, 250012, China; E-mail: shaohuage@sdu.edu.cn;

**Alberto Bianco** – CNRS, Immunology, Immunopathology and Therapeutic Chemistry, UPR3572, University of Strasbourg, ISIS, Strasbourg, 67000, France; E-mail: a.bianco@ibmc-cnrs.unistra.fr

**Hong Liu** – State Key Laboratory of Crystal Materials, Shandong University, Jinan, Shandong 250013, China; E-mail: [hongliu@sdu.edu.cn](mailto:hongliu@sdu.edu.cn);

**Baojin Ma** – Department of Periodontology & Tissue Engineering and Regeneration, School and Hospital of Stomatology, Cheeloo College of Medicine, Shandong University & Shandong Key Laboratory of Oral Tissue Regeneration & Shandong Engineering Laboratory for Dental Materials and Oral Tissue Regeneration & Shandong Provincial Clinical Research Center for Oral Diseases, Jinan, Shandong, 250012, China; E-mail: baojinma@sdu.edu.cn

## **Abstract**

Physical cues like morphology, light, electric signal, mechanic signal, magnetic signal, and heat can be used as alternative regulators for expensive but short-acting growth factors in bone tissue engineering to promote osteogenic differentiation and bone regeneration. As physical stimulation applied directly to the tissue cannot be focused on the bone defect area to regulate the cell behaviors and fate in situ, this limits the efficiency of precise bone regeneration. Biomaterials-mediated in situ physical cues, as an effective strategy combining the synergistic effect of materials themselves, have been put forward and studied widely to promote osteogenic differentiation and bone repair efficiently and precisely. Different types of physical cues provide different choices to better satisfy the requirements for targeted bone defect repair. In this review, we will introduce the recent research about different biomaterials-mediated physical cues accelerating osteogenesis *in vitro* and promoting in situ bone formation *in vivo*. Meanwhile, the corresponding possible mechanisms of various physical cues regulating cell responses will be also discussed. This review provides useful and enlightening guidance for the utilization of intrinsically physical properties of functional materials to achieve efficient bone regeneration, leading to the design and construction of smart biomaterials for practical applications, and eventually promoting clinical translation.

## 1. Introduction

Bone is one of the bases for the human body by providing high stiffness to bear loading from own weight or outside force,<sup>[1]</sup> and bone metabolism mediated by a balance between bone formation by osteoblasts and resorption by osteoclasts plays a crucial role in the formation of a mature and dynamic bone structure.<sup>[2]</sup> In mature bone, anabolic and catabolic actions are balanced by tightly regulating the activity of bone-forming cells (osteoblasts) and bone-resorbing cells (osteoclasts), a process known as coupling.<sup>[3]</sup> Bones are mainly made of nanocrystalline hydroxyapatite (HAp) as an inorganic component and collagen nanofibers as an organic constituent, forming complex and ordered hierarchical structures comprising nano–micro–macro scales, which endow bone with excellent mechanical properties of self-remodeling and regenerative capability.<sup>[4]</sup> Bone defects are very common in daily life and small-size bone defects can be usually repaired naturally by simple fixation and without other interventions. During bone regeneration, cell recruitment, immune response, angiogenesis, osteogenesis, and mineralization happen dynamically and sequentially, finally finally controlling bone metabolism. Meanwhile, these processes are concomitant and represent a continuum of changing cell populations and signal transduction processes within regenerating tissues.<sup>[5]</sup> However, bone defects beyond critical size would fail to achieve self-regeneration.<sup>[6]</sup> Therefore, how to repair these types of bone defects efficiently becomes a vital problem to be resolved. Bone tissue engineering (BTE) and regenerative medicine have opened potentially filled and stirred multiple possibilities for bone defect regeneration.<sup>[7]</sup> For ideal BTE, the whole complex of cells, growth factors, and biomaterials is considered an optimal repair system.<sup>[8]</sup> However, until now the limited cell resources, the relatively low viability of cells after implantation, and the high price and short function period of growth factors have hindered the expected tissue engineering far from practical clinical translation.<sup>[9]</sup> Therefore, more and more researchers have made enormous efforts to seek a breakthrough in functional material preparation and design to optimize bone repair.

With the development of technology, nanomaterials, and multifunctional scaffolds have flourished and have been widely applied in BTE, from stem cell fate regulation to bone defect repair.<sup>[10]</sup> Due to the diversity of nanomaterials and multifunctional scaffolds, many attractive and efficient strategies have been developed. As one of the traditionally popular biomaterials, HAp-based materials possess great advantages to promote the osteogenic differentiation of stem cells by regulating gene expression.<sup>[4a, 11]</sup> Meanwhile, compositing with other materials to construct multifunctional scaffolds is

a common strategy to extend the bio-applications. For example, a HAp-calcium sulfate-hyaluronic acid composite encapsulated with collagenase was prepared as a bone substitute to promote alveolar bone regeneration,<sup>[12]</sup> and a gelatin methacrylamide/HAp porous composite with biomimetic bone matrix and customizable porous structure was able to accelerate the formation of new bone in rabbit skull defects.<sup>[13]</sup> It is worth noting that bone repair efficiency is relatively low when depending only on traditional materials. Therefore, various growth factors were widely applied to achieve a satisfactory repair efficiency. Chitosan-HAp scaffolds can enhance osteoblastic differentiation of bone mesenchymal stem cells (BMSCs) by sustained release of bone morphogenetic protein bone morphogenetic proteins (BMP)-2,<sup>[14]</sup> and facilitate bone regeneration *in vivo* when decorated with vascular endothelial growth factor (VEGF).<sup>[15]</sup> Meanwhile, due to the high loading rate, varied hydrogels have also wide applications in BTE. A covalent cross-linking chondroitin sulfate hydrogel loaded with BMP-4 with injectable and self-healing capabilities was developed for cranial bone repair,<sup>[16]</sup> and a functionalized silk fibroin (SF)/arginine–glycine–aspartic acid (RGD) hydrogel was designed to enhance osteogenesis of mesenchymal stem cells (MSCs) for bone defect repair.<sup>[17]</sup> Although the repair efficiency was improved, the short validity period of growth factors weakens the long-term functions, and the relatively high price also increases the cost of the scaffolds, thus hindering the wide applications and the potential clinical translation. Therefore, alternative efficient strategies need to be conceived to weaken the dependency on growth factors for better bone defect repair at low costs.

Varied nanostructures have been constructed to promote osteogenic differentiation and bone repair.<sup>[18]</sup> Unexpectedly, an appropriate degree of disorder in the nanostructures can promote higher osteogenic differentiation than a high symmetry degree, with the differentiation efficiency comparable to the osteogenic media.<sup>[19]</sup> Similarly, the surface epitaxial crystallization-directed nano-topography can be also used to accelerate pre-osteoblast proliferation and osteogenic differentiation.<sup>[17]</sup> For example, MSCs showed enhanced osteogenic differentiation on BMP-2-functionalized nanopatterned substrates.<sup>[20]</sup> Besides, cells are also sensitive to other physical cues, such as force, light, electric signals, magnetic signals, and heat, which can be used to regulate stem cell differentiation and bone regeneration.<sup>[21]</sup> Notably, there is force-dependent cell signaling in the regulation of stem cell differentiation, and bioprocess forces can regulate bone regeneration.<sup>[22]</sup> Alternatively, red light irradiation can increase the proliferation and osteogenic differentiation of MSCs by regulating the

extracellular signal-regulated kinase (ERK) pathway.<sup>[23]</sup> Alternating electric fields and pulsed direct current stimulation, both promoted differentiation of MSCs into osteoblasts.<sup>[24]</sup> Besides, external positive or negative electrical fields were found to enhance peri-implant lamellar bone volume compared with sham-treated animals.<sup>[25]</sup> Furthermore, a static magnetic field (SMF) and pulsed magnetic fields significantly promoted the osteogenic differentiation of stem cells, as well as the repair of bone defects.<sup>[26]</sup> Interestingly, accelerated proliferation and osteogenic differentiation of dental follicle stem cells happened at 40 °C, meaning that mild heat can function as beneficial stimulation to regulate osteogenic differentiation.<sup>[27]</sup> Herein, we can state that physical cues can be used as multifunctional regulators similar to varied growth factors to promote osteogenic differentiation and bone regeneration. However, the direct applications of the above physical cues usually show a low efficiency for bone repair due to the fact that the physical cues cannot be focused on the bone defect area to regulate cell behaviors and fate *in situ*.

Recently, biomaterials-mediated *in situ* physical cues have been put forward and widely studied to promote osteogenic differentiation and bone regeneration efficiently. For example, we demonstrated that a TiO<sub>2</sub> nanorod array with high biocompatibility can promote the osteogenic differentiation of MSCs compared with the smooth TiO<sub>2</sub> ceramic.<sup>[28]</sup> In another study, the stiffness of polyacrylamide hydrogels was shown to have an obvious effect on the morphology, adhesion, proliferation, and osteogenic differentiation of MSCs.<sup>[29]</sup>

To illustrate the efficiencies of materials-mediated physical cues on bone regeneration, this review summarizes the applications in BTE of varied *in situ* physical cues mediated by functional materials *in vitro* and *in vivo*. Different types of physical cues provide more choices to better satisfy the requirements for targeted bone defect repair. In addition, the corresponding mechanisms of the different physical cues and how they affect cell differentiation are also discussed to comprehensively understand the interaction between cells and physical stimulations. This review provides useful and enlightening guidance to design and construct smart biomaterials based on physical properties and shows an alternative strategy for traditional growth factors regulation mode in BTE.

## **2. Impact of the morphology**

Due to the developed nanotechnologies and the great potential in clinical applications, the studies of

the effects of nanostructures on cell behavior and regulation have attracted much attention, and innumerable nanostructures based on varied biomaterials have been explored for bone regeneration. Besides the intrinsic properties of biomaterials, an optimized nanostructure can further accelerate the efficiency of osteogenic differentiation and bone regeneration. Below we will describe the different types of (bio)materials that have been designed for BTE.

## 2.1 Ti-based nanostructures

Ti-based materials are the common implants in orthopedic, dental, and bone tissue repair due to their excellent resistance to corrosion, good mechanical properties, and biocompatibility.<sup>[30]</sup> However, Ti-based biomaterials usually lack osteogenic bioactivity, and how to improve surface bioactivity and osteogenic induction ability of Ti-based biomaterials has assumed an important role in osteointegration.<sup>[31]</sup> One of the efficient and convenient strategies is to modify Ti-based biomaterials to integrate nanostructures.<sup>[18, 32]</sup> Surface nanostructures can be fabricated by different methods (such as hydrothermal methods, sandblast-acid etching, anodization, and laser treatment)<sup>[33]</sup> and were significantly effective to regulate cell mobility, proliferation, and differentiation.<sup>[34]</sup>

Applied as suitable surface nanostructures, Ti-based materials possess a high capability to regenerate damaged bones.<sup>[35]</sup> Compared to smooth and macro-micro rough Ti-6Al-4V, Ti-6Al-4V with hierarchical, a macro-micro-nano rough structure can form a stellate morphology, which is the typical feature leading to mature osteoblasts/osteocytes, rapid and random cell migration, and improved osteogenic differentiation of MSCs (**Figure 1a**).<sup>[36]</sup> Furthermore, the Ti surface with a nanonetwork structure prepared by sodium hydroxide treatment could promote osteogenic differentiation of BMSCs,<sup>[37]</sup> while the Ti surface with a nanopetal-like structure prepared by hydrothermal method could favor osteogenesis after implantation *in vivo* for 12 weeks.<sup>[38]</sup> Besides, our group found that TiO<sub>2</sub> nanorod with 1.5 μm in length and 100 nm in diameter arrays grown on TiO<sub>2</sub> ceramic and Ti substrate ameliorated the adhesion, the proliferation, and the osteogenic differentiation of stem cells (**Figure 1b**),<sup>[28, 39]</sup> and optimized micro-/nano-topography consisting of 39 nm diameter TiO<sub>2</sub> nanotubes prepared by anodization method enhanced osteogenesis in MSCs.<sup>[40]</sup> Additionally, the clustered TiO<sub>2</sub> nanotube surface modified by platelet-derived growth factor (PDGF)-BB, boosted the osteogenic differentiation of MSCs and bone regeneration *in vivo*.<sup>[41]</sup> Interestingly, besides osteogenic differentiation, arrays of TiO<sub>2</sub> nanotubes with a diameter of 30 nm showed the potential for

vascularization by increasing the activity of endothelial cells,<sup>[42]</sup> and the ~85 nm spaced Ti nanorod array switched macrophage (M $\phi$ ) from M1 to M2 phenotype.<sup>[43]</sup> Notably, nanoporous Ti surface with about 30 nm diameter alleviated the inhibition of osteoclasts on osteogenesis by changing the secretion of cytokines and accelerated bone regeneration by macrophage cytokine profiles, which indicated that the morphology of Ti surface was critical for modulating monocyte/M $\phi$  lineage commitment, thereby providing guidance for promoting osseointegration by coupling the osteogenesis and osteoclastogenesis (**Figure 1c**).<sup>[44]</sup>

To further promote bone generation, a bioactive ion-assisted strategy has been developed. For example, Sr<sup>2+</sup> was incorporated in Ti nanostructured substrates to further promote angiogenesis of human umbilical vein endothelial cells (UVECs), switch M $\phi$  polarization towards the M2 phenotype *in vitro* and trigger rapid bone regeneration *in vivo* (**Figure 1d**),<sup>[45]</sup> and nanostructured titanium foams with magnesium ions or Ca<sup>2+</sup> incorporation showed higher efficiency for the promotion of osteogenic differentiation of MSCs.<sup>[46]</sup>

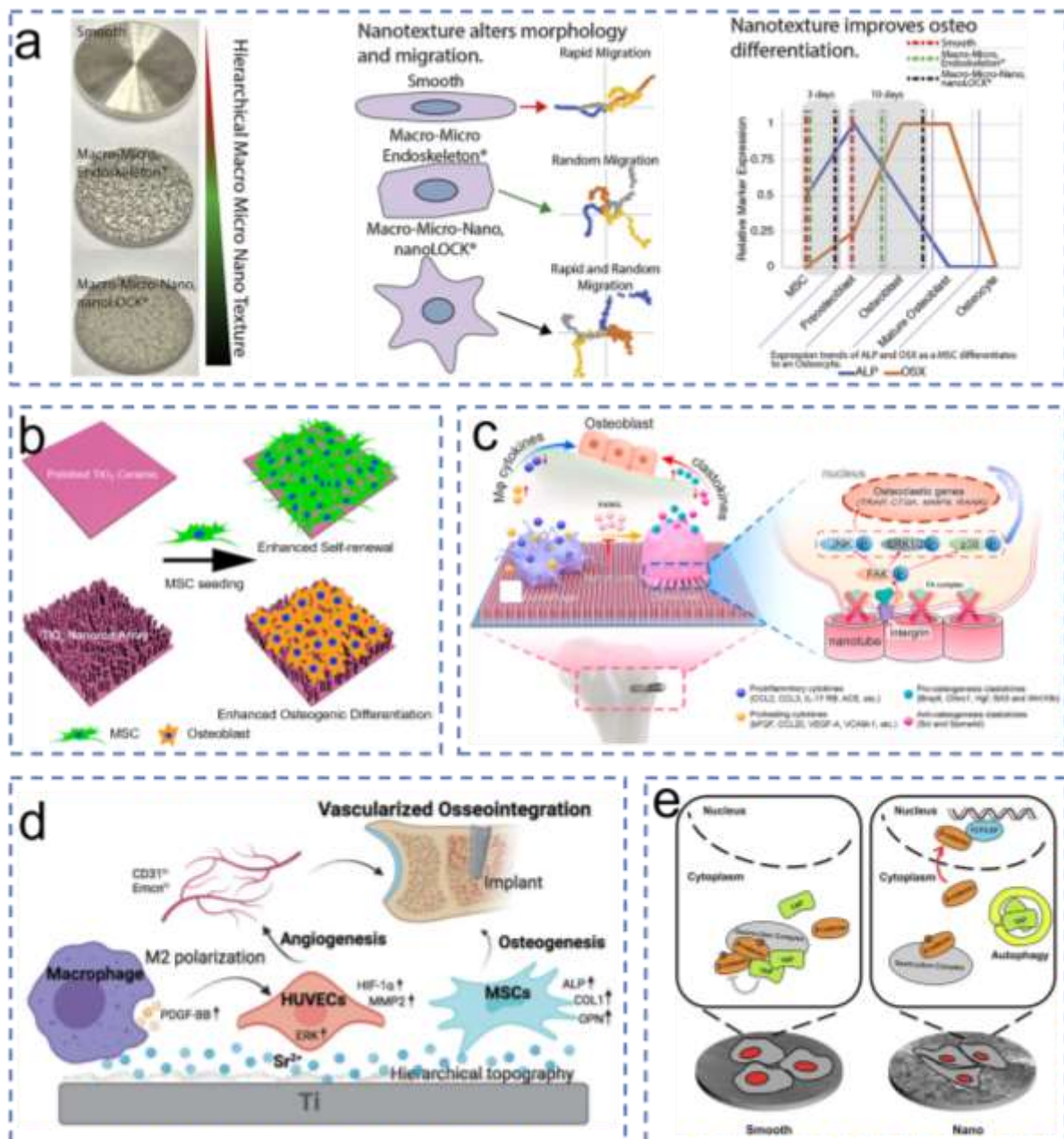


**Figure 1.** Ti-based nanostructures for bone regeneration. (a) Schematic presentation for the influence of the hierarchical macro-micro-nano roughness of Ti surface on the morphology of osteoblasts/osteocytes and osteogenesis of MSCs. Reproduced with permission.<sup>[36]</sup> Copyright 2019, Elsevier Ltd. (b) Schematic illustration of the different fates of MSCs on TiO<sub>2</sub> substrates with different surface nanotopographies. Reproduced with permission.<sup>[28]</sup> Copyright 2016, Wiley Ltd. (c) Schematic diagram of the modulation of osteogenesis by monocyte/Mφ lineage on Ti surface nanoarchitecture. Reproduced with permission.<sup>[44]</sup> Copyright 2021, Elsevier Ltd. (d) Schematic representation of overall cues involved in the process of vascularized implant osseointegration. Reproduced with permission.<sup>[45a]</sup> Copyright 2022, Royal Society of Chemistry. (e) Schematic of the mechanism of

nanotopography-induced osteogenic differentiation via the autophagy-mediated signaling link between YAP and  $\beta$ -catenin. Reproduced with permission.<sup>[47]</sup> Copyright 2019, Elsevier Ltd.

To elucidate how the nanostructure morphology affects osteogenic differentiation and bone repair, varied mechanisms were studied. Nanostructures on Ti may regulate osteogenic differentiation: 1) by autophagy-mediated signaling between yes-associated protein (YAP) and  $\beta$ -catenin (**Figure 1e**),<sup>[47]</sup> 2) the crosstalk between cell division cycle 42 protein (Cdc42, as a key modulator of rat MSC morphology and cytoskeletal reorganization) and Wnt/ $\beta$ -catenin signaling,<sup>[48]</sup> 3) a rho-associated kinase (Rock)-Wnt5a feedback loop,<sup>[49]</sup> 4) the activation of mitogen-activated protein kinases (MAPK) pathway through ras-related C3 botulinum toxin substrate 1 (Rac1),<sup>[50]</sup> Wnt11,<sup>[51]</sup> 5) the role of p53 mediated miR-23a/C-X-C motif chemokine ligand 12 (CXCL12) pathway,<sup>[52]</sup> 6) the participation of integrin  $\beta$ 3<sup>[53]</sup> and so on. Besides regulating osteogenesis, a nanoporous surface on the Ti implant inhibited osteoclastogenesis via integrin  $\beta$ 1/focal adhesion kinase phosphorylation of tyrosine (FAKpY)397/MAPK (**Figure 1c**).<sup>[44]</sup> Furthermore, the nanoscale geometry of TiO<sub>2</sub> nanotubes can influence the osteogenic differentiation of human adipose-derived stem cells (ADSCs) by modulating H3K4 trimethylation<sup>[54]</sup> and the regulation of lncRNA C-C motif chemokine ligand 3 (CCL3-AS).<sup>[55]</sup> Interestingly, a spaced nanorods array on Ti implants switched M $\phi$  to M2 phenotype via the fibronectin(FN)-integrin  $\beta$ 1-Akt1 pathway and subsequent M2 cytokines enhanced by arrays facilitated osteogenesis via BMP2-transforming growth factor (TGF)-SMAD pathway.<sup>[43]</sup> Therefore, optimally nanostructured Ti-based biomaterials possess more efficient osteogenesis acceleration by activating varied signal pathways and M $\phi$  polarization, which is helpful for further clinical applications.

## 2.2 HAp-based nanostructures

As the main inorganic component of bone, HAp possesses great potential in BTE due to its high biocompatibility, bioactivity, and biodegradability.<sup>[56]</sup> To facilitate osteogenic differentiation and bone repair, various nanostructured HAp-based biomaterials have been designed and fabricated. HAp nanostructures (e.g., nanorods, nanowires, nanorods) can be deposited on substrates including metals, polymers, ceramics, etc., using bottom-up and top-down techniques such as electrochemical deposition,<sup>[57]</sup> spray coating,<sup>[58]</sup> hydrothermal deposition,<sup>[59]</sup> and biomimetic.<sup>[60]</sup> Nanostructured HAp can be not only used to regulate stem cell differentiation and bone regeneration directly but it is often

coated on the surface of other biomaterials as an osteoinductive layer.<sup>[56b, 61]</sup>

By regulating the viscosity in the reaction system, our group prepared HAp nanostructures with tunable length and demonstrated that HAp short nanowire (5  $\mu\text{m}$  in length) modified substrate could promote osteogenic differentiation more efficiently than a nanorod (100 nm in length) substrate or a long nanowire (50  $\mu\text{m}$  in length) substrate (**Figure 2a**).<sup>[62]</sup> Meanwhile, HAp nanowires have been also blended with polylactic acid (PLA) as a Janus membrane with osteoinduction/barrier dual functions for bone defect repair.<sup>[63]</sup> Moreover, compared to nanosheets and nanorods, a micro-nano-hybrid surface topography significantly enhanced protein adsorption, cell attachment and viability, and osteogenic differentiation of stem cells.<sup>[56b, 64]</sup> Interestingly, imprinted HAp surfaces with isolated island topographies (a scattered form of wells with a mean depth of 5  $\mu\text{m}$ , and width of 12  $\mu\text{m}$ ) significantly promoted osteogenic differentiation of ADSCs, while honeycomb topographies (e.g., a complex form of pits with a mean depth of 12  $\mu\text{m}$ , opening diameter of 18  $\mu\text{m}$  and a basal diameter of 6  $\mu\text{m}$ ) hampered the process (**Figure 2b**).<sup>[11]</sup> It was also reported that the osteogenic differentiation level of MSCs was significantly higher when cultured on a spherical nanostructured HAp coating rather than on a plate-like or wire-like nanostructured HAp coating.<sup>[65]</sup> Furthermore, the synergistic promotion of osseointegration by nanostructures and bioactive ions on HAp coatings has been studied. As a principle-of-proof,  $\text{Si}^{4+}$  substitution of HAp nanostructure coatings enhanced cell proliferation, improved osteogenic and angiogenic differentiation, and repressed osteoclastogenesis in diabetes mellitus BMSCs, following an effective promotion of bone formation and bone-implant osseointegration *in vivo*.<sup>[66]</sup> Thus, varied nanostructures of HAp have different effects on cell behavior and differentiation, and optimal nanotopographies are obviously helpful to the osteogenic differentiation of stem cells and bone repair.

To enhance the bone regeneration ability of other biomaterials, nanostructured HAp coatings have been sprayed on their surface.<sup>[67]</sup> For instance, HAp nanorods coating on Ti-6Al-4V implants promoted the attachment, proliferation, and differentiation of rat BMSCs, further improving the osseointegration between Ti implants and the surrounding bone tissue.<sup>[68]</sup> Interestingly, besides Ti-based materials, HAp coating was also widely used to modify biodegradable and bioabsorbable scaffolds. Our group successfully constructed HAp nanostructure on the surface of chitosan and collagen scaffolds by simulated body fluid mineralization according to Kokubo's method. We found that mineralized HAp with interconnected nanonetwork could regulate cell shape and cytoskeleton organization and

promote osteogenic differentiation efficiently.<sup>[69]</sup> Meanwhile, the HAp nanostructure assembled on the chitosan-HAp scaffold can function as well as an absorption/release platform to deliver BMP-2 for optimal bone repair.<sup>[14]</sup> Additionally, the influence of nanostructure on the immune response should be considered when applied *in vivo* and in future clinical practice. Ti surfaces coated with HAp nanoparticles were found to modulate the inflammatory response resulting in an osteoimmune microenvironment more favorable for osteogenesis/angiogenesis while Ti surfaces coated with nanorod-shaped HAp harmed the same process and the osteoimmunomodulation (**Figure 2c**).<sup>[68]</sup>

To better understand the effect of HAp nanostructures on osteogenic differentiation and bone regeneration, many mechanisms have been explored. Phosphoinositide 3-Kinase (PI3K)-protein kinase B (AKT) pathway has been widely studied, and the activation of PI3K can up-regulate AKT and consequently activate phosphorylation of mammalian target of rapamycin (mTOR) (**Figure 2d**), which not only participates in osteogenic differentiation but also up-regulates the formation of blood vessels.<sup>[67a, 70]</sup> HAp nanoparticle (NP) coating up-regulated osteogenesis through the integrin  $\alpha 7$ -mediated PI3K-AKT signaling pathway,<sup>[71]</sup> and HAp nanorods promoted osteoblast differentiation by mediating mTOR signaling pathway and autophagy.<sup>[72]</sup> In addition, the topographical features of HAp including nanorod and micropattern structures stimulated osteogenesis by activating the BMP/Smad pathway,<sup>[11]</sup> which in turn activated some integrin subunits and connexin protein (Cx43)-related cell-cell communication.<sup>[73]</sup> Moreover, HAp nanostructures can promote osteogenesis by regulating the immune response. As proof, the rod-shaped HAp (300-400 nm) induced M2 polarization via the PI3K-Akt and Wnt/ $\beta$ -catenin pathways, thereby promoting osteogenesis.<sup>[74]</sup> Similarly, bone-mimicking HAp nanorods with different aspect ratios can regulate osteogenesis through modulation of T cells and interleukin (IL)-22 in the bone regeneration process. Specifically, HAp nanorods stimulated osteogenesis by activating T cells, which produced IL-22 to activate the janus kinase-1 (JAK1)-signal transducer and activator of transcription (STAT3) signaling pathway of BMSCs (**Figure 2e**).<sup>[75]</sup> Therefore, HAp nanostructures can promote osteogenic differentiation and improve the efficiency of bone regeneration by activating a variety of pathways, but the specific mechanisms are still uncertain and the relationships between these pathways need to be furtherly investigated.

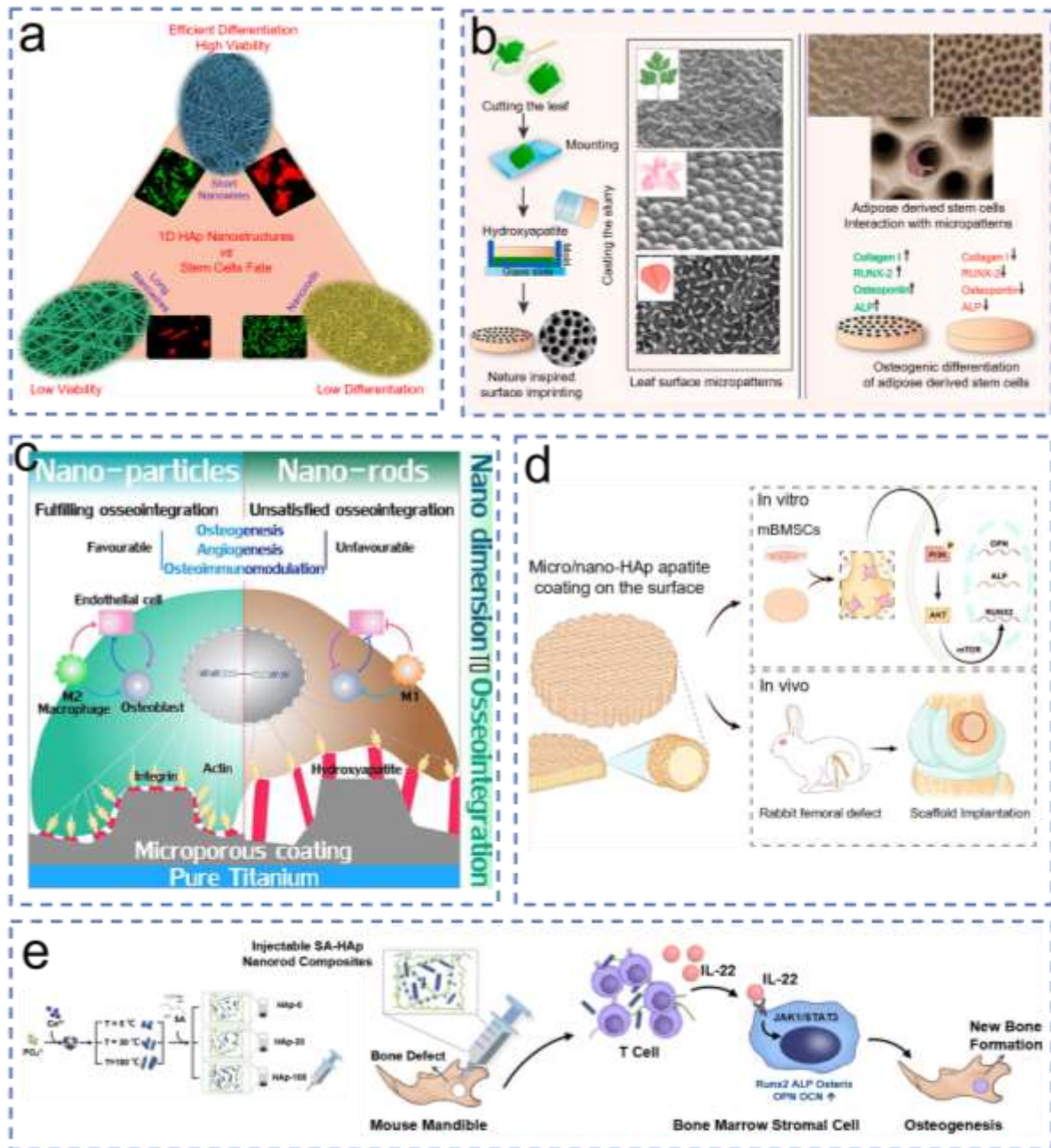


**Figure 2.** HAp-based nanostructures for bone regeneration. (a) Illustration of how the length of 1D HAp nanostructures regulates the fate of the stem cells without any growth factors. Reproduced with permission.<sup>[62]</sup> Copyright 2017, American Chemical Society. (b) Schematic diagram of the nature-inspired micron-scale topographies to control the osteogenic differentiation of stem cells. Reproduced with permission. Reproduced with permission.<sup>[11]</sup> Copyright 2021, Elsevier Ltd. (c) Illustration of the mechanism of the coating with nano-micro dimension on osteogenesis/angiogenesis and osteoimmunomodulation. Reproduced with permission.<sup>[68]</sup> Copyright 2018, Elsevier Ltd. (d) Schematic diagram showing the biomimetic hydroxyapatite coating constructed on the ceramic

scaffold promoting osteogenic differentiation via PI3K/AKT/mTOR signaling pathway. Reproduced with permission.<sup>[67a]</sup> Copyright 2023, Elsevier Ltd. (e) Schematic diagram of the mechanism of HAp nanorods with different aspect ratios-induced osteogenic differentiation via T cells and T cell-derived cytokines. Reproduced with permission.<sup>[75]</sup> Copyright 2022, American Chemical Society.

### 2.3 Polymer-based nanostructures

In the last few years, a wide range of polymers has been extensively investigated for BTE applications. According to the origin, polymeric materials can be categorized into natural and synthetic polymers.<sup>[76]</sup> Some of the most common techniques for the preparation of polymer-based nanostructures for bone regeneration are surface epitaxial crystallization,<sup>[17]</sup> sulfonation reaction,<sup>[77]</sup> hot die formation technique,<sup>[78]</sup> and freeze-drying.<sup>[79]</sup> In this section, we will briefly introduce the impact of polymer-based nanostructures on in situ osteogenesis.

#### 2.3.1 Synthetic polymers

Synthetic polymers can be stably produced on a large scale, with adjustable physical, chemical, and mechanical properties. The most widely used synthetic polymers in BTE are PLA, poly(glycolic acid) (PGA), poly (lactic-co-glycolic acid) (PLGA), and polycaprolactone (PCL).<sup>[80]</sup> The nanostructured PLA film with a 200 nm pillar array exhibited an improved osteogenic ability both *in vitro* and *in vivo* compared with a planar PLA film,<sup>[81]</sup> while PLGA nanopatterned patch (BNP) (**Figure 3a**) with a size of 800-800-600 nm (ridge-groove-height) enhanced bone regeneration *in vivo* by promoting the recruitment, migration, and osteogenic differentiation of osteoblasts without external stimuli.<sup>[82]</sup> Moreover, surface lamellar PCL nanosheets constructed on PCL substrates by surface epitaxial crystallization significantly enhanced the proliferation and osteogenic differentiation of preosteoblasts by activating the corresponding transcriptional coactivator (**Figure 3b**).<sup>[17]</sup>

In addition to the common polymers mentioned above, poly-ether-ether-ketone (PEEK) has recently become popular in BTE for its elastic modulus (3-4 GPa), which is comparable to the cortical bone of humans.<sup>[83]</sup> A 3D nanostructured network on PEEK was fabricated through a sulfonation reaction with concentrated sulfuric acid (sulfonation-treated PEEK/SPEEK), improving the osteogenic differentiation of stem cells.<sup>[76b, 77, 84]</sup> However, sulfuric acid is extremely dangerous, and SPEEK has a porous surface, which generally weakens the mechanical properties of PEEK.<sup>[85]</sup> To solve these

problems, a type of facile hot die formation technique was developed for modifying PEEK materials with in situ patterned nanorod (200 nm diameter) arrays on the surface (**Figure 3c**). This method could maintain the excellent properties of PEEK and facilitate osteogenic activity in the absence of any organic/inorganic differentiation-inducing factors.<sup>[78]</sup>

Moreover, other synthetic polymers have been also developed for BTE. Surface patterns of polyimide enhanced the differentiation of MSCs towards specific lineages: patterns with 15  $\mu\text{m}$  ridges increased adipogenic differentiation whereas patterns with 2  $\mu\text{m}$  ridges enhanced osteogenic differentiation.<sup>[86]</sup> When compared to an unpatterned polyurethane surface, the osteogenic differentiation of MSCs was more enhanced on the surfaces of nanostructured polyurethane substrate with a dot pattern (400 nm diameter).<sup>[87]</sup> These results suggest that surface nanotopography, in the presence of suitable biochemical signals, can exert a significant influence on regulating stem cell differentiation.

### 2.3.2 Natural polymers

Natural polymers, including cellulose, chitosan, gelatin, and SF, are similar to the native extracellular matrix (ECM) and typically exhibit increased cell adhesion and biocompatibility in comparison to synthetic polymers.<sup>[88]</sup> Given the superiority of natural polymers, various nanostructures have been designed to improve their applications in BTE. The natural polymer-based, micro-nanostructured matrix (CAc), which was formed by self-assembly of type I collagen (Col I) on a porous microstructured matrix prepared by cellulose acetate (CA), effectively induced osteogenic differentiation of BMSCs.<sup>[89]</sup> Additionally, it has been demonstrated that  $\sim 32$  nm pores present within Col I fibers were the most effective to induce osteogenic differentiation of stem cells.<sup>[90]</sup> Furthermore, nanopillared chitosan/gelatin films with  $\sim 90$  nm pillar diameter,  $\sim 300$  nm height, and  $\sim 50$  nm pitch between pillars remarkably enhanced the mineralization capacity of BMSCs and osteoblast-like saos-2 cells (**Figure 3d**).<sup>[91]</sup> Moreover, biomimetic ECM porous nanostructures prepared through self-assembling chitosan, oxidized sodium alginate (SA), and bovine serum albumin (BSA)-based NPs, promoted the attachment, proliferation, and differentiation of BMSCs and ultimately enhanced bone formation.<sup>[92]</sup>

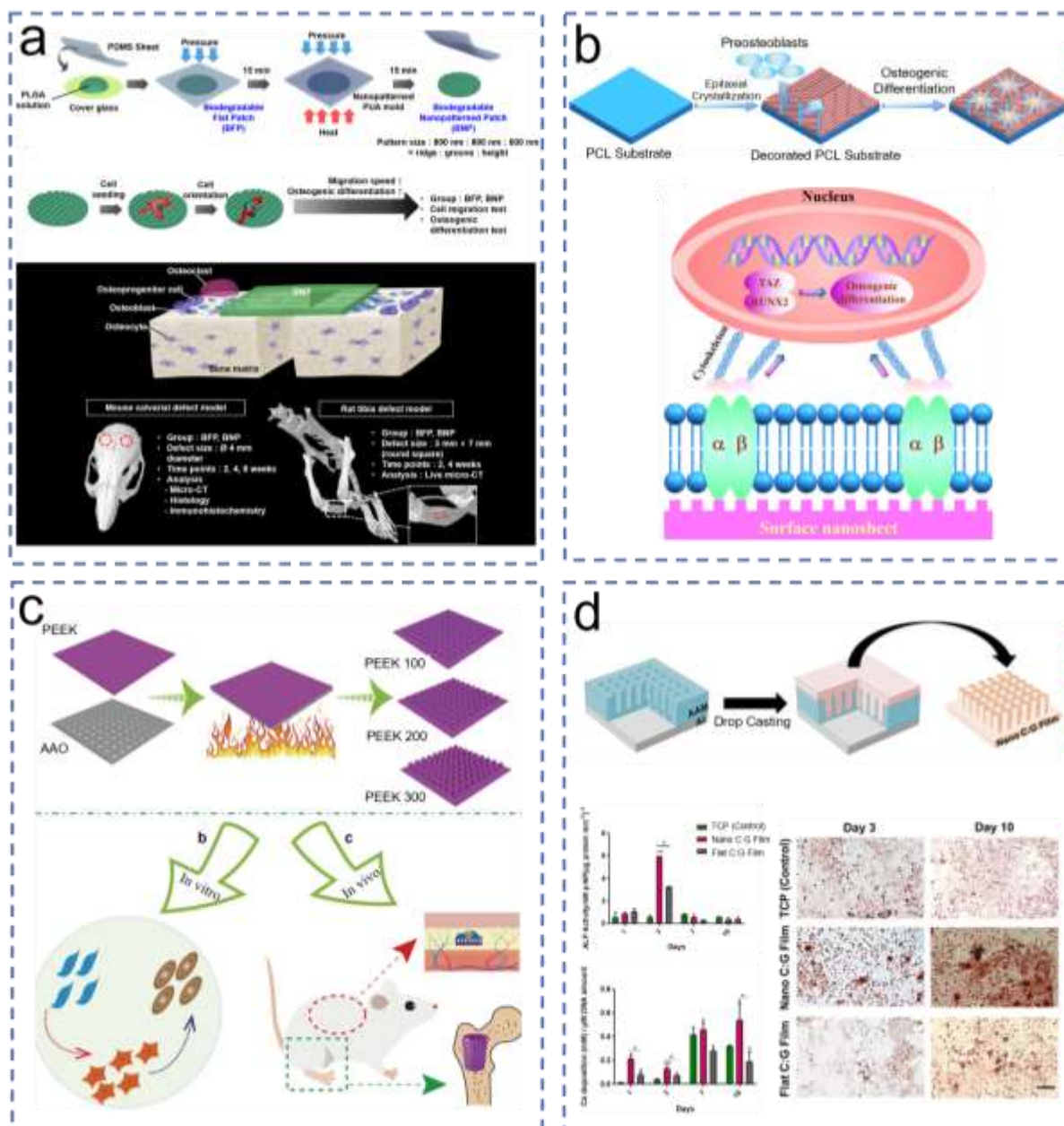


**Figure 3.** Polymer-based nanostructures for modulating osteogenesis. (a) Schematic illustration of the preparation of BNP and its influences on *in vitro* osteogenic differentiation of MSCs and *in vivo* bone formation to repair bone defects. Reproduced with permission.<sup>[82]</sup> Copyright 2018, American Chemical Society. (b) Schematic illustration of surface epitaxial crystallization-induced nanotopography for osteogenic differentiation and the underlying mechanism of surface nanosheets to promote osteogenic differentiation. Reproduced with permission.<sup>[17]</sup> Copyright 2019, American Chemical Society. (c) Flow diagram of the fabrication process of the PEEK material and the regulation of nanorod arrays on osteogenic differentiation *in vitro*. Reproduced with permission.<sup>[78]</sup> Copyright 2021, Wiley Ltd. (d) Schematic representation of nanopillared chitosan/gelatin film and its influence

on mineralization and osteoblast differentiation of saos-2 cells. Reproduced with permission.<sup>[91a]</sup>  
Copyright 2019, American Chemical Society.

## 2.4 Other materials-based nanostructures

In addition to the above nanostructures, other materials including graphene and its derivative graphene oxide (GO),<sup>[93]</sup> molybdenum disulfide,<sup>[94]</sup> and gold<sup>[95]</sup> have been used to construct different nanostructures for bone regeneration. Here we will briefly introduce several commonly used nanostructures that can regulate the differentiation fate of stem cells and promote in situ bone regeneration. The nanostructures of graphene and GO can offer desirable conductivity, biocompatibility, and chemical stability, and have been recently widely used in BTE.<sup>[96]</sup> Highly wrinkled cross-linked GO films with a rough surface nanotopography and high in-plane stiffness were able to enhance the adhesion, proliferation rate, and bone matrix formation of human stem cells.<sup>[97]</sup> To further improve the efficiency of graphene on bone differentiation, 3D graphene/RGD composites were prepared to accelerate the osteogenic differentiation of ADSCs through the synergistic effect of the nanostructure and the peptide.<sup>[98]</sup> Apart from graphene, a nanoporous MoS<sub>2</sub> interface consisting of many interconnected nanoflakes with a size of 5–8 nm accelerated as well the osteogenesis of MSCs.<sup>[99]</sup> Moreover, nanostructured porous Si coatings with highly ordered sub-10 nm porosity accelerated early osteoblast adhesive response, promoted the osteogenic differentiation of MSCs,<sup>[100]</sup> and accelerated the formation of bone tissue in the periphery of the implant.<sup>[101]</sup> Recently, flower-like nanostructures with thicknesses of 20–50 nm prepared in situ on biodegradable calcium silicate bioceramics, via hydrothermal treatment, significantly stimulated osteogenesis of BMSCs through the focal adhesion kinase (FAK)/p38 signaling pathway.<sup>[102]</sup>

## 3. Impact of mechanical signals

Bone tissues are very sensitive to mechanical stress. The proliferation and formation of osteoclasts and osteoblasts, as well as their distinct roles in bone formation and resorption, heavily depend on the unloading and loading of mechanical stress, respectively.<sup>[103]</sup> Therefore, mechanical stress has a significant impact on bone microenvironment and metabolism. In addition to osteoblasts and osteoclasts, osteocytes, bone lining cells, and Mφs can sense mechanical stimulation and respond

directly or indirectly as well.<sup>[104]</sup> It is well-known that a complex but precise regulation mechanism called mechanical transduction occurs between cells and their microenvironment, between nearby cells, and between mechanical sensors with various functions within a single cell.<sup>[105]</sup> Ion channels, integrins, gap junction proteins, FAK, ECM, cellular skeletal components (such as intermediate filaments, microtubules, and actin filaments), and primary cilia are mechanical sensors that have been proven to regulate intracellular signaling pathways.<sup>[106]</sup> In this context, the study of mechanical stimulation-mediated cell fate regulation has attracted much attention in BTE. In this section, we will detailly discuss the most common mechanical stimulation mediated by biomaterials in BTE, mainly including stiffness and biodegradability effects.

### 3.1 Stiffness

The inherent stiffness of ECM has a profound impact on cell morphology, proliferation, and cell fate, with subsequent consequences on the promotion of osteogenic differentiation of stem cells and bone repair.<sup>[107]</sup> Recently, it was reported that aligned PCL fibers with lower elastic modulus had an evident accelerating effect on inducing stem cell osteogenic differentiation when compared to fibers with high elastic modulus (**Figure 4a**).<sup>[108]</sup> Even though osteogenic differentiation was commonly thought to be positively correlated with stiffness,<sup>[109]</sup> investigations have shown that there is likely a threshold at which further increase in stiffness did not correspond to increased osteogenic differentiation.<sup>[110]</sup> However, the threshold is still uncertain. It was worth noting that higher expression of alkaline phosphatase (ALP), RUNX2, and Col I by MSCs in soft composites compared to stiffer hybrids.<sup>[111]</sup> Similarly, smooth muscle cells showed the highest extent of osteogenesis and calcium deposition when cultured on a polydimethylsiloxane (PDMS) substrate with moderate stiffness (0.909 MPa).<sup>[112]</sup> In addition, it has been gradually accepted that stiffness matching the native ECM may induce stem cells to differentiate into residential tissue cell lines. As shown in **Figure 4b**, MSCs were reported to differentiate into neuron-like cells, myoblasts, and osteoblasts, on various gels whose elasticity mimicked the corresponding tissues.<sup>[113]</sup> Subsequently, extensive studies have confirmed the relationship between matrix elasticity and MSC differentiation, including osteogenesis, myogenesis, adipogenesis, angiogenesis, and neurogenesis. In general, stem cells tend to differentiate to the target tissue on substrates that have similar elasticity to the target tissue.<sup>[114]</sup>

Furthermore, dynamic conditions have been identified as an important regulator in tissue

development as many ECM components are locally synthesized and continuously reorganize to modulate diverse intracellular processes.<sup>[115]</sup> A recent study reported that osteogenic differentiation of BMSCs was regulated by the starting high stiffness and subsequent stiffness relaxation.<sup>[116]</sup> Moreover, a dynamic stiffening methacrylated gelatin (GelMA)/SA hydrogel that could be uninterruptedly stiffened from  $14.63 \pm 1.18$  kPa to  $68.37 \pm 4.99$  kPa within 7 days accelerated the calvarial defect repair when compared with a low stiffness ( $10.20 \pm 2.39$  kPa) or a high stiffness ( $66.30 \pm 4.40$  kPa) hydrogel. The dynamic nature of the hybrid had a consequence on the treated group *in vivo* particularly enhancing angiogenesis *in vivo*, leading to bone regeneration (**Figure 4c**).<sup>[117]</sup>

Interestingly, M $\phi$  involvement in a co-culture system altered previously identified stiffness-related effects on BMSCs. The increasing stiffness of transglutaminase cross-linked gelatin (TG-gels) harnessed osteogenic differentiation of BMSCs when cultured alone. However, the high-stiffness matrix was more alike than the medium and low-stiffness matrices to push M $\phi$  toward the M1 phenotype, which would negatively influence the osteogenesis of BMSCs. When cultured in the conditioned medium (CM) derived from the gel-encapsulated M $\phi$ s or when placed into co-culture systems, the M $\phi$ s in the low ( $1.58 \pm 0.42$  kPa) and high stiffness ( $60.54 \pm 10.45$  kPa) TG-gels were able to regulate BMSCs osteogenesis positively and negatively, respectively. When the M $\phi$ s and BMSCs were encapsulated within the same TG-gel and placed in a transwell system, similar levels of cell osteogenesis were instead found in BMSCs encapsulated in the low and high-stiffness matrices (**Figure 4d**).<sup>[118]</sup> Therefore, in the development of biomimetic biomaterials for regenerative applications, M $\phi$ -stem cell interactions should be taken into account when establishing proper matrix parameter-associated cell fate regulation.

Several studies aimed to illustrate the mechanisms between stiffness and osteogenesis, indicating that an increase in stiffness could induce osteogenic differentiation via the mechanotransduction mediators YAP/TAZ and the canonical Wnt (cWnt) signaling pathway.<sup>[119]</sup> As shown in **Figure 4e**, once the integrins bound to the ECM, the stiffness stimulation propagated to the intracellular activated mechanosensory system, including FAK and ROCK, and then controlled actin assembly. The actin skeleton can then be detected by YAP/TAZ and activated into the nucleus. As a final step, osteogenic differentiation was enhanced by YAP1/TAZ activation.<sup>[109]</sup> However, several researchers discovered that YAP was not related to BMSCs differentiation<sup>[110b, 120]</sup> Moreover, the cWnt signaling may play an integral role in osteogenesis induced by the substrate in a stiffness-dependent manner.<sup>[121]</sup> It is worth

that cWnt and  $\beta$ -catenin were demonstrated as negative regulators of osteogenic differentiation on the stiffer substrate, which could explain why further increases in stiffness did not correlate to stronger osteogenic differentiation.<sup>[122]</sup> Furthermore, there may be other pathways in the process of ECM stiffness to regulate MSC differentiation, such as BMP2,<sup>[119c]</sup> ERK, c-Jun N-terminal kinase (JNK),<sup>[123]</sup> or p38 MAPK signaling, and downstream TAZ signal molecules.<sup>[124]</sup> It is worth noting that the role of integrin-mediated phosphatidylinositol 4-phosphate 5-kinase (PIP5k)-phosphatidylinositol 4,5-bisphosphate (PIP2)-B cell lymphoma 6 (BCL-6) and the osteogenic differentiation pathways on aligned nanofibers with lower elastic modulus in promoting the growth and differentiation of BMSCs. It was reported that the overexpression of BCL-6 and/or the inhibition of miR-126a-5p promoted the expression of PIP5k-PIP2 pathway and thus stimulated the proliferation and differentiation of stem cells (**Figure 4a**).<sup>[108]</sup> Overall, the mechanism of how stiffness regulates the osteogenic differentiation of stem cells is still not clear, and further research is needed.

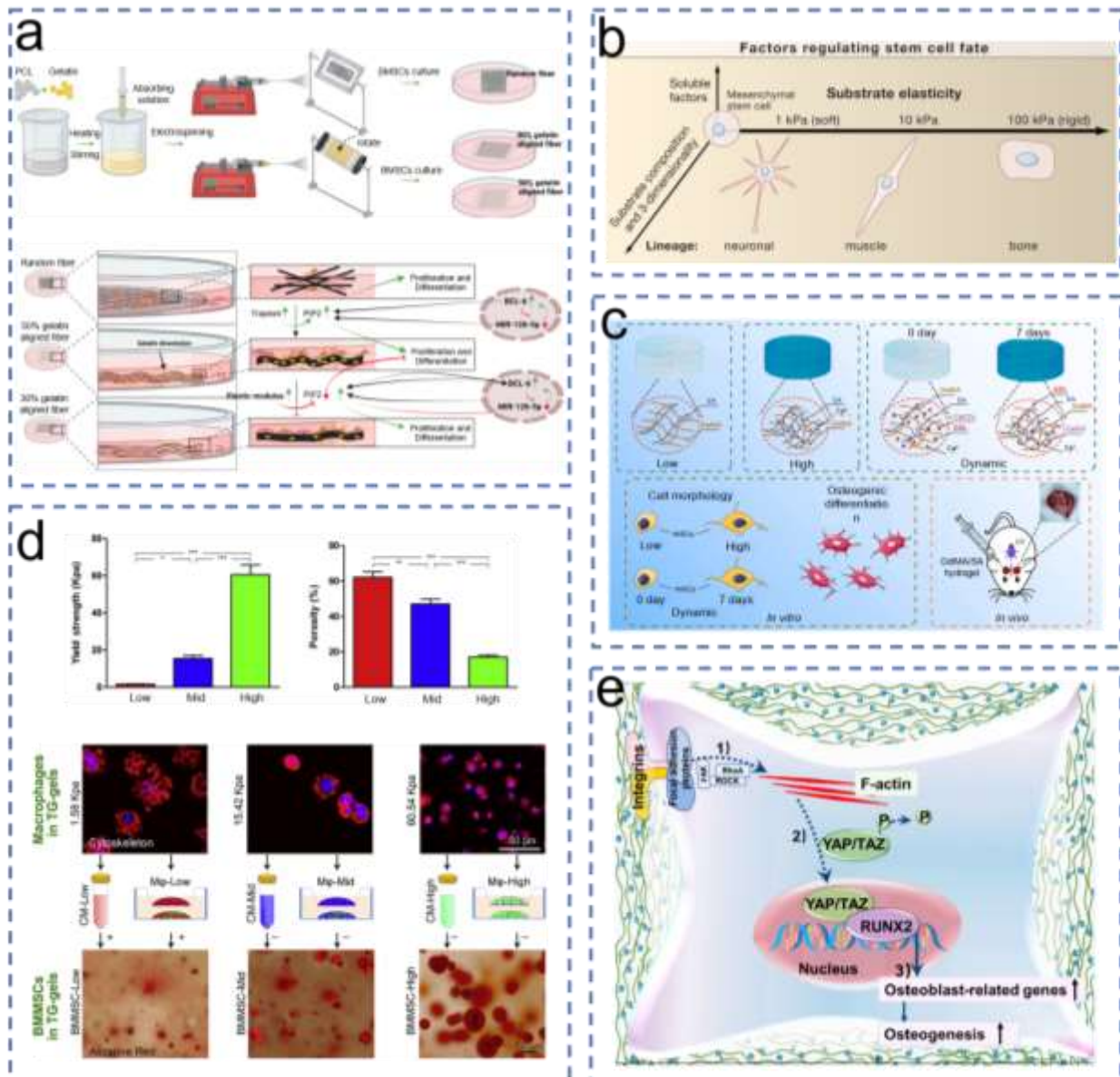


**Figure 4.** Stiffness-related regulation for osteogenesis. (a) Schematic illustration of the fabrication of aligned and random submicron fibers with different elastic modulus and influences on proliferation and differentiation. Reproduced with permission.<sup>[108]</sup> Copyright 2023, Wiley Ltd. (b) Schematic diagram of the effect of matrix elasticity on the differentiation of MSCs. Reproduced with permission.<sup>[113]</sup> Copyright 2006, Elsevier Ltd. (c) Schematic illustration of the fabrication of a dynamic hydrogel and its effect on osteogenic differentiation of MSCs and regeneration of defected bones. Reproduced with permission.<sup>[117]</sup> Copyright 2022, Elsevier Ltd. (d) Schematic diagram of the effect of substrate stiffness on the MSC-M $\phi$ -matrix interplay. Reproduced with permission.<sup>[118]</sup> Copyright 2018, Elsevier Ltd. (e) Illustration of the mechanism of matrix stiffness-mediated osteogenic differentiation via a cytoskeleton-mediated mechanical signaling transduction pathway. Reproduced with

permission.<sup>[109]</sup> Copyright 2021, Elsevier Ltd.

### 3.2 Biodegradability

Biodegradability is an important indicator to assess the impact of biomaterials, and the degradation rate of biomaterials has shown the power to regulate osteogenic differentiation.<sup>[125]</sup> The combination of biomaterials with different degradation rates has been a simple and practical strategy to regulate their decomposition.<sup>[76a, 126]</sup> However, the degradation rate is not in direct proportion to the increase in osteogenic efficiency. It was reported that the rapid degradation of a PLGA/HAp scaffold harmed the late growth and reconstruction of new bone tissues.<sup>[127]</sup> In a recent study, regenerated SF/gelatin (RSF/G) hydrogels at different ratios were prepared, and the 9%RSF/3%G hydrogel with a moderate degradation rate (approximately three months *in vivo*) remarkably enhanced the osteogenesis efficiency compared to the rapidly degrading gelatin hydrogel and the slowly degrading RSF hydrogel (**Figure 5a**).<sup>[128]</sup> Similarly, PCL/magnesium hydroxide composite scaffolds<sup>[129]</sup> and Sr<sup>2+</sup>-tricalcium phosphate (TCP)/bioactive glass (BG) nanocomposite scaffolds showed good capability to form new bone both *in vitro* and *in vivo* due to their moderate degradation profile.<sup>[130]</sup>

Moreover, the accelerated repair of bone defects can be achieved by regulating the dynamic process of artificial bone degradation and new bone formation, which requires the degradation rate of the bone scaffold to match the growth rate of new bone.<sup>[131]</sup> The new bone will not grow out if the degradation is too fast, and the formation of new bone will be hindered if the degradation is too slow.<sup>[132]</sup> In particular, the stepwise-degraded scaffold of PLGA/PCL/HA: Yb/Ho/Zn (PPHZ) exhibited better osteogenesis than the fast-degradable scaffold PLGA/HA: Yb/Ho/Zn (PLHZ), revealing that the maintenance of relatively long-term scaffold integrity is more favorable to the bone reconstruction (**Figure 5b**).<sup>[133]</sup> Furthermore, a calcium sulfate and HAp biphasic bone graft (CS/HAp), possessing a time-dependent degradation rate, was constructed to promote osteogenesis. Since the degradation rate of CS is much faster than that of HAp, CS/HAp could be degraded rapidly (~10 wt%/week) in the first stage and slowly (~1 wt%/week) in the second stage. The different degradation rate could initially release a large amount of calcium ions and remains structurally stable throughout the degradation process, thereby effectively promoting the formation of new bone and blood vessels.<sup>[134]</sup> Overall, the degradability and structure stability of biomaterials is competing with each other during bone

regeneration and an optimal degradation rate should be carefully controlled to achieve higher efficiency.

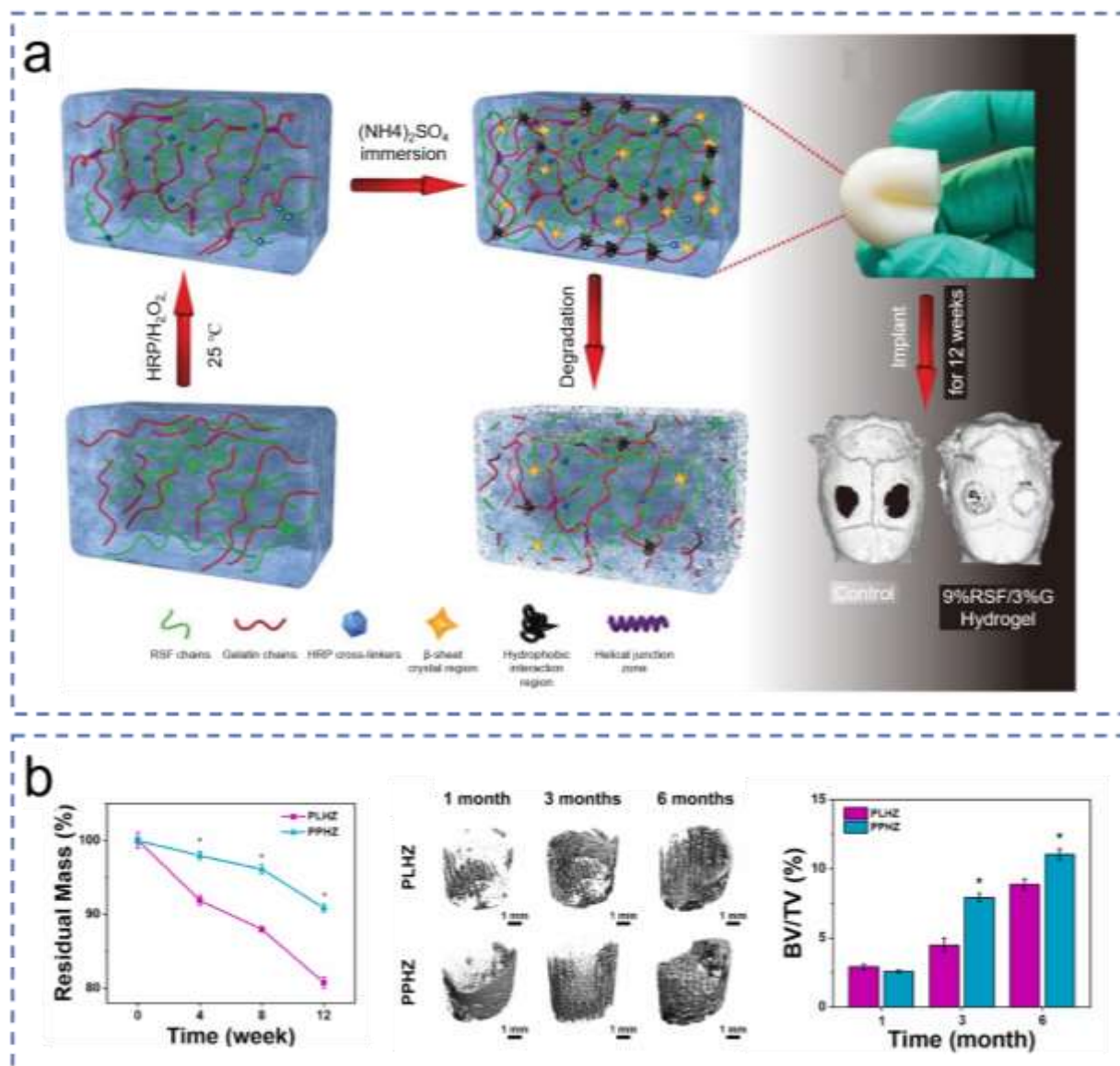


**Figure 5.** Degradation-related regulation of osteogenesis. (a) Schematic of the fabrication of a physically and chemically double-crosslinked RSF/G hydrogel with controlled degradation for bone regeneration; the 9%RSF/3%G hydrogel which possessed a moderate degradation rate showed the highest expression of osteogenic genes and proteins among all groups. Reproduced with permission.<sup>[128]</sup> Copyright 2019, Wiley Ltd. (b) Weight loss of PLHZ and PPHZ scaffolds before and after immersion in PBS for 12 weeks; Micro-CT reconstructed new bone images and bone fraction BV/TV ratio at different implantation times. Reproduced with permission.<sup>[133]</sup> Copyright 2021, Elsevier Ltd.

## 4. Impact of electric signals

Electrical signals are ubiquitous in the human body and can affect many cellular behaviors and physiological processes.<sup>[135]</sup> Electrical stimulation has been applied widely in tissue regeneration engineering. Since electroactive biomaterials can create an electrophysiological microenvironment under an external stimulus,<sup>[136]</sup> they can not only transfer electrical signals to cells but also regulate the growth of cells and the repair of tissues *in situ*, attracting more and more attention, especially in bone reconstitution.<sup>[137]</sup> It has been demonstrated that electrical stimulation could accelerate bone regeneration both in animal experiments and in clinical practice.<sup>[138]</sup> Currently, two types of electroactive biomaterials have been developed in tissue repair.<sup>[139]</sup> One consists of piezoelectric materials such as piezopolymers, piezoceramics, and their composites, while the other includes conductive materials such as conductive polypyrrole (PPy), polyaniline (PANi), poly(3,4-ethylenedioxythiophene) (PEDOT), and carbon-based materials.<sup>[73, 140]</sup> In this section, we will discuss how piezoelectric and conductive materials affect stem cell osteogenic differentiation under an external stimulus, assess the effects *in vivo*, and briefly discuss the mechanisms underneath.

### 4.1 Piezoelectric materials

Piezoelectricity is the ability of a material to generate an electric field in response to applied mechanical stress. As shown in **Figure 6a**, the generation of surface charges is due to the distortion of internal dipoles arising from the applied mechanical force.<sup>[141]</sup> Since native bone tissue exhibits a typical piezoelectric property, electroactive piezoelectric materials have drawn increasing attention to boost the therapeutic effectiveness in bone tissue repair and regeneration.<sup>[142]</sup> Piezoelectric materials can exploit the natural deformation of bone tissue during movement as a platform for mechanical-electrical translation, generating immediate bioelectric stimulation and converting it into electrophysiological signals that mimic physiological activities (**Figure 6b**).<sup>[142b]</sup> When these materials are implanted, their surface charges serve as electrical cues under mechanical stress, leading to protein adhesion, altering membrane potential, controlling voltage-gated calcium channels, and ultimately changing cell behavior.<sup>[141b]</sup> To date, the effectiveness of using piezoelectric materials to promote bone regeneration at the local defect sites has been well demonstrated.<sup>[143]</sup> Additionally, piezoelectric materials can skew M $\phi$  polarization toward the M2 phenotype,<sup>[144]</sup> which helps to

modulate the local inflammatory responses and creates a proper microenvironment for tissue regeneration. Hence, piezoelectric materials have been considered promising electroactive biomaterials in the process of repairing bone defects.<sup>[145]</sup> Piezopolymers like polyvinylidene fluoride (PVDF), poly(vinylidene fluoride-trifluoroethylene) [P(VDF-TrFE)], poly-L-lactide (PLLA), and polyhydroxyalkanoates (PHAs), and piezoceramics like barium titanate (BT), ZnO, and potassium sodium niobate (KNN) and their composites have been extensively used.<sup>[146]</sup>

#### 4.1.1 Piezoelectric polymers

Among piezoelectric polymers, PVDF and its copolymer P(VDF-TrFE) have been regarded as a research hotspot in tissue engineering due to their good biocompatibility, moderate mechanical properties, and easy processing. The polycrystalline structural polymer PVDF has four different crystal forms:  $\alpha$ ,  $\beta$ ,  $\gamma$ , and  $\delta$ . Among them, only the  $\beta$  crystal possesses good piezoelectricity, and the content of  $\beta$  crystal correlates with the piezoelectric properties.<sup>[147]</sup> Thus, one of the key strategies for enhancing the piezoelectric performance is to increase the concentration of the  $\beta$  phase in PVDF and P(VDF-TrFE). The researchers explored a variety of manufacturing techniques including polar additive addition,<sup>[148]</sup> annealing,<sup>[149]</sup> electrospinning,<sup>[150]</sup> and mechanical stretching<sup>[147]</sup> to improve the efficacy of PVDF and P(VDF-TrFE) in BTE. A flexible P(VDF-TrFE) membrane fabricated by annealing treatment to increase its  $\beta$  phases showed appropriateness as a bone substitute (**Figure 6c**).<sup>[149]</sup> Besides, another study showed that negatively polarized P(VDF-TrFE) membrane, obtained via casting and external electric field polarization, could promote promoted the osteogenic differentiation of rBMSCs. However, P(VDF-TrFE) is a bioinert material that cannot bind to bone tissue before new bone is generated, which may slow down the process of bone healing and affect its effectiveness. Additionally, unlike conventional inorganic bone repair materials such as HAp, P(VDF-TrFE) seems unable to supply sufficient mineral ions ( $\text{Ca}^{2+}$  and  $\text{PO}_4^{3-}$ ) which are necessary for bone formation.<sup>[151]</sup> Therefore, BG particles, which possesses superior biocompatibility, osteoconductive, and osteoinductive abilities, were introduced into P(VDF-TrFE) to form P(VDF-TrFE)-BGM scaffolds. These bioactive multifunctional scaffolds remarkably improved the proliferation, adhesion, and osteogenesis differentiation of BMSCs, and significantly enhanced the formation of periosteum-like tissue and the bone regeneration at the center of bone defect.<sup>[141d]</sup> Moreover, when severe medical conditions restrict patients' free movement, thereby preventing natural mechanical stimulation, the benefits of piezoelectric scaffolds are diminished. Such a constraint requires further measures of

remote mechanical or electrical stimulation of cells and tissues.<sup>[152]</sup> Thus pulsed electromagnetic fields (50 Hz, 0.6 mT, 30 min/day) were adapted to PVDF-coated PCL-TCP scaffolds ( $d_{33} = -1.2$  pC/N) to provide local mechanical stimulation and were proved to have a synergetic effect with PVDF on the osteogenic differentiation of MC3T3-E1 cells.<sup>[153]</sup>

Nonetheless, both PVDF and P(VDF-TrFE) are poorly degradable materials, raising concerns about the biosecurity of *in vivo* implants. Consequently, other polymers like PLA or PLLA, and PHA have recently attracted increasing attention for their good piezoelectricity and biodegradability. Particularly, the modulation of piezoelectric properties in PLLA nanofibers significantly affected the differentiation of stem cells in a cell type-specific manner, where neurogenesis and osteogenesis were enhanced by orthogonal and shear piezoelectricity, respectively.<sup>[154]</sup> Furthermore, the polymers belonging to the family of PHAs, e.g., polyhydroxybutyrate (PHB) and poly(hydroxybutyrate-hydroxyvalerate) [P(HB-HV)], which are completely biodegradable, degrading to produce CO<sub>2</sub> and water, have attracted a lot of attention in the last years.<sup>[155]</sup> PHB-based composites have shown an excellent capacity to induce osteogenesis and promising potential application in BTE due to their piezoelectric properties.<sup>[156]</sup> However, PHAs' relatively hydrophobic nature and weak mechanical characteristics have largely limited their application.<sup>[157]</sup>

#### 4.1.2 Piezoceramic inorganic materials

BT is a type of Pb-free piezoceramic that has been widely investigated in bone repair. The hydrothermal method was used to create a BT layer on the surface of Ti-6Al-4V scaffolds, and the layer could promote osteoblasts adhesion, proliferation, and differentiation, as well as significantly improve osteogenesis and osseointegration in the bone defect area.<sup>[158]</sup> However, due to the inherent brittleness of ceramic materials, BT was seldom used alone.<sup>[159]</sup> It was instead blended with PVDF, PVDF-TrFE, or other piezoelectric polymers to improve flexibility. Meanwhile, the incorporation of BT NPs into the polymeric matrix would improve the mechanical properties of the hybrid scaffold.<sup>[160]</sup> Nevertheless, piezoelectric organic-inorganic composites are mainly limited to PVDF/BT systems, whose low degradation rate is not suitable for *in vivo* applications.<sup>[141b]</sup> Therefore, PVDF was replaced with biodegradable PLA to fabricate BT/PLA piezoelectric composite membrane showing good osteogenic properties both *in vitro* and *in vivo*.<sup>[161]</sup> In addition, ion (e.g., barium) doping can improve the degradability of BT nanofibers by accelerating the release of ions while minimizing the potential cytotoxicity of Ba<sup>2+</sup>.<sup>[162]</sup> For example, PLLA/CMBT composites, which were constructed by blending

Ca<sup>2+</sup>/Mn<sup>4+</sup> co-doped BT nanofibers into the PLLA matrix; possessed great biodegradability, electroactivity, antibacterial, and anti-inflammatory activities.<sup>[163]</sup>

Besides, other piezoelectric inorganic materials have been reported to promote bone regeneration. Nanostructured ZnO layers can generate a local electric field in response to cellular mechanical forces, enhancing the biochemical activity of human saos-2 osteoblast-like cells without applying chemical or physical external stimulation.<sup>[164]</sup> Moreover, piezoelectric KNN ceramics were used to create microscale piezoelectric zones to mimic the piezoelectricity distribution in natural bone, and as a result, the microscale piezoelectric zones promoted osteogenic differentiation both *in vitro* and *in vivo*.<sup>[165]</sup>

Furthermore, the microenvironment of bone tissue is dynamic, namely it changes in response to mechanical stresses. Thus, when a piezoelectric material is implanted *in vivo*, its surface potential varies with stress. In other words, it is difficult for piezoelectric materials to maintain a sustained and stable electrical potential that can be adapted to the charge polarity required for bone regeneration.<sup>[166]</sup> To enhance the intensity and sustainability of electrical stimulus of piezoelectric inorganic materials, a strategy of combining ultrasound and piezoelectric materials may be effective. For instance, BT piezoelectric ceramic coating<sup>[167]</sup> and piezoelectrical whitlockite (Ca<sub>18</sub>Mg<sub>2</sub>(HPO<sub>4</sub>)<sub>2</sub>(PO<sub>4</sub>)<sub>12</sub>) nanoparticles (WH NPs) under low-intensity pulsed ultrasound (LIPUS) produced a microcurrent and significantly promoted osteogenic differentiation *in vitro* (**Figure 6d**).<sup>[168]</sup> Our team also found that piezoelectric nylon-11 NPs with the value of the piezoelectric amplitude of ~10 mV could promote the osteogenic differentiation of dental pulp stem cells efficiently with the assistance of ultrasound.<sup>[169]</sup> In addition to improving the osteogenic behavior *in vitro*, BT coating was proved to promote osteogenesis in rabbit bone defects (**Figure 6e**),<sup>[170]</sup> and M2 polarization of Mφs, and bone repair in a sheep bone defect, under LIPUS stimulation.<sup>[158]</sup>

#### 4.1.3 Mechanisms of piezoelectric stimulation

Numerous studies on the mechanisms of piezoelectric materials promoting osteogenesis have been conducted recently, but the precise pathway is still unclear. Free Ca<sup>2+</sup> is considered a major factor in both direct and indirect mechanisms of electrical stimulation. Specifically, as a second messenger, intracellular Ca<sup>2+</sup> has been widely studied, including the involvement in multiple signaling pathways, regulation of the activity of many proteins, and modulation of several cellular responses.<sup>[171]</sup> As shown in **Figure 6f**, the mechanical stimulation of a piezoelectric scaffold generated an electrical signal, which activated the voltage-gated Ca<sup>2+</sup> channels. The increase of the intracellular Ca<sup>2+</sup> concentration

triggered the calcium-modulated protein calmodulin, further activating the calcineurin (a calcium and calmodulin-dependent serine/threonine protein phosphatase). The activated calcineurin dephosphorylates the nuclear factor of activated T cells, which translocates to the nucleus and binds co-operatively with other transcription factors to the regulatory regions of the inducible genes.<sup>[172]</sup> These genes further induced the translation of several growth factors like TGF- $\beta$  and BMP, which were responsible for the regulation of ECM production as well as the up/down-regulation of several proteins and cellular metabolic pathways.<sup>[173]</sup> Additionally, the membrane mechanical receptors can also be activated by mechanical stimulation, subsequently triggering the protein kinase C and MAPK signaling pathways.<sup>[173c]</sup> Moreover, due to the electrostatic interactions on the surface of piezoelectric materials,  $\text{Ca}^{2+}$  concentration increases, subsequently activating the calcium-sensing receptor of osteoblasts to promote osteogenesis and mineralization.<sup>[141d, 174]</sup>

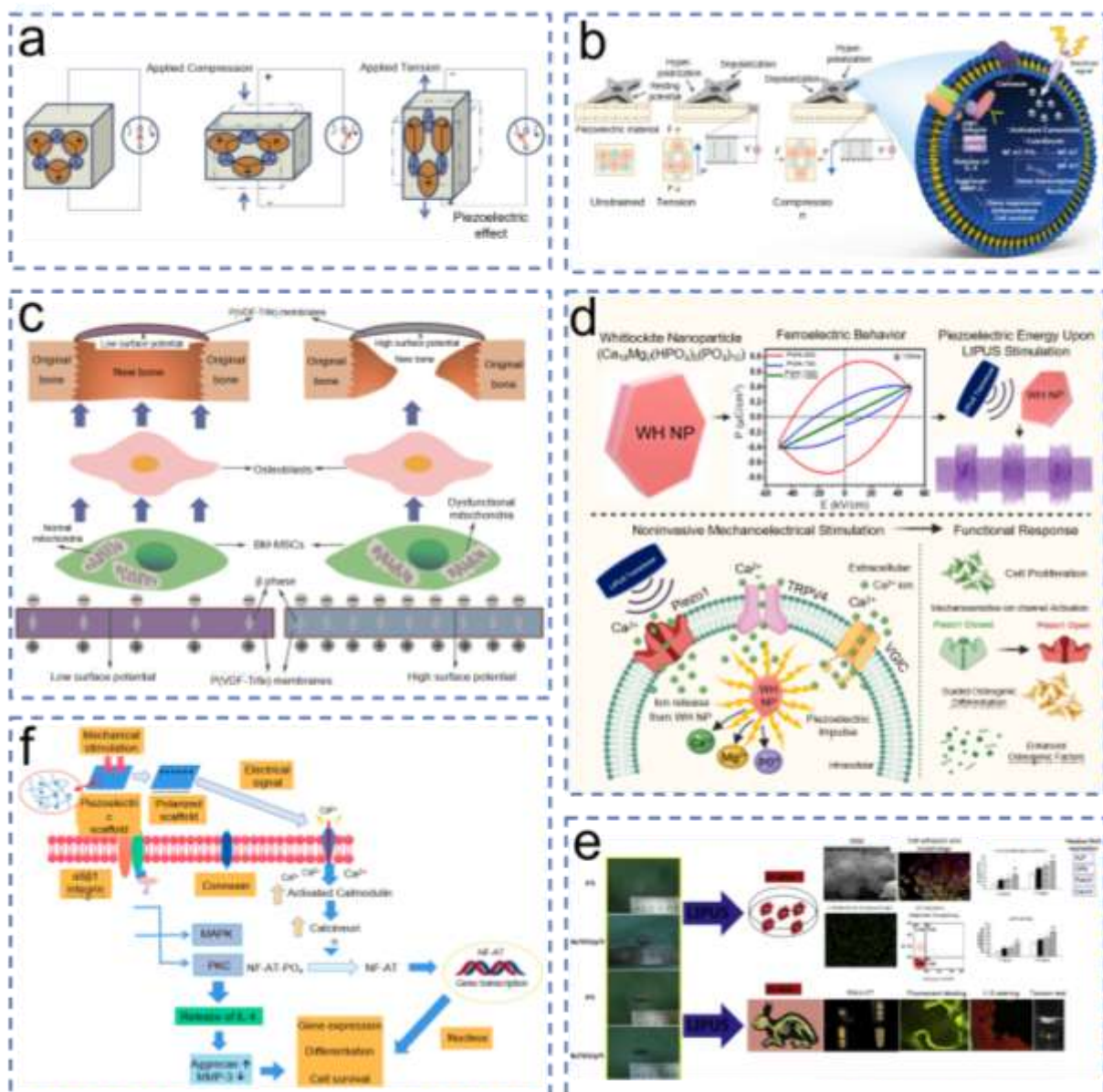


**Figure 6.** Piezoelectric materials for in situ osteogenesis. (a) Schematic diagram of the piezoelectricity phenomenon. Reproduced with permission.<sup>[141b]</sup> Copyright 2018, Elsevier Ltd. (b) Illustration of mechanical strain induced electric charge generation on piezoelectric material surface triggering cell signaling pathways. Reproduced with permission.<sup>[142b]</sup> Copyright 2020, Wiley Ltd. (c) Scheme showing different surface potentials created by P(VDF-TrFE) membranes with different  $\beta$  phase contents for bone regeneration. When the P(VDF-TrFE) membranes were implanted to cover the bone defects, the lower surface potential P(VDF-TrFE) membranes provided the optimal electrical stimulation, activating the mitochondria in the MSCs and inducing them to differentiate the cells into osteoblasts. Reproduced with permission.<sup>[149]</sup> Copyright 2018, Wiley Ltd. (d) Schematic illustration of LIPUS-mediated electric field produced by the piezoelectric WH NPs promoting osteoblast

proliferation and differentiation. Reproduced with permission.<sup>[168]</sup> Copyright 2021, Elsevier Ltd. (e) Illustration of BT coating on bone promoting repair in rabbit bone defect with the assistance of LIPUS. Reproduced with permission.<sup>[170]</sup> Copyright 2020, Elsevier Ltd. (f) Schematic diagram of Ca<sup>2+</sup> signal transduction pathway and other miscellaneous pathways activated in response to the electrical and mechanical stimulation. Reproduced with permission.<sup>[172]</sup> Copyright 2022, Frontiers Media S. A. Ltd.

## 4.2 Conductive materials

Carbon-based biomaterials, metal oxides, and conductive polymers are the three typical types of conductive biomaterials. The most recently investigated conductive bone repair materials are carbon-based materials and conductive polymers (**Figure 7a**).<sup>[140]</sup> Under external electrical fields, conductive materials can generate in situ electrical cues, following to regulate cell fate and bone regeneration.

### 4.2.1 Carbon-based biomaterials

Highly conductive and easy-processing carbon-based materials are outstanding candidates for conductive nanocomposite preparation and have been widely applied as additives to improve the mechanical properties and electrical conductivity in BTE.<sup>[175]</sup> The most frequently utilized carbon-based materials in tissue regeneration engineering are graphene-based materials and carbon nanotubes (CNTs) because of their superior mechanical properties, chemical stability, electrical conductivity, and big surface area.<sup>[176]</sup> Especially, to produce an environment that supports bone regeneration, some researchers have combined the strong electrical conductivity of graphene with the bone conductivity of ceramic materials, such as BG<sup>[177]</sup> and HAp.<sup>[178]</sup> Moreover, due to their antibacterial properties, graphene-based materials have demonstrated more practical utility as electroactive biomaterials for tissue implantation.<sup>[179]</sup> The PLGA/GO conductive composite accelerated neovascularization and formation of Col1 *in vitro* when coupled with electrical stimulation (**Figure 7b**).<sup>[180]</sup> Externally applied electrical stimulation (1 V/cm with a current density of approximately 300  $\mu\text{A}/\text{cm}^2$ ) augmented ADSC proliferation and osteogenic differentiation when cultured on a conductive graphene-cellulose scaffold (**Figure 7c**).<sup>[181]</sup> Furthermore, when implanted *in vivo*, the electro-active PCL/graphene scaffolds were able to mediate in situ electrical cues, accelerate bone regeneration and the formation of more organized new bone through a fast angiogenesis and a rapid transition to the mineralization.<sup>[182]</sup>

Moreover, when used in a scaffold, the other type of carbon-based materials, namely CNTs, resulted in appealing materials with excellent electrical conductivity and acceptable biocompatibility, once dispersed throughout the composite network, eliciting bone formation.<sup>[183]</sup> For example, a CNT-based conductive layer enabled the modulation of cell behavior through *in situ* electrical stimulation, leading to cellular proliferation and osteogenic gene marker expression (**Figure 7d**).<sup>[184]</sup> Nevertheless, the problem is that some of CNTs are cytotoxic and can induce inflammatory responses.<sup>[185]</sup> To overcome the aforementioned adverse effects, polyacrylonitrile was employed as a precursor polymer, synthesized as electrospun nanofibers, and subjected to a specific regime of heat treatment, resulting in carbon nanofibers (CNFs).<sup>[186]</sup> Electrospun CNFs are currently replacing CNTs as a viable substitute due to their similar mechanical and electrical properties, superior biocompatibility, and chemical inertness. Meanwhile, under electrical stimulation, the CNFs present increased osteoblast proliferation and ALP activity *in vitro*.<sup>[187]</sup>

#### 4.2.2 Conductive polymers

Conductive polymers, mainly including PPy, PANi, and PEDOT, are also appealing material candidates for the fabrication of conductive scaffolds.<sup>[188]</sup> In addition to high conductivity similar to those of metals and inorganic semiconductor materials, this type of polymer also benefits from superior biocompatibility and simplicity in the synthesis.<sup>[138a, 142b, 189]</sup> Thus, several reports have mentioned the use of these systems in bone regeneration in conjunction with external electrical stimulation.<sup>[190]</sup> It was reported that PANi coating,<sup>[190a]</sup> PPy coating,<sup>[191]</sup> and PEDOT coating<sup>[192]</sup> all facilitated the proliferation and differentiation of MC3T3 and mineralization *in vitro* under electrical stimulation. Additionally, conductive polymers have the potential to modulate and remove reactive oxygen species (ROS), which poses pernicious impacts on cell metabolism and fates in bone repair.<sup>[193]</sup> Despite the above data suggesting that conductive polymers are effective in promoting osteogenesis, there are currently not many *in vivo* evaluations of conductive polymers for promoting bone regeneration. Challenges remain in the development of these polymers due to their manufacturing limitation (e.g., some of them cannot be melted), potential toxicity, and poor solubility in solvents.<sup>[194]</sup> From this viewpoint, biodegradable composites containing conductive polymers or biodegradable copolymers containing conductive oligomers may be considered for future *in vivo* studies.

#### 4.2.3 Mechanism of conductive materials

External electrostimulation is reported to influence the potential of cell membranes as well as membrane receptors, ion channels, gap junctions, etc.<sup>[140]</sup> When electrical stimulation is applied, a conductive polymer activates the  $\text{Ca}^{2+}$  channel of the cell membrane, thus facilitating extracellular  $\text{Ca}^{2+}$  entry into cells and subsequently stimulating the  $\text{Ca}^{2+}$  signal transduction pathway, upregulating related gene expression and promoting osteogenesis differentiation.<sup>[195]</sup> This process is the same as the previously described downstream pathway following the increase in intracellular calcium concentration caused by piezoelectric materials. Conductive materials have been also reported to promote calcium deposition, contributing to the formation of the bone matrix.<sup>[193]</sup> Several pathways (**Figure 7e**) have the potential of regulating cell activity and differentiation,<sup>[140]</sup> including intracellular  $\text{Ca}^{2+}$  signaling, membrane receptors, and integrins. For  $\text{Ca}^{2+}$  signaling, on one hand, electrical stimulation activates voltage-gated  $\text{Ca}^{2+}$  channels to allow extracellular  $\text{Ca}^{2+}$  to flow into the cell, and on the other hand, causes the release of intracellular  $\text{Ca}^{2+}$  reservoirs. These two conditions cause a  $\text{Ca}^{2+}$  transient that activates the cytoskeletal calmodulin, promoting cell differentiation and proliferation.<sup>[142b, 164, 196]</sup> Meanwhile, electrical stimulation can influence the distribution, expression, or conformation of transmembrane proteins, influencing relevant intracellular signaling pathways in cell migration or differentiation via ligand-receptor binding.<sup>[197]</sup> Integrins are also sensitive to the changes in the ECM altered by electrical stimulation, including changes in protein structures and charges.<sup>[198]</sup> Furthermore, the electrical stimulation can control ROS generation at the physiological level, triggering pathways associated with osteogenic differentiation.<sup>[149]</sup> In addition, electrical stimulation can regulate cell behavior by accelerating the depletion of intracellular ATP.<sup>[199]</sup> In this case, the original electrical stimulus is converted into a biochemical stimulus that activates downstream signaling pathways related to cell proliferation and differentiation, such as MAPK, ERK1/2, and JNK pathways.<sup>[140]</sup>

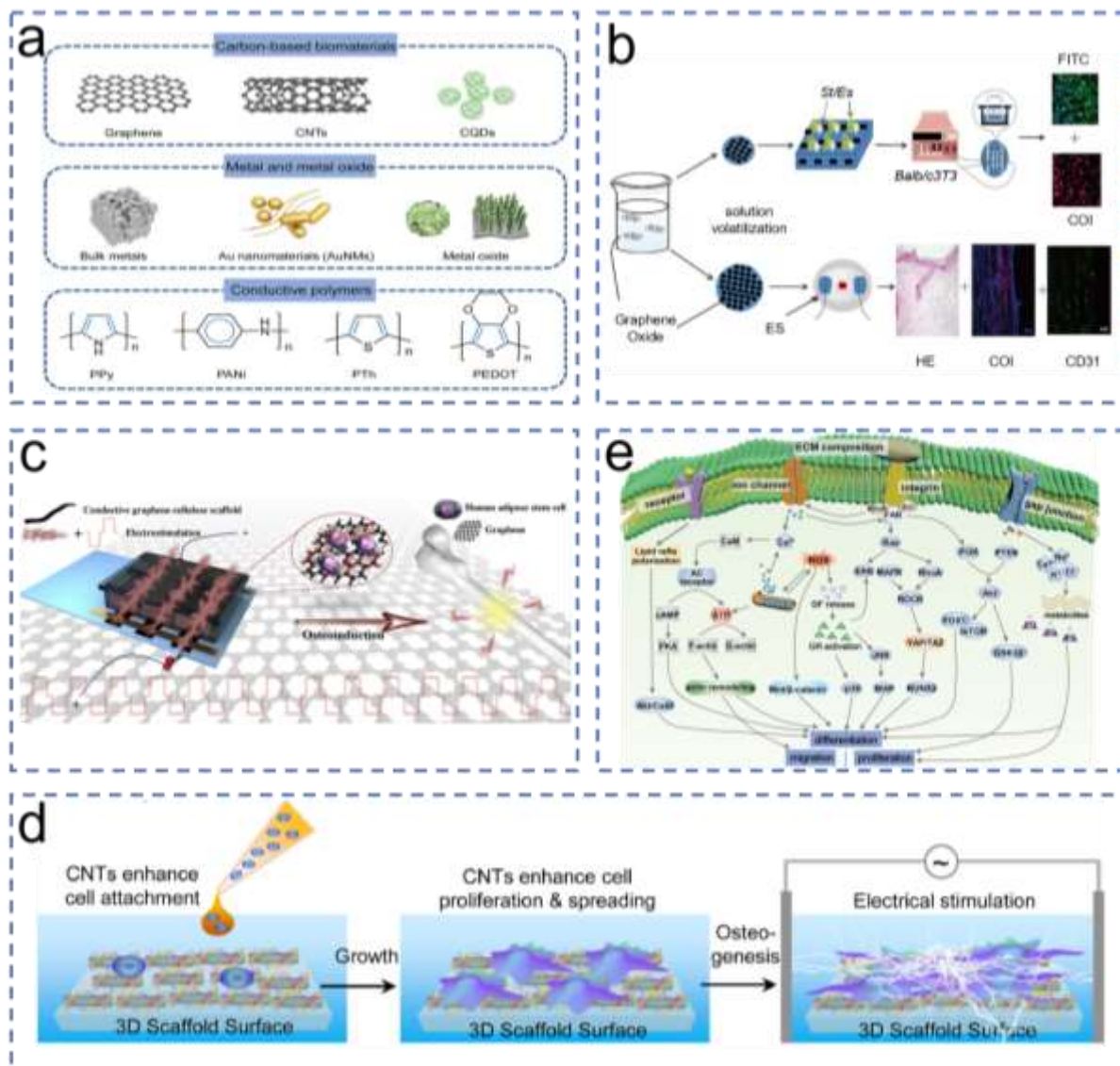


**Figure 7.** Conductive material-related osteogenesis. (a) Typical conductive biomaterials used for tissue engineering. Reproduced with permission.<sup>[140]</sup> Copyright 2021, Wiley Ltd. (b) Schematic plot of the preparation of PLGA/GO composite and its application for wound treatment. Reproduced with permission.<sup>[180]</sup> Copyright 2019, Dove Medical Press Ltd. (c) Schematic diagram illustrating the effect of the combination of an electroactive graphene-cellulose scaffold and an external electrical stimulation on osteoinduction of human ADSCs. Reproduced with permission.<sup>[181]</sup> Copyright 2020, Elsevier Ltd. (d) Schematic presentation showing enhanced cell proliferation and osteogenesis under electrical stimulation in the presence of a CNT-based conductive layer. Reproduced with permission.<sup>[184]</sup> Copyright 2020, Elsevier Ltd. (e) Schematic illustration of the pathways involved in the biological response to electrostimulation. Reproduced with permission.<sup>[140]</sup> Copyright 2021, Wiley Ltd.

## 5. Impact of magnetic signals

The magnetic field has been proven to enhance bone tissue repair by affecting cell metabolic behavior.<sup>[200]</sup> Different magnetic field strengths have various effects on cells, while medium-strength magnetic fields are the most widely used, promoting attachment, proliferation, migration, and differentiation of cells.<sup>[201]</sup> Furthermore, increasing evidence has indicated the potential of in situ magnetic strategies mediated by magnetic materials for bone regeneration.<sup>[202]</sup> Magnetic materials with external SMF significantly increased the expression of diverse osteogenic markers and the deposition of the mineralized matrix, as well as an enhancement in the CD31<sup>+</sup> cell population, suggesting that, besides boosting osteogenesis, they also favored angiogenesis both of which are important moments in bone regeneration.<sup>[203]</sup>

### 5.1 Magnetic materials

Magnetic materials with magnetic elements like iron, cobalt, manganese, and nickel demonstrated excellent potential for tissue regeneration engineering.<sup>[204]</sup> Iron oxide NPs (IONPs), which have prominent advantages like superparamagnetism, nontoxicity, large surface area, high surface-to-volume ratio, and rapid and easy methodology of target separation from solution exploiting the external magnetic field attraction, are the most widely used among various magnetic NPs in magnetic cue to promote bone formation, drug loading, bone formation with stem cells, and bone formation with scaffolds.<sup>[201, 205]</sup> The most common forms of IONPs are present in nature: magnetite ( $\text{Fe}_3\text{O}_4$ ), maghemite ( $\gamma\text{-Fe}_2\text{O}_3$ ), and hematite ( $\alpha\text{-Fe}_2\text{O}_3$ ).<sup>[206]</sup>

There are several available studies concerning the use of IONPs alone. For example,  $\text{Fe}_3\text{O}_4$  was demonstrated to increase the osteogenic differentiation of MC3T3 osteoblasts significantly when exposed to a magnetic field.<sup>[207]</sup> Besides, many researchers have combined magnetic nanoparticles with other desirable scaffolds to create nanocomposites with comprehensive properties for biomedical applications. Preparation methods that have been extensively studied include selective laser sintering,<sup>[208]</sup> grafting, layer-by-layer assembly in combination with electrospinning techniques,<sup>[209]</sup> and co-deposition.<sup>[210]</sup> It was reported that  $\text{Fe}_3\text{O}_4$  NPs embedded within the scaffold would be magnetized by an SMF via their dipole moment rearrangement, which generates a locally enhanced magnetic field.<sup>[209, 211]</sup> The enhanced magnetic field provided direct magnetic stimulation (55-65 mT) to human umbilical cord-derived MSCs grown on a scaffold containing  $\text{Fe}_3\text{O}_4$  NPs, subsequently promoting

osteogenic differentiation.<sup>[208]</sup> Magnetic PLGA/PCL scaffolds manufactured using an electrospinning technique and a layer-by-layer assembly of superparamagnetic IONPs significantly promoted the osteogenesis of ADSCs.<sup>[209]</sup> Moreover, a superparamagnetic Col I hydrogel, obtained by grafting  $\alpha$ - $\text{Fe}_2\text{O}_3/\gamma\text{-Fe}_2\text{O}_3$  NPs on collagen nanofibers, induced the M $\phi$  phenotype transition from M1 to M2, subsequently promoting osteogenic differentiation of BMSCs *in vitro*, which reminded us of a novel strategy utilizing biomaterial-mediated in situ magnetic stimulation to generate an immune microenvironment favorable to bone regeneration (**Figure 8a**).<sup>[212]</sup>

Furthermore, IONPs implanted *in vivo* could convert the applied external magnetic field stimulation into a local magnetic field, which in turn promoted bone regeneration. To illustrate, a study has shown that an implanted porous PGA/ $\text{Fe}_3\text{O}_4$  scaffold into rabbit forearmed radius defect, meanwhile, an external SMF was used to provide a magnetic source. In this case, the magnetic moment of the  $\text{Fe}_3\text{O}_4$  NPs oriented along the direction of the SMF (1.2-70 mT), thereby generating an in situ enhanced magnetic field. It is clear that the integration of the scaffold and the SMF further synergistically accelerated bone regeneration (**Figure 8b**).<sup>[208]</sup> Similarly, a magnetic  $\text{Fe}_3\text{O}_4$ /polydopamine(PDA) coating improved in situ osteogenesis of 3D-printed porous Ti scaffolds *in vivo* under an external SMF (15 mT).<sup>[210]</sup> These above findings suggest that the combined application of external (SMF) and internal (scaffold) magnetism can be a promising tool to precisely regulate in situ bone regeneration.

Besides IONPs,  $\text{CoFe}_2\text{O}_4$  (CFO), is the other popular ferrite material exploited for a variety of applications due to its strong intrinsic magnetocrystalline anisotropy, excellent mechanical toughness, and mild magnetic saturation.<sup>[213]</sup> In another aspect, the high magnetostrictiveness of CFO particles enables them to change form or size once they are magnetized.<sup>[214]</sup> These changes are beneficial in achieving the desired magnetomechanical/electrical response of the scaffold and CFO was thus incorporated into the matrix of piezoelectric polymers.<sup>[215]</sup> CFO/P(VDF-TrFE) coatings containing CFO with a mass fraction of 6% improved osteogenic differentiation of MC3T3-E1 cells under an SMF condition.<sup>[216]</sup> Moreover, a type of magnetoactive 3D porous scaffold comprised of PVDF and CFO was found to exert both local magnetomechanical and magnetoelectric response, thereby significantly promoting the proliferation of preosteoblasts through the application of magnetic stimuli.<sup>[215b]</sup> Furthermore, applied together with a remote direct current (DC) magnetic field, CFO/P(VDF-TrFE) magnetoelectric membranes containing 10 wt% CFO can generate a built-in magnetoelectric microenvironment for precisely controlling bone regeneration in situ. The magnetoelectric

microenvironment provided by the membranes not only directly enhanced the osteogenic differentiation of BMSCs but also triggered an initial inflammation and subsequently promoted the M1 to M2 transition of M $\phi$ s to improve bone regeneration (**Figure 8c**).<sup>[215c]</sup>

The strategy of in situ bone formation through localized magnetic fields mediated by magnetically responsive materials has proven promising, but the safety of nanoparticles applied in vivo and the lack of effective magnetic field gradient are the main challenges limiting their clinical translation. Specifically, prolonged retention of magnetic nanoparticles in rats induced severe toxicity, leading to weight loss and damage to the liver and spleen, the interaction between the surface charge of the particles and biocomponents greatly influence their toxic response besides. Based on this, toxic reactions can be effectively minimized by reducing the particle diameter, designing a suitable surface coating, reducing the amount used, and avoiding aggregation. Therefore, when using magnetic nanoparticles, it is crucial to understand their physical properties. In addition to the magnetic material itself, the magnetic controllers in most studies are permanent magnets placed near the target site, but most commercially available magnets currently only penetrate a few millimeters of tissue depth. The development of novel magnetic control systems and the synthesis of magnetic nanoparticles with high magnetic moments may solve this problem.<sup>[204b, 217]</sup>

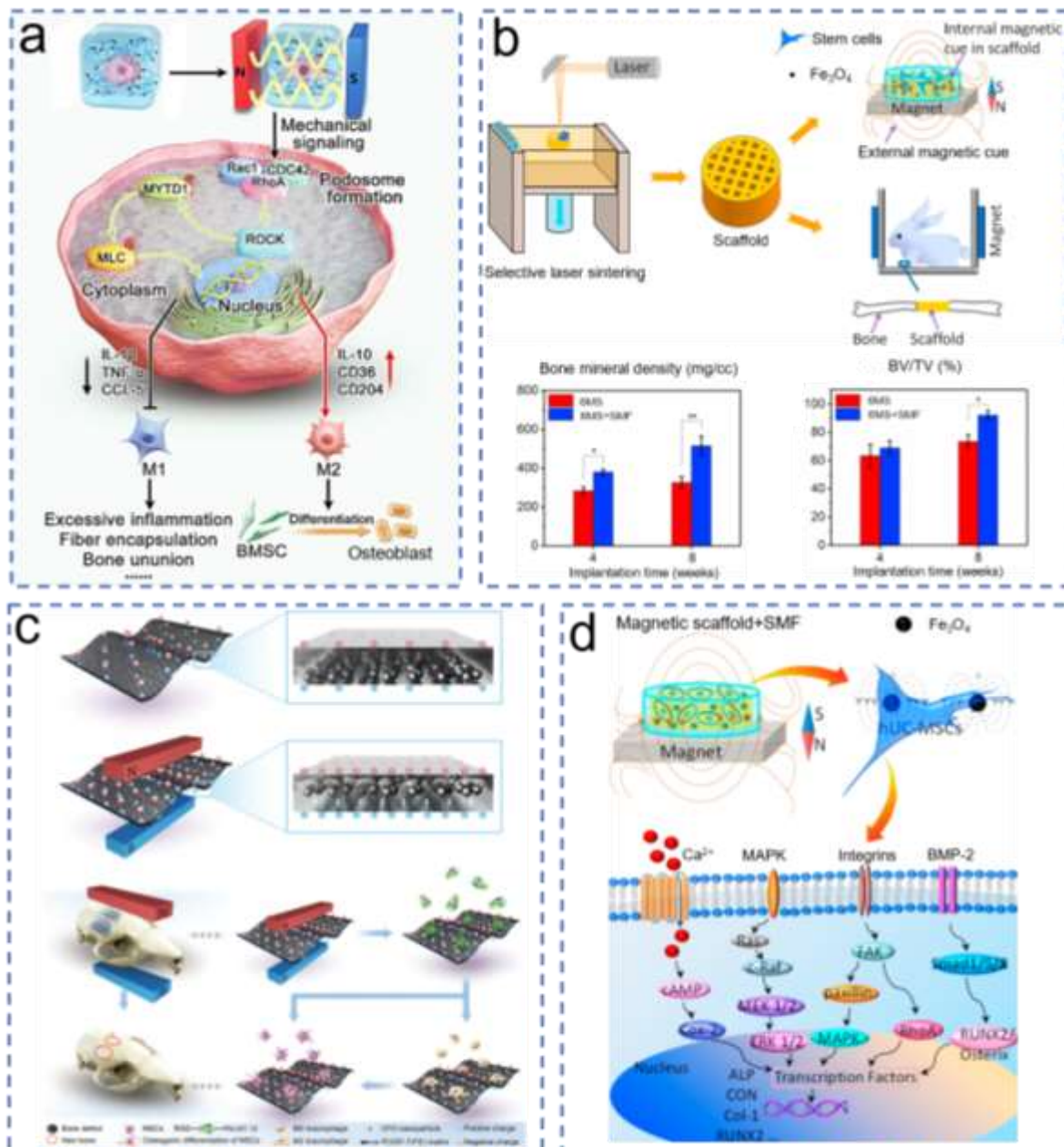


**Figure 8.** Magnetic materials-mediated in situ stimulus for osteogenesis. (a) Schematic illustration of magnetized nanocomposite hydrogels for on-demand immunomodulation via temporally controlled Mφ phenotypic transition in response to a magnetic field. Reproduced with permission.<sup>[212]</sup> Copyright 2022, Wiley Ltd. (b) Schematic diagram of the osteogenic effect of a scaffold integrated with SMF *in vivo*. Reproduced with permission.<sup>[208]</sup> Copyright 2020, Elsevier Ltd. (c) Illustration of magnetolectric effect and biological effect of CFO/P(VDF-TrFE) magnetolectric membrane. Reproduced with permission.<sup>[215c]</sup> Copyright 2020, Wiley Ltd. (d) Schematic illustration of the integration of magnetic scaffold and SMF in promoting osteogenic differentiation. Reproduced with permission.<sup>[208]</sup> Copyright 2020, Elsevier Ltd.

## 5.2 Mechanisms of magnetic signals

The mechanisms of magnetic NPs and scaffolds under external magnetic fields that improve bone regeneration remain unidentified yet. As shown in **Figure 8d**,<sup>[208]</sup> several signaling pathways, including integrin, MAPK, BMP, and nuclear factor-kappa B (NF- $\kappa$ B), may be activated during the process.<sup>[201]</sup> It was reported that integrins, the major molecular force transducers, mediated the mechanotransduction process of magnetic nanoparticles and SMF.<sup>[207a]</sup> RhoA/Rho-associated kinase (Rho-kinase/ROCK) and MAPK signaling pathways, which are downstream of integrins, are subsequently activated, facilitating osteogenic differentiation.<sup>[218]</sup> Meanwhile,  $\alpha$ -Fe<sub>2</sub>O<sub>3</sub>/ $\gamma$ -Fe<sub>2</sub>O<sub>3</sub> are not only able to enhance the osteogenic activities of stem cells through activating integrin alpha-3 (INT $\alpha$ -3)<sup>[207a]</sup> but also by upregulating WNT/ $\beta$ -catenin signaling.<sup>[219]</sup> Moreover, the BMP-2/Smad/RUNX2 pathway was observed to be activated within BMSCs upon magnetic stimulation, as evidenced by the higher expression of its components.<sup>[200a]</sup> The downstream transcription factors of these signaling pathways are then altered, increasing the expression of the genes for osteogenic differentiation-related genes, such as ALP, OCN, Coll, and RUNX2.<sup>[208]</sup>

## 6. Impact of light

Non-invasive light stimulation is one of the most common external stimuli with promising application aspects.<sup>[220]</sup> Three subcategories of light are frequently used in photoresponsive therapies: 1) ultraviolet (UV) (200-400 nm), 2) visible (Vis) (400-700 nm), and 3) near-infrared (NIR) (700-1300 nm) lights, which have different effects on controlling stem cell differentiation fate.<sup>[220a, 220b, 221]</sup> In terms of osteogenic differentiation, Vis light has been demonstrated with great potential. An obvious increase of ALP and OCN expression in rat BMSCs was observed with multiple exposures of red light emitting (630 nm) at 15 mW/cm<sup>2</sup> and 4 J/cm<sup>2</sup>.<sup>[222]</sup> Compared to red light, the osteogenic differentiation of amniotic fluid-derived stem cells (AFSCs) was facilitated more significantly by green (525 nm) and blue light (470 nm) irradiation.<sup>[220c]</sup>

Nevertheless, visible light clinical applications are constrained by its lack of penetrating depth and worse adverse effects on tissues when compared to NIR light. Thus researchers have paid great attention to the in situ conversion of NIR into Vis light to provide localized visual stimulation of stem

cells.<sup>[223]</sup> A typical case is that lanthanide-doped upconversion nanoparticles (UCNPs) have been demonstrated to possess the capacity to convert NIR light into high-energy UV, Vis, or NIR (shorter wavelength) light.<sup>[224]</sup> Furthermore, a new way to modulate the multidirectional differentiation of MSCs by using a NIR-based upconversion substrate was conceived. **Figure 9a** illustrates the substrate (named UCNP/P1/P2-RGD) made of UCNPs, 4-(hydroxymethyl)-3-nitrobenzoic acid (ONA, a commonly employed photo-cleavage molecule) modified poly(ethylene glycol) (PEG) (abbreviated as P1) and RGD-modified PEG (abbreviated as P2). The RGD moieties of P2 on UCNP/P1/P2-RGD can capture MSCs, while the PEG moieties of P1 can block the interaction between MSCs and the substrate. Upon NIR irradiation, P1 is released from the substrate by photocleavage, with the level of NIR irradiation controlling the percentage of P1 detachment and subsequently change in cell–matrix interactions. Interestingly, it was found that MSCs differentiated into adipose tissues when exposed to low-power ( $0.5 \text{ W/cm}^2$ ) NIR light irradiation, whereas they differentiated into osteoblasts when exposed to high-power ( $6 \text{ W/cm}^2$ ) NIR light irradiation.<sup>[225]</sup> Moreover, NIR-controllable nanomaterials were utilized for regulating stem cell differentiation by controlling intracellular calcium, both *in vitro* and *in vivo*. For example, thulium (Tm)- and ytterbium (Yb)-doped  $\text{NaYF}_4$  (Y=Yb or Tm) upconversion nanotransducer-based nanocomplexes were found to promote MSC differentiation into osteoblasts through increasing intracellular calcium levels when converting light from NIR to UV (**Figure 9b**).<sup>[226]</sup>

In general, there are relatively few studies on the promotion of *in situ* bone regeneration by light cue alone. Even though light stimulation can control the osteogenic differentiation of stem cells, there are still certain issues associated with its repeated use. For example, Vis and UV light penetration is limited, and the process of light penetration may damage the tissues around the target. Meanwhile, the strategy of converting NIR to Vis or UV light faces the problems of low conversion efficiency and non-degradability of NPs.<sup>[223]</sup> Solving these problems will be of great significance to expand the applications of *in situ* light stimulation in BTE.

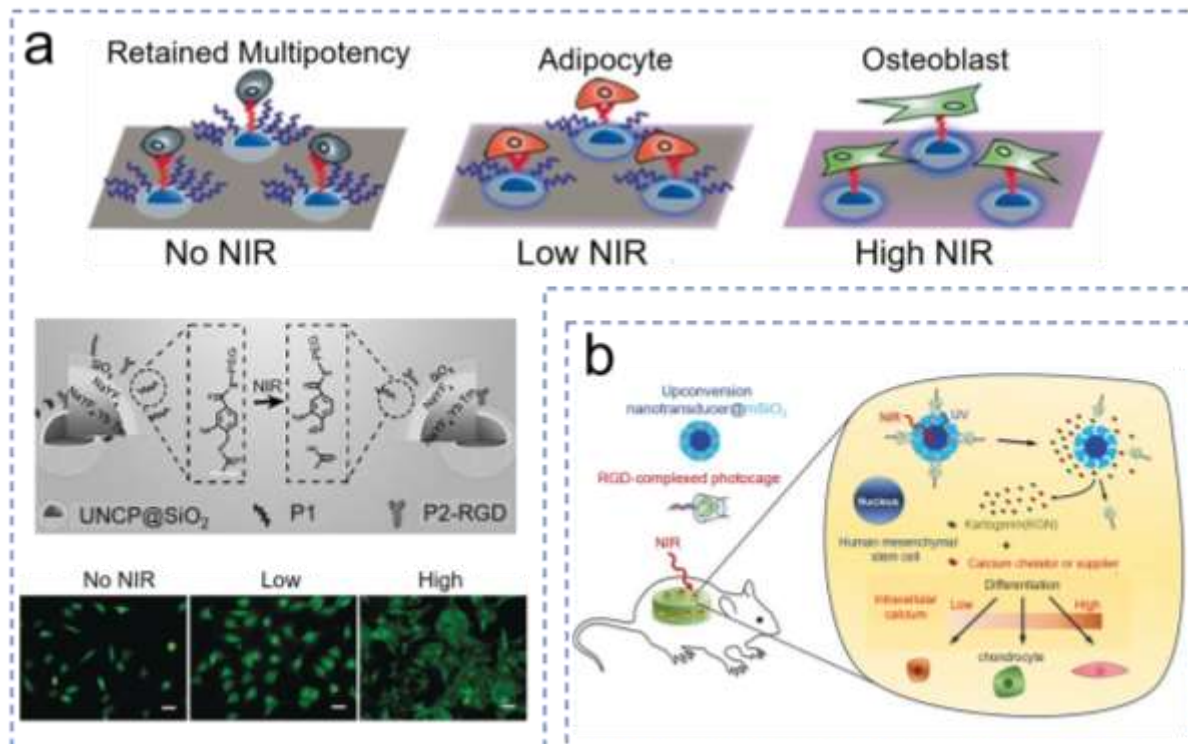


**Figure 9.** The light stimulus for osteogenesis promotion. (a) Schematic illustration of modulating cell-matrix interactions and fate commitment of MSCs by using a UCNP-based substrate; Representative fluorescence microscopy images of cells cultured on UCNP/P1/P2-RGD with exposure to no NIR, low-power NIR, or high-power NIR irradiation; Reproduced with permission.<sup>[225]</sup> Copyright 2018, Wiley Ltd. (b) Schematic representation of NIR-triggered differentiation of hMSCs after subcutaneous implantation *in vivo*. Reproduced with permission.<sup>[226]</sup> Copyright 2018, Wiley Ltd.

## 7. Impact of heat

Heat is an indispensable stimulus in the bone-repair process, boosting osteogenesis and mineralization. An early study reported that following initial surgical trauma, rabbit femur hyperthermia through 915 MHz microwave heating enhanced the formation of new bone trabeculae and an increase in cortical bone density, thereby accelerating bone remodeling.<sup>[227]</sup> Previous studies have shown that heat stimulation produced by an external heater (e.g., 2-4 °C higher than body temperature) massively increased osteogenic activity, such as ALP expression and mineralization in MSCs.<sup>[228]</sup> Mild heating (e.g., to 40-43 °C) facilitated the healing of bone defects<sup>[229]</sup> and when the osteogenesis temperature of hyperthermia was controlled at about 42 °C, osteogenesis activity resulted in the highest.<sup>[230]</sup> Moreover, the efficiency of differentiation was influenced by the heating frequency, which was shown

to work best when applied twice a day.<sup>[228a]</sup> The effect was mainly achieved by upregulating the heat shock proteins (HSP) in MSCs, enhancing blood flow, and promoting nutrient exchange.<sup>[231]</sup> As proof, periodic heat significantly upregulated both HSP70 and HSP27 in differentiated MC3T3-E1 cells.<sup>[228a]</sup>

According to previous studies, moderate thermal therapy can effectively promote bone regeneration. Nevertheless, the strategies based on direct heating are less efficient in stimulating osteogenesis, particularly when the lesion is deep. Therefore, to induce temperature enhancement in deep tissues, externally non-invasive stimuli have gained popularity and have been applied recently for tissue engineering. By combining with the specific agents or nanoparticles, mild photothermal therapy (PTT) and magnetic thermotherapy (MTT) have shown new interests because of their easy regulation and precise thermal positioning.<sup>[232]</sup> In this section, we will briefly describe the applications of these therapies in promoting in situ bone regeneration.

### 7.1 Photothermal therapy

In PTT, converting light energy into heat, photothermal agents (PTAs) are generally irradiated by light at the target tissue to increase the local temperature. PTT has gained importance among externally non-invasive thermal therapeutic strategies in BTE due to the benefits of great selectivity and non-invasiveness. PTT is commonly carried out by applying tissue transparent NIR light in the area where PTAs are present to produce an in situ thermal effect.<sup>[232a, 233]</sup> Therefore, when the PTAs at the damage site photothermally respond to external NIR light, mild hyperthermia therapy, enhancing bone regeneration, can be easily achieved. Recent studies have shown that gentle photothermal radiation can promote MSC differentiation, osteoblast maturation, and mineralization (**Figure 10a**).<sup>[229, 234]</sup> Consequently, PTT has received growing attention in BTE as a relatively gentle and targeted treatment.<sup>[233c]</sup> PTAs that have been applied in tissue engineering include carbon-based PTAs (such as graphene), metal-based PTAs (such as gold nanoparticles), and other types of PTAs.<sup>[235]</sup> Among them, graphene and GO are commonly used due to their great NIR light absorbance and strong photothermal conversion efficiency.<sup>[233c, 236]</sup> Scaffolds incorporating graphene and GO, including nHAp/GO scaffold (**Figure 10b**)<sup>[237]</sup> and HAp/GO/CS scaffold (**Figure 10c**),<sup>[233c]</sup> can not only promote osteogenesis of BMSCs *in vitro* but also show excellent photothermal properties *in vivo*, thus significantly supporting bone regeneration. Additionally, other carbon-based PTAs, including carbon dots (CDs), CNTs, and carbon aerogel also showed promising potential in BTE.<sup>[238]</sup>

Moreover, metal-based PTAs comprised of metal NPs, metal-oxide NPs, and metal compounds showed excellent photothermal conversion efficiency as well. After being internalized by cells, hyperthermia porous AuPd alloy NPs (pAuPds) produced a mild localized heat (e.g., 40-43 °C) under NIR light irradiation, greatly accelerating cell proliferation and bone regeneration. Almost 97% of the cranial defect area was covered into the newly formed bone after 6 weeks of PTT (**Figure 10d**).<sup>[239]</sup> Apart from metal oxides, other metal compounds such as MoS<sub>2</sub> possess photothermal effects and corresponding applications in bone biomaterials.<sup>[233b, 240]</sup>

In the last years, black phosphorus (BPs) is considered a superior PTA as it can naturally decompose into the nontoxic PO<sub>4</sub><sup>3-</sup>, which serves as an essential bone component.<sup>[241]</sup> Thus based on the above unique superiority, BPs@PLGA osteoimplants were fabricated and showed a moderate but effective heat-induced osteogenesis impact *in vivo* when exposed to NIR light, reaching a depth of 7 mm into the biological tissue.<sup>[231]</sup> Recently, a fish-derived scaffold consisting of GelMA and BP nanosheets, not only accelerated the proliferation and osteogenesis of MSCs, but also reduced the inflammation process due to the low immunogenicity. Furthermore, BP nanosheets contributed to photothermal conversion, which enabled the NIR photothermal therapy, further facilitating osteogenesis and bone regeneration (**Figure 10e**).<sup>[242]</sup> However, due to their easy decomposition, the degradation speed of BP needs to be controlled when applied *in vivo*, which limits its clinical translation.<sup>[243]</sup>

Furthermore, it is worth highlighting that a core-shell structural nanorod-like array with HAp as a core and PDA as an amorphous shell (PDA@HAp) was found to achieve periodic PTT at a mild temperature (41±1 °C), further accelerating the transition of MΦ adhered to PDA@HAp from M1 to M2 phenotype both *in vitro* and *in vivo* (**Figure 10f**).<sup>[244]</sup> This behavior suggests us a method of employing mildly periodic PTT to induce a favorable immunomodulatory microenvironment for osteogenesis.

Nonetheless, most of these studies focused on the first NIR window (NIR-I, 700-950 nm), it would be preferable to develop PTT agents spanning the second NIR window (NIR-II, 1000-1350 nm) to maximize the photothermal effects for effective bone regeneration in deep tissues.<sup>[245]</sup> As an example, CDWS<sub>2</sub> complexes were fabricated to achieve photothermal conversion at 1064 nm and showed 56.3% efficiency, thus greatly enhancing bone regeneration.<sup>[238b]</sup>



defect repair. Reproduced with permission.<sup>[237]</sup> Copyright 2022, Elsevier Ltd. (c) Schematic diagram of the fabrication of nHA/GO/CS scaffold and its osteogenesis promotion under 808-nm NIR irradiation. Reproduced with permission.<sup>[233c]</sup> Copyright 2020, Elsevier Ltd. (d) Schematic illustration of pAuPds for PTT of cranial defect reparation. Reproduced with permission.<sup>[239]</sup> Copyright 2022, American Chemical Society. (e) Illustration of the components of the fish-derived scaffold and its osteogenesis function combined with MSCs and PTT. Reproduced with permission.<sup>[246]</sup> Copyright 2023, Tsinghua Univ Press. (f) Schematic illustration showing the PTT process *in vitro* for evaluation of the phenotypic transformation of Mφs cultured on PDA@HAp (top) and the experimental process *in vivo* to evaluate the immune responses and osteogenesis modulated by the implant with NIR radiation (bottom). Reproduced with permission.<sup>[244]</sup> Copyright 2022, Wiley Ltd.

There are several hypotheses about which pathways are involved in the promotion of osteogenesis during the process of PTT. The osteogenic pathways which are activated during the photothermal effect include MAPK, PI3K-Akt,<sup>[247]</sup> BMP2/Smad,<sup>[233c]</sup> ERK,<sup>[248]</sup> and Wnt signaling pathways.<sup>[239]</sup> Moreover, a study revealed that the activation of the PI3K-Akt1 signaling pathway was responsible for the periodic PTT-induced acceleration of the M1 to M2 transition of MΦs.<sup>[244]</sup> More studies are needed in the future to elucidate the related mechanisms of photothermal therapy to improve the effect of PTA-mediated in situ thermal stimulation in promoting bone regeneration.

In conclusion, NIR light-assisted phototherapies have shown great potential to treat bone-related diseases and BTE. Numerous NIR-absorbing PTAs have been developed for PTT, but their clinical applications are hindered by several factors, including the potential for photodamage of tissues under high power excitations, the relatively shallow depth of penetration of NIR to reach deep tissues, and potential long-term toxicity.<sup>[249]</sup> Therefore, increased efforts should be made to design and synthesize more nanomaterials with both high phototherapeutic efficiency and enhanced biocompatibility. In future research, on the one hand, other controllable and non-invasive physical triggers should be explored to improve tissue penetration, and on the other hand, more accurate and sensitive real-time monitoring techniques should be developed to adjust the irradiation parameters to avoid unnecessary damage caused by overheating.

## 7.2 Magnetic thermotherapy

Similar to the action of PTT, MTT can promote tissue regeneration by magnetic field-mediated heat generation, regulating cell behavior and promoting osteogenic differentiation.<sup>[232b]</sup> In some cases, MTT showed higher tissue-penetrating capability than PTT and possessed other outstanding characteristics as well, such as non-invasiveness, remote controllability, and nano-scale spatial resolution.<sup>[250]</sup>

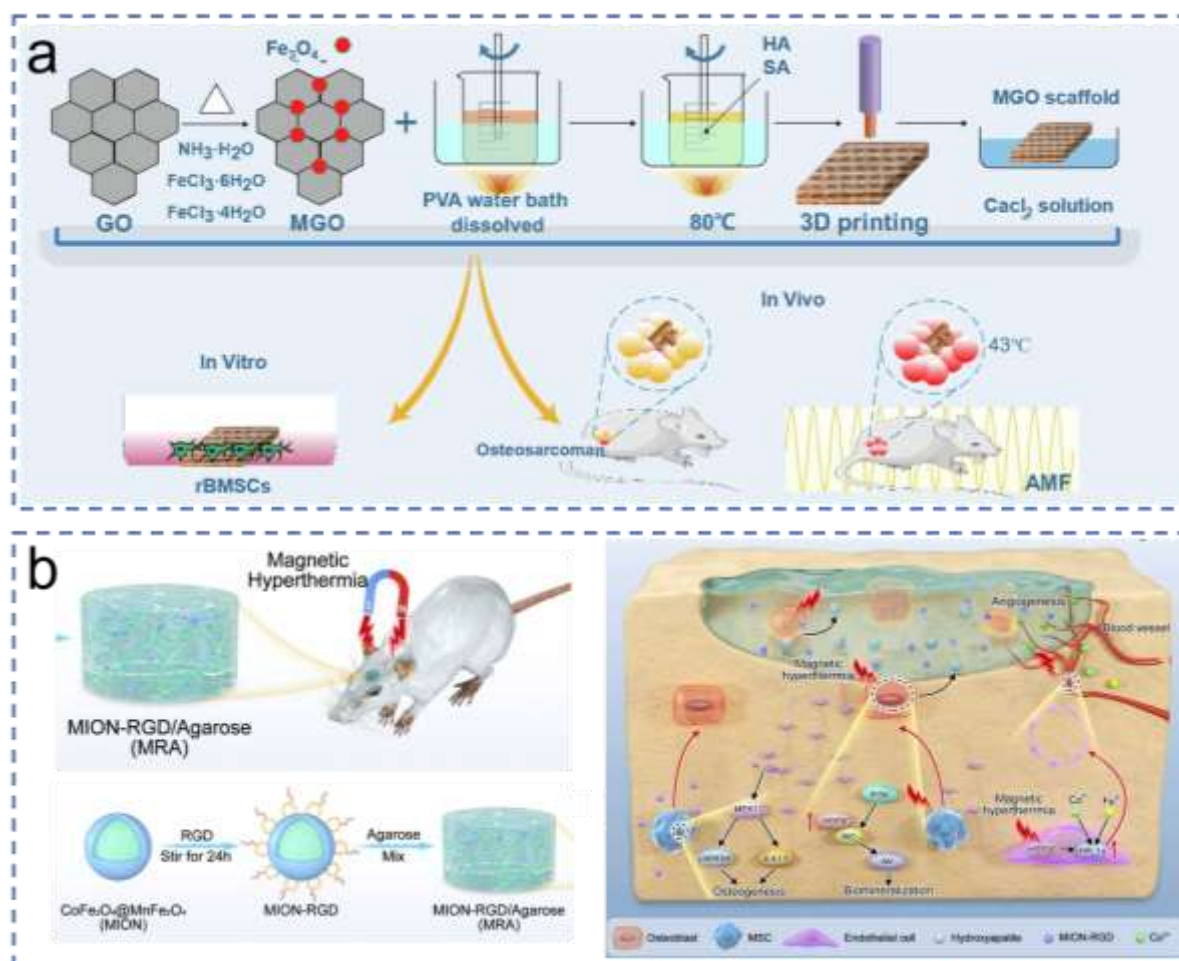


**Figure 11.** Schematic illustration of MTT applied for in situ osteogenesis. (a) Schematic diagram of MGO hydrogel composite fabrication (top) and its application to bone tumor defect regeneration *in vitro* and *in vivo* (bottom). Reproduced with permission.<sup>[232b]</sup> Copyright 2022, Elsevier Ltd. (b) Schematic diagram of the synthesis of MRA hydrogels (left), and its mechanism of osteogenesis, biomineralization, and angiogenesis in the bone defect site under mild magnetic hyperthermia (right). Reproduced with permission.<sup>[251]</sup> Copyright 2022, Elsevier Ltd.

As proof of concept, a nanocomposite hydrogel fabricated by incorporating magnetic  $\text{Fe}_3\text{O}_4$  NPs

into chitosan/PEG hydrogel achieved high temperatures under an alternative magnetic field (AMF). The elevated temperature induced by the magnetic hydrogel contributed to a higher osteogenic differentiation ability of MSCs compared with direct heat treatment applied under equal temperatures.<sup>[252]</sup> Furthermore, when implanted *in vivo*, magnetic GO (MGO)@Fe<sub>3</sub>O<sub>4</sub> NPs realized effective geomagnetic thermal conversion and supported osteogenesis remarkably (**Figure 11a**).<sup>[232b]</sup> In addition to promoting osteogenesis, a magnetothermal composite hydrogel fabricated by embedding RGD-coated, core-shell structured magnetic iron oxide NPs (CoFe<sub>2</sub>O<sub>4</sub>@MnFe<sub>2</sub>O<sub>4</sub>, MION) in the agarose (MION-RGD/Agarose, MRA) was able to generate mild magnetic hyperthermia to promote angiogenesis and biomineralization, thus accelerating the repairing of bone defects. As shown in **Figure 11b**, an alternating magnetic field with deep tissue penetration evoked a mild magnetic hyperthermia therapy (e.g., 41-42°C), significantly stimulating the osteogenic differentiation and biomineralization of pre-osteoblasts via the HSP90-activated PI3K/Akt pathway.<sup>[251]</sup>

Therefore, MTT has shown great promise for potential clinical applications due to its deep tissue penetration depth and remote controllability. However, there are still several drawbacks of MTT, such as unsatisfactory magnetothermal efficiency and potential toxicity.<sup>[235b]</sup> Currently, there are few studies on the application of MTT for BTE, and further explorations are necessary.

## 8. Multiple cues

The previous sections were concerned predominantly with the material-mediated modulation of bone regeneration by a single type of physical stimulus, whereas the introduction of multiple physical cues in biomaterials is important to improve bioactivity and osteoinductive capacity. Silk nanofibre hydrogels with anisotropic morphology and higher stiffness of 120 kPa were developed by a synergistic horseradish peroxidase-electric field crosslinking strategy. This strategy demonstrated that the structure and stiffness of the nanofibers contribute to the regulation of stem cell adhesion, aggregation, and osteogenic differentiation *in vitro* and *in vivo*.<sup>[253]</sup> Homogeneous magnetic biomaterials prepared using oleic acid-modified IONPs underwent nano deformation upon application of SMF, which in turn generated mechanical stress and stimulated mechanosensitive proteins Piezo1 thus synergistically accelerating osteogenesis in conjunction with local magnetic stimulation.<sup>[254]</sup> In addition, bone growth is closely related to electrical and magnetic signals. If dual electric stimulation

and magnetic stimulation are applied at the same time, effective and accurate induction can be achieved through the synergistic effect of electric stimulation and magnetic stimulations, which is conducive to the improvement of cell viability, bone mineralization rate, and repair. PEDOT/Fe<sub>3</sub>O<sub>4</sub>/PLGA magnetic-conductive bi-functional fibrous scaffold was demonstrated to further promote bone cell/tissue growth in response to magneto-electric dual stimulation.<sup>[255]</sup> Electromagnetic fields can only produce induced electric and magnetic fields perpendicular to each other and cannot provide induced electric and magnetic fields parallel or in any other direction. Instead, the combination of an independent electric field, magnetic field, and magnetic-conductive bi-functional scaffolds could be applied to regulate the effects of electric stimulation and magnetic stimulation to meet practical demands.

We focus in this review on the influence of physical cues mediated by materials on osteogenesis, and indeed the microenvironment of bone regeneration also includes chemical and biological factors.<sup>[256]</sup> Some works have combined physical and chemical factors, demonstrating that they can act synergistically to enhance bone regeneration. For example, the high stiffness of TG-gels and the BMP-2 loaded in a gel can act synergistically to promote osteogenesis both *in vivo* and *in vitro*,<sup>[257]</sup> and the increase of stiffness of GelMA and alendronate density was found to improve osteogenesis of MSCs synergistically.<sup>[258]</sup> In addition, combining chemical factors and intrinsic physical properties of the material, the PLGA/HAp/PLA/BMP-4 conductive scaffold released BMP-4 in a controlled manner under external electrical stimulation, and the synergistic effect of BMP-4 and the scaffold-mediated electric field facilitated cell proliferation and osteogenic differentiation.<sup>[259]</sup> Further, as we have discussed above, various physical cues are able to promote osteogenesis by different signal pathways, such as BMP/Smad and Wnt/ $\beta$ -catenin pathways,<sup>[260]</sup> which can be also activated by chemical factors, promoting osteogenic differentiation synergistically. These studies suggest that material-mediated physical signals can be combined with chemokines to achieve precise and effective bone regeneration.

## 9. Conclusion and perspectives

The three main components of BTE involve biomaterials, cells, and growth factors. Cells, particularly stem cells, have been at the forefront of the field as they can self-renew and differentiate into

functional cells for bone tissue regeneration.<sup>[261]</sup> But there are several limitations, particularly regarding controlling or manipulating the ECM microenvironments to determine cell fate. Growth factors play key roles in determining the behavior and differentiation of stem cells, bringing efficient bone repair.<sup>[7a]</sup> However, the high price, easily decomposed *in vivo*, short function period, and potential side effects of growth factors-mediated BTE restrain their clinical applications. Therefore, an alternative strategy that we have discussed in this review, replacing growth factors with materials-mediated *in situ* physical cues, is emerging in BTE. Physical signals are widely present in the human body and play crucial roles in physiologic functions. For example, myelin envelopes neuronal axons to ensure their health and rapid propagation of electrical impulses in the central nervous system.<sup>[262]</sup> Vitamin D is synthesized under sunlight to maintain the functions of human bones and teeth and protect cardiovascular and cerebrovascular tissues.<sup>[263]</sup> Therefore, physical signals with a suitable intensity not only are safe and biocompatible but also necessary to human bodies. Meanwhile, physical signals mediated by biomaterials can be conveniently regulated to match the requirements at a safe intensity. Hence, biomaterials-mediated *in situ* physical cues combining the synergistic effect of materials themselves have opened a new perspective to expand the applications of BTE.

Nevertheless, there are still deficiencies in the field of biomaterials-mediated *in situ* stimulation to promote osteogenesis. The first thing is that the efficiency of materials-mediated physical cues to promote bone regeneration is generally low compared with growth factors. The optimal parameters of each type of stimulation for bone tissue regeneration have not been determined clearly, resulting in low efficiency in promoting osteogenesis. As a result, most studies have no precise reference for determining the intensity, time, and frequency when applying external physical stimulation. Besides, the bone repair is a complex process involving a variety of physiological signals, but recently a large number of studies only have focused on transforming a single external stimulus into a biomaterials-mediated *in situ* stimulus to support bone regeneration. It is a worthy thing that some researchers have begun to combine various cues to improve the efficiency of bone regeneration, such as magnetoelectric nanocomposite membranes mediated electric and magnetic stimulation.<sup>[220a]</sup> Therefore, designing multifunctional biomaterials with the capacity to combine multiple stimulation to improve bone repair efficiency still needs much effort in the future.

In addition, there are some concerns about the degradation and biological security of biomaterials after being implanted *in vivo*. The research on the biocompatibility of most materials, especially

inorganic materials and non-degradable polymer materials *in vivo*, is still in its infancy and needs more effort. Most of the biomaterials implanted *in vivo* in the current studies, such as PDMS, are non-degradable, and maybe require a second surgery to be removed, resulting in secondary trauma. Besides, the main current biosafety assessment of materials through observing whether the structures of main viscera organs are damaged during the period after the materials are implanted *in vivo* failed to assess long-term biological safety and the influence on other body tissues. Thus, there are increasing queries about the long-term biological safety of biomaterials when applied in clinics and increased efforts should be put into designing and constructing fully biodegradable and biocompatible biomaterials in the future.

Figuring out the mechanisms by which biomaterials-mediated *in situ* physical cues promoting osteogenesis is critical for improving the performance of functional materials. Although various studies of the mechanisms of materials-mediated physical stimulation promoting osteogenic differentiation have been put forward, some of them are inconsistent and even conflicting. The studies on signaling pathways summarized in this review are based on different materials-mediated different physical stimuli under different parameters, causing confusion and difficulty to construct satisfactory signal transduction and intracellular molecular mechanisms for each physical stimulation. Besides, almost all studies have focused on conventional pathways during the process of osteogenesis, such as the Wnt signaling pathway,<sup>[48, 219, 239, 264]</sup> and the mechanism of how the process is triggered deserves more attention.

Besides osteogenesis, immune response and angiogenesis show great power to promote bone regeneration.<sup>[265]</sup> Unfortunately, there is almost no research on the synergistic effect of materials-mediated *in situ* physical cues on angiogenesis, osteogenesis, and immunoregulation. Moreover, the immune microenvironment plays a crucial role in bone tissue regeneration. Tissue regeneration generally begins with early immune-inflammatory responses, thus triggering the boosting of immune cells and secretion of inflammatory cytokines and chemokines, which subsequently mobilize and recruit immune cells to injured sites.<sup>[266]</sup> A variety of immune cells including Mφs, natural killer cells, dendritic cells, and regulatory T cells play different roles in the process of bone tissue regeneration.<sup>[267]</sup> However, the current research on the regulation of immunity by biomaterials-mediated *in situ* physical stimulation mainly concentrates on Mφs while barely put attention to other immune cells. Hence, establishing a favorable immune microenvironment through modulating various immune cells and

factors and arising the synergetic effect on osteogenesis, angiogenesis, and immune regulation is of great significance for biomaterials-mediated in situ stimulation applied in BTE.

It is worth noting that the coupling of osteoblasts and osteoclasts plays a key role in bone repair and metabolism,<sup>[268]</sup> while osteocytes can communicate with osteoclasts and osteoblasts via distinct signaling molecules.<sup>[269]</sup> Thus, it is theoretically envisageable the use of biomaterial-mediated physical stimulation to modulate the correlation among osteoblasts, osteoclasts, and osteocytes to achieve more efficient in situ bone regeneration. However, most studies have focused on material-mediated physical stimuli acting on BMSCs and osteoblasts, with fewer studies on osteoclasts or osteocytes, and even less attention on material-mediated physical stimuli affecting the interaction between osteoblasts, osteoclasts, and osteocytes.

In conclusion, biomaterials-mediated in situ physical cues including nanostructures, mechanical stimulation, electric signals, magnetism, light, and heat as an approach to stimulate bone regeneration present attractive prospects in BTE. Developing biodegradable and multifunctional biomaterials, which can utilize multiple physical cues to regulate immune response, angiogenesis, and osteogenesis, is vital to promote the clinical translation of this strategy. Besides, increased efforts should be made to clarify the optimal parameters when applying external stimulation to biomaterials. Thus, the strategy of biomaterials-mediated in situ physical cues to promote bone regeneration has great application possibilities and development in the field of bone repair and regenerative medicine in the future.

**Table 1.**

Physical cues associated with the different biomaterials to promote in situ osteogenesis.

| Cues       | Biomaterials | Realization form   | External stimulation | <i>In vitro</i> results               | <i>In vivo</i> results          | Ref  |
|------------|--------------|--|----------------------|---------------------------------------|---------------------------------|------|
| Morphology | Ti-based     | Hierarchical macro-micro-nano roughness                              | /                    | Human MSCs—osteogenic differentiation | /                               | [36] |
|            |              | Nanopetal-like structure with pore size (264.1 ± 45.2 nm)            | /                    | MG63 cells—osteogenic differentiation | Rabbit femur defect—bone repair | [38] |
|            |              | Nanotubes (39 nm diameter) layer                                     | /                    | Human MSCs—osteogenic differentiation | /                               | [40] |
|            |              | Clustered TiO <sub>2</sub> nanotubular surface with PDGF-BB covalent | /                    | Human MSCs—osteogenic differentiation | Rat femur defect—bone repair    | [41] |

|                                  |                                    |   |   |   |  |       |
|----------------------------------|------------------------------------|---|---|---|--|-------|
|                                  |                                    | modification<br>(235.55 ± 37.70 nm<br>roughness)  |   |   |  |       |
|                                  |                                    | Sr-incorporated<br>micro/nano Ti  | / | Human<br>BMSCs—<br>osteogenic<br>differentiation,<br>Human<br>UVECs—<br>angiogenic<br>differentiation,<br>Raw264.7—<br>M2<br>polarization | Rat tibial<br>defect—<br>bone repair                   | [45a] |
|                                  |                                    | HAp nanorods (45–<br>70 nm in length and<br>10–15 nm in width)  | / | BMSCs—<br>osteogenic<br>differentiation   | Mouse<br>mandibular<br>defect—<br>bone repair          | [75]  |
|                                  | HAp-based                          | Topography<br>imprinting of<br>Isolated islands<br>patterns on HAp  | / | Human<br>ADSCs—<br>osteogenic<br>differentiation  | /  | [11]  |
|                                  |                                    | HAp coating of rod-<br>cluster<br>micro/nanocrystals  | / | Mouse<br>BMSCs—<br>osteogenic<br>differentiation  | Rabbit<br>femoral<br>condyle<br>defect—<br>bone repair | [67a] |
|                                  |                                    | PLGA BNP with<br>well-aligned ridge<br>and groove<br>features (ridge:<br>groove: height =<br>800: 800: 600 nm)          | / | Rat<br>osteoblasts—<br>osteogenic<br>differentiation<br>and<br>mineralization   | Mouse<br>calvarial<br>defect—<br>bone repair           | [82]  |
|                                  | Polymer-<br>based                  | PCL substrate with<br>nanoridges<br>(thickness:<br>distance= ~74 nm:<br>~556 nm)  | / | Mouse<br>MC3T3-E1—<br>osteogenic<br>differentiation   | /  | [17]  |
|                                  |                                    | PEEK surface with<br>patterned nanorod<br>arrays (diameter:<br>height: distance=<br>195 ± 21: 711 ± 61:<br>452 ± 34 nm) | / | Rat ADSCs—<br>osteogenic<br>differentiation   | Rat femur<br>defect—<br>bone repair                    | [78]  |
|                                  |                                    | Chitosan/gelatin<br>film with arrays of<br>ordered nanopillars<br>(diameter: heigh:<br>pitch= ~90: ~300:<br>~50 nm)     | / | Human<br>BMSCs—<br>osteogenic<br>differentiation  | /  | [91a] |
|                                  | Other<br>materials                 | CS with flower-like<br>nanostructures<br>(thicknesses= 20–<br>50 nm)  | / | Rat BMSCs—<br>osteogenic<br>differentiation   | Rat<br>calvarial<br>defect—<br>bone repair             | [102] |
| Mecha<br>nical<br>propert<br>ies | Stiffness-<br>related<br>materials | PDMS substrate<br>with intermediate<br>stiffness (0.909<br>MPa)   | / | Smooth<br>muscle cell—<br>osteogenic<br>differentiation   | /  | [112] |
|                                  |                                    | GeIMA/ SA<br>hydrogel, dynamic  | / | Rat MSCs—<br>osteogenic   | Rat<br>calvarial                                       | [117] |

|                               |                          |   |  |   |   |        |
|-------------------------------|--------------------------|---|--|---|---|--------|
|                               |                          | stiffness from 14.63 ± 1.18 kPa to 68.37 ± 4.99 kPa                   |  | differentiation                               | defect—bone repair                                    |        |
| Degradation-related materials |                          | 9%RSF/3%G hydrogel, approximately 3 months                            | /  | Rat BMSCs—osteogenic differentiation          | Rat calvarial defect—bone repair                      | [128]  |
|                               |                          | PLGA/PCL/HA: Yb/Ho/Zn (PPHZ) scaffold, stepwise-degraded              | /  |   | Rabbit femoral defect—bone repair                     | [133]  |
| Electricity                   | Piezoelectric materials  | P(VDF-TrFE) coating, $d_{33} = -22 \pm 0.5$ pC/N                      | /  | Mouse M $\phi$ —M2 polarization               | /   | [144b] |
|                               |                          | BTO/P(VDF-TrFE) membrane, $d_{33} = 9.21$ pC/N                        | /  | Rat BMSCs—osteogenic differentiation          | Rabbit mandible defect—bone repair                    | [160]  |
|                               |                          | SiO <sub>2</sub> /PDMS membrane, $\zeta$ -potential = -61.5 mV        | /  | Rat BMSCs—osteogenic differentiation          | Rat calvarial defect—bone repair                      | [270]  |
|                               | Conductive materials     | PPy-coated PLLA fibers  | Electrical stimulation, 75 mV mm <sup>-1</sup> , 3 h day <sup>-1</sup> | /   | Rat BMSC—osteogenic differentiation                   | /      |
| CNFs                          |                          | 100 $\mu$ A DC electrical stimulation, 1 h day <sup>-1</sup> , 7 days | /  | MG63 cell—osteogenic differentiation          | /   | [187]  |
| Magnetism                     | Magnetic materials       | PGA/Fe <sub>3</sub> O <sub>4</sub> scaffold                           | SMF, 1.2 to 70 mT  | Human UC-MSCs—osteogenic differentiation      | Rabbit radius defect—bone repair                      | [208]  |
|                               |                          | PLLA/PGA@Fe <sub>3</sub> O <sub>4</sub> scaffold                      | SMF, 0.35 T  | MG63 cell—osteogenic differentiation          | Rabbit radius defect—vessel formation and bone repair | [271]  |
|                               |                          | MNPs/collagen hydrogel  | SMF, 280 mT  | Rat BMSCs—osteoblast M1 M $\phi$ —M2 M $\phi$ | Rat calvarial defect—bone repair                      | [212]  |
|                               |                          | Fe <sub>3</sub> O <sub>4</sub> /PDA coating                           | SMF, 15 mT   | Human BMSCs—osteogenic differentiation        | Rabbit femoral defect—bone repair                     | [210]  |
|                               |                          | CFO/P(VDF-TrFE) membrane  | Remote DC magnetic field   | BMSCs—osteogenic differentiation              | Rat cranial defect—bone repair                        | [220a] |
| Light                         | Photoresponsive material | UCNT-based nanocomplex  | 6 W cm <sup>-2</sup> , NIR light                                       | MSCs—osteogenic differentiation               | /   | [225]  |
| Heat                          | PTT-related materials    | HAp@graphene scaffold   | 980 nm NIR radiation, 0.2 W/cm <sup>2</sup>                            | Rat BMSCs—osteogenic differentiation          | Rat calvaria defect—bone repair                       | [237]  |
|                               |                          | CD/WS <sub>2</sub> HJs  | 1064 nm NIR  | Human   | /   | [238b] |

|                          |  |  |   |  |       |
|--------------------------|--|--|---|--|-------|
|                          |  | light  | MSCs—<br>osteogenic<br>differentiation  |  |       |
|                          | AuPd nanoparticle  | 808 nm NIR                                     | MC3T3-E1—<br>osteogenic<br>differentiation  | Rat cranial<br>defect—<br>bone repair    | [239] |
|                          | MoS <sub>2</sub> -biotin-<br>agarose-gelatin<br>scaffold           | 808 nm NIR<br>light, 1.5<br>W/cm <sup>2</sup>  | Rat BMSCs—<br>osteogenic<br>differentiation   | Rat cranial<br>defect—<br>bone repair    | [240] |
|                          | PDA@HAp core-<br>shell structure                                   | 808 nm NIR<br>light, 0.75<br>W/cm <sup>2</sup> | Mouse<br>BMSCs—<br>osteogenic<br>differentiation  | Rat femoral<br>defect—<br>bone repair    | [244] |
| MTT-related<br>materials | CoFe <sub>2</sub> O <sub>4</sub> @MnFe <sub>2</sub> O <sub>4</sub> | AMF, 1.35<br>kA/m, 5min<br>day <sup>-1</sup>   | MC3T3-E1—<br>osteogenic<br>differentiation,<br>HUVECs—<br>angiogenic<br>differentiation | Rat<br>cranium<br>defect—<br>bone repair | [251] |

## ACKNOWLEDGMENTS

The authors greatly acknowledge the financial support from National Natural Science Foundation of China (No. 82100974, 82170964, and 82101020), Natural Science Foundation of Shandong Province (ZR2021QH241 and ZR202102180927), The Construction Engineering Special Fund of “Taishan Scholars” of Shandong Province (No.ts20190975 and tsqn202211327), Shandong Province Key Research and Development Program (No. 2021ZDSYS18), Shandong Province Major Scientific and Technical Innovation Project (No. 2021SFGC0502), Collaborative Innovation Center of Technology and Equipment for Biological Diagnosis and Therapy in Universities of Shandong, Qilu Young Scholars Program of Shandong University, and Young Elite Scientist Support Program by CSA (2021PYRC001). This work was partly supported by the Interdisciplinary Thematic Institute SysChem via the IdEx Unistra (ANR-10-IDEX-0002) within the program “Investissement d’Avenir”. We wish to also acknowledge the Centre National de la Recherche Scientifique (CNRS), and the International Center for Frontier Research in Chemistry (icFRC). ToC figure was partly from Servier Medical Art with some modification (<http://smart.servier.com/>), licensed under a Creative Commons Attribution 3.0 Generic License (<https://creativecommons.org/licenses/by/3.0/>).

## Declaration of Competing Interest

The authors declare no conflict of interest.

## Keywords:

Physical cues; biomaterials; in situ; bone regeneration; bone tissue engineering.

## Reference

- [1] a) A. D. Berendsen, B. R. Olsen, *Bone* **2015**, *80*, 14; b) J. E. Shea, S. C. Miller, *Adv. Drug Deliv. Rev.* **2005**, *57*, 945.
- [2] a) N. van Gestel, G. Carmeliet, *Nat. Metab.* **2021**, *3*, 11; b) G. Karsenty, S. Khosla, *Cell Metab.* **2022**, *34*, 805.
- [3] S. Kim, E. Macfarlane, M. J. Seibel, H. Zhou, in *Encyclopedia of Molecular Pharmacology*, Springer, Cham **2021**, p. 336.
- [4] a) J. Xie, C. Peng, Q. Zhao, X. Wang, H. Yuan, L. Yang, K. Li, X. Lou, Y. Zhang, *Acta Biomater.* **2016**, *29*, 365; b) Y. Liu, D. Luo, T. Wang, *Small* **2016**, *12*, 4611; c) A. Salhotra, H. N. Shah, B. Levi, M. T. Longaker, *Nat. Rev. Mol. Cell Biol.* **2020**, *21*, 696.
- [5] T. A. Einhorn, L. C. Gerstenfeld, *Nat. Rev. Rheumatol.* **2015**, *11*, 45.
- [6] T. Tosounidis, G. Kontakis, V. Nikolaou, A. Papathanassopoulos, P. V. Giannoudis, *Trauma* **2009**, *11*, 145.
- [7] a) R. Subbiah, R. E. Guldborg, *Adv. Healthc. Mater.* **2019**, *8*, 1801000; b) G. Zhu, T. Zhang, M. Chen, K. Yao, X. Huang, B. Zhang, Y. Li, J. Liu, Y. Wang, Z. Zhao, *Bioact. Mater.* **2021**, *6*, 4110; c) K. L. Christman, *Science* **2019**, *363*, 340.
- [8] a) S. Ruiz-Alonso, M. Lafuente-Merchan, J. Ciriza, L. Saenz-del-Burgo, J. L. Pedraz, *J. Controlled Release* **2021**, *333*, 448; b) R. Shi, Y. Huang, C. Ma, C. Wu, W. Tian, *Front. Med-Prac.* **2019**, *13*, 160.
- [9] a) M. S. V. Ferreira, W. Jahnen-Dechent, N. Labude, M. Bovi, T. Hieronymus, M. Zenke, R. K. Schneider, S. Neurs, *Biomaterials* **2012**, *33*, 6987; b) R. Visser, G. A. Rico-Llanos, H. Pulkkinen, J. Becerra, *J. Controlled Release* **2016**, *244*, 122; c) L. G. Griffith, G. Naughton, *Science* **2002**, *295*, 1009.
- [10] a) A. K. Gaharwar, I. Singh, A. Khademhosseini, *Nat. Rev. Mater.* **2020**, *5*, 686; b) R. A. Perez, S.-J. Seo, J.-E. Won, E.-J. Lee, J.-H. Jang, J. C. Knowles, H.-W. Kim, *Mater. Today* **2015**, *18*, 573; c) C. Sealy, *Mater. Today* **2018**, *21*, 205.
- [11] Y. Ramaswamy, I. Roohani, Y. J. No, G. Madafiglio, F. Chang, F. Zhao, Z. Lu, H. Zreiqat, *Bioact. Mater.* **2021**, *6*, 1107.
- [12] S. Subramaniam, Y.-H. Fang, S. Sivasubramanian, F.-H. Lin, C.-p. Lin, *Biomaterials* **2016**, *74*, 99.
- [13] P. Song, M. Li, B. Zhang, X. Gui, Y. Han, L. Wang, W. Zhou, L. Guo, Z. Zhang, Z. Li, C. Zhou, Y. Fan, X. Zhang, *Composites, Part B* **2022**, *244*, 110163.
- [14] G. Wang, J. Qiu, L. Zheng, N. Ren, J. Li, H. Liu, J. Miao, *J. Biomat. Sci-Polym. E.* **2014**, *25*, 1813.
- [15] L. Casarrubios, N. Gómez-Cerezo, S. Sánchez-Salcedo, M. J. Feito, M. C. Serrano, M. Saiz-Pardo, L. Ortega, D. de Pablo, I. Díaz-Güemes, B. Fernández-Tomé, S. Enciso, F. M. Sánchez-Margallo, M. T. Portolés, D. Arcos, M. Vallet-Regí, *Acta Biomater.* **2020**, *101*, 544.
- [16] S. Lü, X. Bai, H. Liu, P. Ning, Z. Wang, C. Gao, B. Ni, M. Liu, *J. Mater. Chem. B* **2017**, *5*, 3739.
- [17] H.-M. Yin, W. Liu, Y.-F. Huang, Y. Ren, L. Xu, J.-Z. Xu, B. Zhao, Z.-M. Li, *ACS Appl. Mater. Interfaces* **2019**, *11*, 42956.
- [18] Y. Zhao, L. Bai, Y. Zhang, R. Yao, Y. Sun, R. Hang, X. Chen, H. Wang, X. Yao, Y. Xiao, R. Hang,

*Biomaterials* **2022**, *288*, 121684.

- [19] M. J. Dalby, N. Gadegaard, R. Tare, A. Andar, M. O. Riehle, P. Herzyk, C. D. Wilkinson, R. O. Oreffo, *Nat. Mater.* **2007**, *6*, 997.
- [20] M.-J. Kim, B. Lee, K. Yang, J. Park, S. Jeon, S. H. Um, D.-I. Kim, S. G. Im, S.-W. Cho, *Biomaterials* **2013**, *34*, 7236.
- [21] a) H. Wei, J. Cui, K. Lin, J. Xie, X. Wang, *Bone Res.* **2022**, *10*, 17; b) A. Higuchi, Q.-D. Ling, S. S. Kumar, Y. Chang, A. A. Alarfaj, M. A. Munusamy, K. Murugan, S.-T. Hsu, A. Umezawa, *J. Mater. Chem. B* **2015**, *3*, 8032; c) A. Higuchi, Q.-D. Ling, Y. Chang, S.-T. Hsu, A. Umezawa, *Chem. Rev.* **2013**, *113*, 3297; d) J. Li, Y. Liu, Y. Zhang, B. Yao, Enhejirigala, Z. Li, W. Song, Y. Wang, X. Duan, X. Yuan, X. Fu, S. Huang, *Front Cell Dev. Biol.* **2021**, *9*, 640388; e) S. Wang, S. Hashemi, S. Stratton, T. L. Arinzeh, *Adv. Healthc. Mater.* **2021**, *10*, 2001244.
- [22] a) E. K. Yim, M. P. Sheetz, *Stem Cell Res. Ther.* **2012**, *3*, 41; b) D. Brindley, K. Moorthy, J.-H. Lee, C. Mason, H.-W. Kim, I. Wall, *J. Tissue Eng.* **2011**, *2011*, 620247.
- [23] N. Yamauchi, Y. Taguchi, H. Kato, M. Umeda, *J. Periodontol.* **2018**, *89*, 351.
- [24] a) Y. Zhang, L. Xu, Z. Liu, X. Cui, Z. Xiang, J. Bai, D. Jiang, J. Xue, C. Wang, Y. Lin, Z. Li, Y. Shan, Y. Yang, L. Bo, Z. Li, X. Zhou, *Nano Energy* **2021**, *85*, 106009; b) F. Sahm, J. Ziebart, A. Jonitz-Heincke, D. Hansmann, T. Dauben, R. Bader, *Int. J. Mol. Sci.* **2020**, *21*, 6944.
- [25] G. A. Giannunzio, R. C. Speerli, M. B. Guglielmotti, *Implant. Dent.* **2008**, *17*, 118.
- [26] a) V. Canè, P. Botti, S. Soana, *J. Orthop. Res.* **1993**, *11*, 664; b) J. Wang, P. Shang, *Prog. Biophys. Mol. Biol.* **2023**, *178*, 91; c) Y. Xia, J. Sun, L. Zhao, F. Zhang, X. J. Liang, Y. Guo, M. D. Weir, M. A. Reynolds, N. Gu, H. H. K. Xu, *Biomaterials* **2018**, *183*, 151.
- [27] M. Rezai Rad, G. E. Wise, H. Brooks, M. B. Flanagan, S. Yao, *Cell Prolif.* **2013**, *46*, 58.
- [28] J. Qiu, J. Li, S. Wang, B. Ma, S. Zhang, W. Guo, X. Zhang, W. Tang, Y. Sang, H. Liu, *Small* **2016**, *12*, 1770.
- [29] C. A. Mullen, T. J. Vaughan, K. L. Billiar, L. M. McNamara, *Biophys. J.* **2015**, *108*, 1604.
- [30] Y. Xie, S. Li, T. Zhang, C. Wang, X. Cai, *Int. J. Oral Sci.* **2020**, *12*, 37.
- [31] T. Stich, F. Alagboso, T. Křenek, T. Kovářik, V. Alt, D. Docheva, *Bioeng. Transl. Med.* **2022**, *7*, e10239.
- [32] L. Salou, A. Hoornaert, G. Louarn, P. Layrolle, *Acta Biomater.* **2015**, *11*, 494.
- [33] a) A. Hayles, J. Hasan, R. Bright, D. Palms, T. Brown, D. Barker, K. Vasilev, *Mater. Today Chem.* **2021**, *22*, 100622; b) J. C. M. Souza, M. B. Sordi, M. Kanazawa, S. Ravindran, B. Henriques, F. S. Silva, C. Aparicio, L. F. Cooper, *Acta Biomater.* **2019**, *94*, 112.
- [34] A. Hoornaert, L. Vidal, R. Besnier, J. F. Morlock, G. Louarn, P. Layrolle, *Clin. Oral Implan. Res.* **2020**, *31*, 526.
- [35] a) I. Lauria, T. N. Kutz, F. Böke, S. Rütten, D. Zander, H. Fischer, *Mat. Sci. Eng. C-Mater.* **2019**, *98*, 635; b) Y. C. Shin, K.-M. Pang, D.-W. Han, K.-H. Lee, Y.-C. Ha, J.-W. Park, B. Kim, D. Kim, J.-H. Lee, *Mat. Sci. Eng. C-Mater.* **2019**, *99*, 1174.
- [36] E. G. Long, M. Buluk, M. B. Gallagher, J. M. Schneider, J. L. Brown, *Bioact. Mater.* **2019**, *4*, 249.
- [37] H. Xing, S. Komasa, Y. Taguchi, T. Sekino, J. Okazaki, *Int. J. Nanomed.* **2014**, *9*, 1741.
- [38] Y.-Z. Huang, S.-K. He, Z.-J. Guo, J.-K. Pi, L. Deng, L. Dong, Y. Zhang, B. Su, L.-C. Da, L. Zhang, *Mat. Sci. Eng. C-Mater.* **2019**, *94*, 1.
- [39] Z. Li, J. Qiu, L. Q. Du, L. Jia, H. Liu, S. Ge, *Mat. Sci. Eng. C-Mater.* **2017**, *76*, 684.
- [40] J. Li, I. Mutreja, S. Tredinnick, M. Jermy, G. Hooper, T. Woodfield, *Mat. Sci. Eng. C-Mater.* **2020**, *109*, 110562.
- [41] Q. Ma, N. Jiang, S. Liang, F. Chen, L. Fang, X. Wang, J. Wang, L. Chen, *Biomaterials* **2020**, *230*, 119650.
- [42] B. Wu, Y. Tang, K. Wang, X. Zhou, L. Xiang, *Int. J. Nanomed.* **2022**, 1865.

- [43] M. Yu, H. Yang, B. Li, R. Wang, Y. Han, *Chem. Eng. J.* **2023**, *454*, 140141.
- [44] Y. He, Z. Li, X. Ding, B. Xu, J. Wang, Y. Li, F. Chen, F. Meng, W. Song, Y. Zhang, *Bioact. Mater.* **2022**, *8*, 109.
- [45] a) W. Lu, C. Zhou, Y. Ma, J. Li, J. Jiang, Y. Chen, L. Dong, F. He, *Biomater. Sci.* **2022**, *10*, 2198; b) A.-t. Xu, Y.-w. Xie, J.-g. Xu, J. Li, H. Wang, F.-m. He, *Colloids Surf., B* **2021**, *207*, 111992.
- [46] J.-W. Park, T. Hanawa, J.-H. Chung, *Int. J. Nanomed.* **2019**, *14*, 5697.
- [47] L. Li, S. Yang, L. Xu, Y. Li, Y. Fu, H. Zhang, J. Song, *Acta Biomater.* **2019**, *96*, 674.
- [48] G. Li, Y. Song, M. Shi, Y. Du, W. Wang, Y. Zhang, *Acta Biomater.* **2017**, *49*, 235.
- [49] Y. Yu, X. Shen, J. Liu, Y. Hu, Q. Ran, C. Mu, K. Cai, *Colloids Surf., B* **2018**, *170*, 1.
- [50] W. Wang, G. Li, J. Wang, W. Song, J. Luo, F. Meng, Y. Zhang, *Mater. Des.* **2018**, *157*, 402.
- [51] B. D. Boyan, R. Olivares-Navarrete, M. B. Berger, S. L. Hyzy, Z. Schwartz, *Sci. Rep.* **2018**, *8*, 1.
- [52] X.-M. Zhuang, B. Zhou, K.-F. Yuan, *Biomed. Pharmacother.* **2019**, *112*, 108649.
- [53] H. B. Lopes, G. P. Freitas, C. N. Elias, C. Tye, J. L. Stein, G. S. Stein, J. B. Lian, A. L. Rosa, M. M. Beloti, *J. Biomed. Mater. Res. Part A* **2019**, *107*, 1303.
- [54] L. Lv, Y. Liu, P. Zhang, X. Zhang, J. Liu, T. Chen, P. Su, H. Li, Y. Zhou, *Biomaterials* **2015**, *39*, 193.
- [55] Z. Jin, X. Yan, K. Shen, X. Fang, C. Zhang, Q. Ming, M. Lai, K. Cai, *Colloids Surf., B* **2019**, *181*, 416.
- [56] a) C. Kim, J. W. Lee, J. H. Heo, C. Park, D.-H. Kim, G. S. Yi, H. C. Kang, H. S. Jung, H. Shin, J. H. Lee, *Biomater. Res.* **2022**, *26*, 7; b) X. Liu, Y. Miao, H. Liang, J. Diao, L. Hao, Z. Shi, N. Zhao, Y. Wang, *Bioact. Mater.* **2022**, *12*, 120; c) L. Wu, X. Pei, B. Zhang, Z. Su, X. Gui, C. Gao, L. Guo, H. Fan, Q. Jiang, L. Zhao, C. Zhou, Y. Fan, X. Zhang, *Chem. Eng. J.* **2023**, *455*, 140699.
- [57] C. Liu, A. Tian, H. Yang, Q. Xu, X. Xue, *Appl. Surf. Sci.* **2013**, *287*, 218.
- [58] M. Roy, A. Bandyopadhyay, S. Bose, *Surf. Coat. Technol.* **2011**, *205*, 2785.
- [59] D. Liu, K. Savino, M. Z. Yates, *Surf. Coat. Technol.* **2011**, *205*, 3975.
- [60] D. Suárez-González, K. Barnhart, F. Migneco, C. Flanagan, S. J. Hollister, W. L. Murphy, *Biomaterials* **2012**, *33*, 713.
- [61] J. Wang, M. Wang, F. Chen, Y. Wei, X. Chen, Y. Zhou, X. Yang, X. Zhu, C. Tu, X. Zhang, *Int. J. Nanomed.* **2019**, *14*, 7987.
- [62] B. Ma, S. Zhang, F. Liu, J. Duan, S. Wang, J. Han, Y. Sang, X. Yu, D. Li, W. Tang, *ACS Appl. Mater. Interfaces* **2017**, *9*, 33717.
- [63] a) B. Ma, J. Han, S. Zhang, F. Liu, S. Wang, J. Duan, Y. Sang, H. Jiang, D. Li, S. Ge, J. Yu, H. Liu, *Acta Biomater.* **2018**, *71*, 108; b) J. Han, B. Ma, H. Liu, T. Wang, F. Wang, C. Xie, M. Li, H. Liu, S. Ge, *J. Biomed. Mater. Res. Part A* **2018**, *106*, 3099.
- [64] L. Xia, K. Lin, X. Jiang, B. Fang, Y. Xu, J. Liu, D. Zeng, M. Zhang, X. Zhang, J. Chang, *Biomaterials* **2014**, *35*, 8514.
- [65] D. Xiao, T. Guo, F. Yang, G. Feng, F. Shi, J. Li, D. Wang, K. Duan, J. Weng, *Ceram. Int.* **2017**, *43*, 1588.
- [66] L. Liu, X. Wang, Y. Zhou, M. Cai, K. Lin, B. Fang, L. Xia, *J. Mater. Chem. B* **2020**, *8*, 2754.
- [67] a) B. Tan, N. Zhao, W. Guo, F. Huang, H. Hu, Y. Chen, J. Li, Z. Ling, Z. Zou, R. Hu, C. Liu, T. Zheng, G. Wang, X. Liu, Y. Wang, X. Zou, *J. Mater. Sci. Technol.* **2023**, *136*, 54; b) L. Xia, Y. Xie, B. Fang, X. Wang, K. Lin, *Chem. Eng. J.* **2018**, *347*, 711.
- [68] L. Bai, Y. Liu, Z. Du, Z. Weng, W. Yao, X. Zhang, X. Huang, X. Yao, R. Crawford, R. Hang, *Acta Biomater.* **2018**, *76*, 344.
- [69] a) H. Zhao, G. Wang, S. Hu, J. Cui, N. Ren, D. Liu, H. Liu, C. Cao, J. Wang, Z. Wang, *Tissue Eng. Part A* **2011**, *17*, 765; b) G. Wang, L. Zheng, H. Zhao, J. Miao, C. Sun, N. Ren, J. Wang, H. Liu, X. Tao, *Tissue Eng. Part A* **2011**, *17*, 1341.

- [70] C. B. Ching, D. E. Hansel, *Lab. Invest.* **2010**, *90*, 1406.
- [71] F. Bao, J. Yi, Y. Liu, Y. Zhong, H. Zhang, Z. Wu, B. C. Heng, Y. Wang, Z. Wang, L. Xiao, H. Liu, H. Ouyang, J. Zhou, *Bioact. Mater.* **2022**, *18*, 539.
- [72] R. X. Wang, H. Hu, J. X. Guo, Q. Wang, J. J. Cao, H. G. Wang, G. P. Li, J. P. Mao, X. N. Zou, D. F. Chen, W. Tian, *J. Biomed. Nanotechnol.* **2019**, *15*, 405.
- [73] C. Zhao, X. Wang, L. Gao, L. Jing, Q. Zhou, J. Chang, *Acta Biomater.* **2018**, *73*, 509.
- [74] D.-W. Zhao, M.-Z. Yu, Y.-X. Zhao, R. Hu, P.-C. Xu, Z.-Y. Sun, K. Bian, C. Liu, L. Cheng, *J. Mater. Sci. Technol.* **2023**, *136*, 109.
- [75] F. Yu, R. Lian, L. Liu, T. Liu, C. Bi, K. Hong, S. Zhang, J. Ren, H. Wang, N. Ouyang, L.-J. Du, Y. Liu, L. Zhou, Y. Liu, B. Fang, Y. Li, S.-Z. Duan, L. Xia, *ACS Nano* **2022**, *16*, 755.
- [76] a) N. Iqbal, A. S. Khan, A. Asif, M. Yar, J. W. Haycock, I. U. Rehman, *Int. Mater. Rev.* **2019**, *64*, 91; b) S. Wang, Y. Yang, Y. Li, J. Shi, J. Zhou, L. Zhang, Y. Deng, W. Yang, *Colloids Surf., B* **2019**, *176*, 38; c) V. Ogay, E. A. Mun, G. Kudaibergen, M. Baidarbekov, K. Kassymbek, Z. Zharkinbekov, A. Saparov, *Polymers*, **2020**, *12*, 2881.
- [77] W. Liu, J. Li, M. Cheng, Q. Wang, K. W. K. Yeung, P. K. Chu, X. Zhang, *Adv. Sci.* **2018**, *5*, 1800749.
- [78] S. Zhang, Z. Feng, Y. Hu, D. Zhao, X. Guo, F. Du, N. Wang, C. Sun, C. Liu, H. J. S. Liu, *Small* **2022**, *18*, 2105589.
- [79] X. Wu, Y. Liu, X. Li, P. Wen, Y. Zhang, Y. Long, X. Wang, Y. Guo, F. Xing, J. Gao, *Acta Biomater.* **2010**, *6*, 1167.
- [80] a) B. Dhandayuthapani, Y. Yoshida, T. Maekawa, D. S. Kumar, *Int. J. Polym. Sci.* **2011**, *2011*, 290602; b) M. R. Iaquinta, E. Mazzone, M. Manfrini, A. D'Agostino, L. Trevisiol, R. Nocini, L. Trombelli, G. Barbanti-Brodano, F. Martini, M. Tognon, in *Int. J. Mol. Sci.* **2019**, *20*, 618.
- [81] S. Zhang, B. Ma, F. Liu, J. Duan, S. Wang, J. Qiu, D. Li, Y. Sang, C. Liu, D. Liu, H. Liu, *Nano Lett.* **2018**, *18*, 2243.
- [82] M. S. Lee, D. H. Lee, J. Jeon, S. H. Oh, H. S. J. A. a. m. Yang, interfaces, *ACS Appl. Mater. Interfaces* **2018**, *10*, 38780.
- [83] S. Najeeb, M. S. Zafar, Z. Khurshid, F. Siddiqui, *J. Prosthodont. Res.* **2016**, *60*, 12.
- [84] Y. Li, J. Wang, D. He, GuoxiongZhu, G. Wu, L. Chen, *J. Mater. Sci. Mater. Med.* **2019**, *31*, 11.
- [85] N. T. Evans, F. B. Torstrick, C. S. D. Lee, K. M. Dupont, D. L. Safranski, W. A. Chang, A. E. Macedo, A. S. P. Lin, J. M. Boothby, D. C. Whittingslow, R. A. Carson, R. E. Guldberg, K. Gall, *Acta Biomater.* **2015**, *13*, 159.
- [86] G. Abagnale, M. Steger, V. H. Nguyen, N. Hersch, A. Sechi, S. Jousen, B. Denecke, R. Merkel, B. Hoffmann, A. J. B. Dreser, *Biomaterials* **2015**, *61*, 316.
- [87] M.-H. You, M. K. Kwak, D.-H. Kim, K. Kim, A. Levchenko, D.-Y. Kim, K.-Y. Suh, *Biomacromolecules* **2010**, *11*, 1856.
- [88] a) A. J. P. i. P. S. Sionkowska, *Prog. Polym. Sci.* **2021**, *122*, 101452; b) L. Guo, Z. Liang, L. Yang, W. Du, T. Yu, H. Tang, C. Li, H. Qiu, *J. Controlled Release* **2021**, *338*, 571.
- [89] A. Aravamudhan, D. M. Ramos, J. Nip, I. Kalajzic, S. G. J. M. b. Kumbar, *Macromol. Biosci.* **2018**, *18*, 1700263.
- [90] J. F. Greiner, M. Gottschalk, N. Fokin, B. Bükler, B. P. Kaltschmidt, A. Dreyer, T. Vordemvenne, C. Kaltschmidt, A. Hütten, B. Kaltschmidt, *Nanomed. Nanotechnol. Biol. Med.* **2019**, *17*, 319.
- [91] a) S. Altuntas, H. K. Dhaliwal, N. J. Bassous, A. E. Radwan, P. Alpaslan, T. Webster, F. Buyukserin, M. J. A. B. S. Amiji, Engineering, *ACS Biomater. Sci. Eng.* **2019**, *5*, 4311; b) P. A. Erturk, S. Altuntas, G. Irmak, F. Buyukserin, *ACS Appl. Bio Mater.* **2022**, *5*, 4913.

- [92] Z. Wang, L. Dong, L. Han, K. Wang, X. Lu, L. Fang, S. Qu, C. W. J. S. r. Chan, *Sci. Rep.* **2016**, 6, 1.
- [93] a) H. Wang, Y. Lai, Z. Xie, Y. Lin, Y. Cai, Z. Xu, J. Chen, *ACS Appl. Mater. Interfaces* **2022**, 14, 54500; b) E.-S. Kang, H. Kim, Y. Han, Y.-W. Cho, H. Son, Z. Luo, T.-H. Kim, *Colloids Surf., B* **2021**, 204, 111807.
- [94] A. Kumar, A. Sood, S. S. Han, *J. Mater. Chem. B* **2022**, 10, 2761.
- [95] L. Yuan, X. Qi, G. Qin, Q. Liu, F. Zhang, Y. Song, J. J. C. Deng, S. B. Biointerfaces, *Colloids Surf., B* **2019**, 184, 110494.
- [96] Y. Liu, J. Ding, Q.-q. Wang, M.-l. Wen, T.-t. Tang, Y. Liu, R. Yuan, Y.-f. Li, M.-w. An, *New Carbon Mater.* **2021**, 36, 779.
- [97] L. A. Tang, W. C. Lee, H. Shi, E. Y. Wong, A. Sadovoy, S. Gorelik, J. Hopley, C. T. Lim, K. P. Loh, *Small* **2012**, 8, 423.
- [98] E.-S. Kang, D.-S. Kim, Y. Han, H. Son, Y.-H. Chung, J. Min, T.-H. Kim, *Int. J. Mol. Sci.* **2018**, 19.
- [99] X. Zhang, J. Nie, X. Yang, Z. Liu, W. Guo, J. Qiu, S. Wang, X. Yu, Y. Guan, H. Liu, *Appl. Mater. Today* **2018**, 10, 164.
- [100] D. Inzunza, C. Covarrubias, A. V. Marttens, Y. Leighton, J. C. Carvajal, F. Valenzuela, M. Díaz - Dosque, N. Mendez, C. Martínez, A. M. J. J. o. B. M. R. P. A. A. O. J. o. T. S. f. B. Pino, The Japanese Society for Biomaterials., T. A. S. f. Biomaterials, t. K. S. f. Biomaterials, *J Biomed Mater Res. A* **2014**, 102, 37.
- [101] C. Covarrubias, M. Mattmann, A. Von Marttens, P. Caviedes, C. Arriagada, F. Valenzuela, J. P. Rodríguez, C. J. A. S. S. Corral, *Appl. Surf. Sci.* **2016**, 363, 286.
- [102] P. Mei, S. Jiang, L. Mao, Y. Zhou, K. Gu, C. Zhang, X. Wang, K. Lin, C. Zhao, M. J. J. o. n. Zhu, *J. Nanobiotechnol.* **2022**, 20, 1.
- [103] a) Z. Li, J. Zheng, D. Wan, X. Yang, *Biomed Res. Int.* **2020**, 2020, 3906426; b) L. Wang, X. You, L. Zhang, C. Zhang, W. Zou, *Bone Res.* **2022**, 10, 16.
- [104] L. Dong, Y. Song, Y. Zhang, W. Zhao, C. Wang, H. Lin, M. K. Al - ani, W. Liu, R. Xue, L. J. J. o. c. p. Yang, *J. Cell. Physiol.* **2021**, 236, 6376.
- [105] a) N. R. Gould, O. M. Torre, J. M. Leser, J. P. Stains, *Bone* **2021**, 149, 115971; b) F. Martino, A. R. Perestrelo, V. Vinarský, S. Pagliari, G. Forte, *Front. Physiol.* **2018**, 9.
- [106] L. Qin, W. Liu, H. Cao, G. J. B. r. Xiao, *Bone Res.* **2020**, 8, 1.
- [107] a) J. H. Park, S. B. Jo, J.-H. Lee, H.-H. Lee, J. C. Knowles, H.-W. Kim, *Bioact. Mater.* **2023**, 20, 381; b) O. Chaudhuri, J. Cooper-White, P. A. Janmey, D. J. Mooney, V. B. Shenoy, *Nature* **2020**, 584, 535; c) V. Irawan, A. Higuchi, T. Ikoma, *Open Phys.* **2018**, 16, 943.
- [108] C. Gao, Y. Lai, L. Cheng, Y. Cheng, A. Miao, J. Chen, R. Yang, F. Xiong, *Adv. Mater.* **2023**, n/a, 2212272.
- [109] L. Chen, C. Wu, D. Wei, S. Chen, Z. Xiao, H. Zhu, H. Luo, J. Sun, H. Fan, *Mat. Sci. Eng. C-Mater.* **2021**, 119, 111613.
- [110] a) L. Wu, A. Magaz, T. Wang, C. Liu, A. Darbyshire, M. Loizidou, M. Emberton, M. Birchall, W. J. B. Song, *Biomaterials* **2018**, 186, 64; b) Y. Zhang, Y. Xing, J. Li, Z. Zhang, H. Luan, Z. Chu, H. Gong, Y. Fan, *Biomed Res. Int.* **2018**, 2018, 4025083; c) A. H. Aziz, K. Eckstein, V. L. Ferguson, S. J. J. J. o. t. e. Bryant, r. medicine, *J. Tissue Eng. Regener. Med.* **2019**, 13, 946.
- [111] K. S. Sen, D. F. Duarte Campos, M. Köpf, A. Blaeser, H. Fischer, *Adv. Healthc. Mater.* **2018**, 7, 1800343.
- [112] J.-y. Chen, Y.-x. Wang, K.-f. Ren, Y.-b. Wang, G.-s. Fu, J. J. C. Ji, S. B. Biointerfaces, *Colloids Surf., B* **2021**, 197, 111388.
- [113] S. Even-Ram, V. Artym, K. M. Yamada, *Cell* **2006**, 126, 645.
- [114] P. A. Janmey, D. A. Fletcher, C. A. Reinhart-King, *Physiol. Rev.* **2020**, 100, 695.
- [115] a) K. M. Ferlin, M. E. Prendergast, M. L. Miller, B.-N. B. Nguyen, D. S. Kaplan, J. P. Fisher, *Mol. Pharmaceutics* **2014**, 11, 2172; b) Y. Ma, T. Han, Q. Yang, J. Wang, B. Feng, Y. Jia, Z. Wei, F. Xu, *Adv.*

*Funct. Mater.* **2021**, *31*, 2100848.

- [116] L. Wu, A. Magaz, A. Darbyshire, A. Howkins, A. Reynolds, I. W. Boyd, H. Song, J.-H. Song, M. Loizidou, M. Emberton, M. Birchall, W. Song, *Adv. Healthc. Mater.* **2019**, *8*, 1801556.
- [117] Z. Chen, Y. Lv, *Composites, Part B* **2022**, *243*, 110162.
- [118] X.-T. He, R.-X. Wu, X.-Y. Xu, J. Wang, Y. Yin, F.-M. Chen, *Acta Biomater.* **2018**, *71*, 132.
- [119] a) Z. Meng, Y. Qiu, K. C. Lin, A. Kumar, J. K. Placone, C. Fang, K.-C. Wang, S. Lu, M. Pan, A. W. J. N. Hong, *Nature* **2018**, *560*, 655; b) G. Brusatin, T. Panciera, A. Gandin, A. Citron, S. J. N. m. Piccolo, *Nat. Mater.* **2018**, *17*, 1063; c) Q. Zhou, S. Lyu, A. A. Bertrand, A. C. Hu, C. H. Chan, X. Ren, M. J. Dewey, A. S. Tiffany, B. A. Harley, J. C. Lee, *Macromol. Biosci.* **2021**, *21*, 2000370.
- [120] a) S. Dupont, L. Morsut, M. Aragona, E. Enzo, S. Giullitti, M. Cordenonsi, F. Zanconato, J. Le Digabel, M. Forcato, S. Biccato, *Nature* **2011**, *474*, 179; b) Y. Guo, Y. Qiao, S. Quan, C. Yang, J. Li, *Mol. Biol. Rep.* **2022**, *49*.
- [121] Q. Zhou, S. Lyu, A. A. Bertrand, A. C. Hu, C. H. Chan, X. Ren, M. J. Dewey, A. S. Tiffany, B. A. C. Harley, J. C. Lee, *Macromol. Biosci.* **2021**, *21*, 2000370.
- [122] Q. Zhou, X. Ren, M. K. Oberoi, M. Bedar, R. M. Caprini, M. J. Dewey, V. Koliopoulos, D. T. Yamaguchi, B. A. C. Harley, J. C. Lee, *Adv. Healthc. Mater.* **2021**, *10*, 2101467.
- [123] J.-H. Hwang, M. R. Byun, A. R. Kim, K. M. Kim, H. J. Cho, Y. H. Lee, J. Kim, M. G. Jeong, E. S. Hwang, J.-H. Hong, *PLoS One* **2015**, *10*, e0135519.
- [124] J.-H. Hwang, U. Han, M. Yang, Y. Choi, J. Choi, J.-M. Lee, H.-S. Jung, J. Hong, J.-H. Hong, *Acta Biomater.* **2019**, *86*, 247.
- [125] A. Barba, Y. Maazouz, A. Diez-Escudero, K. Rappe, M. Espanol, E. B. Montufar, C. Öhman-Mägi, C. Persson, P. Fontecha, M.-C. Manzanares, *Acta Biomater.* **2018**, *79*, 135.
- [126] a) C. Shuai, W. Yang, P. Feng, S. Peng, H. J. B. M. Pan, *Bioact. Mater.* **2021**, *6*, 490; b) X. Xia, J. Huang, J. Wei, S. Jin, Q. Zou, Y. Zuo, J. Li, Y. Li, *Compos. Sci. Technol.* **2022**, *222*, 109368.
- [127] J. Huang, X. Xia, Q. Zou, J. Ma, S. Jin, J. Li, Y. Zuo, Y. Li, *J. Mater. Chem. B* **2019**, *7*, 7690.
- [128] L. B. Jiang, D. H. Su, S. L. Ding, Q. C. Zhang, Z. F. Li, F. C. Chen, W. Ding, S. T. Zhang, J. Dong, *Adv. Funct. Mater.* **2019**, *29*, 1901314.
- [129] A. Abdal-hay, N. T. Raveendran, B. Fournier, S. Ivanovski, *Composites, Part B* **2020**, *197*, 108158.
- [130] M. Kazemi, M. M. Dehghan, M. Azami, *Mat. Sci. Eng. C-Mater.* **2019**, *105*, 110071.
- [131] L. Ren, K. Yu, Y. Tan, *Sensors-Basel* **2018**, *18*, 3066.
- [132] X. Guan, M. Xiong, F. Zeng, B. Xu, L. Yang, H. Guo, J. Niu, J. Zhang, C. Chen, J. Pei, *ACS Appl. Mater. Interfaces* **2014**, *6*, 21525.
- [133] X. Li, Q. Zou, J. Wei, W. J. C. P. B. E. Li, *Composites, Part B* **2021**, *222*, 109084.
- [134] H.-Y. Chang, W.-H. Tuan, P.-L. J. M. S. Lai, E. C, *Mat. Sci. Eng. C-Mater.* **2021**, *118*, 111421.
- [135] L. P. da Silva, S. C. Kundu, R. L. Reis, V. M. Correlo, *Trends Biotechnol.* **2020**, *38*, 24.
- [136] a) P. Wang, X. Wang, *Eng. Regen.* **2022**, *3*, 440; b) B. C. Heng, Y. Bai, X. Li, L. W. Lim, W. Li, Z. Ge, X. Zhang, X. Deng, *Adv. Sci.* **2023**, *10*, 2204502.
- [137] a) D. Khare, B. Basu, A. K. Dubey, *Biomaterials* **2020**, *258*, 120280; b) T. Zheng, Y. Huang, X. Zhang, Q. Cai, X. Deng, X. Yang, *J. Mater. Chem. B* **2020**, *8*, 10221.
- [138] a) L. Leppik, K. M. C. Oliveira, M. B. Bhavsar, J. H. J. E. J. o. T. Barker, E. Surgery, *Eur. J. Trauma Emerg. Surg.* **2020**, *46*, 231; b) C. Zhao, K. Lin, X. Wang, *Appl. Mater. Today* **2020**, *19*, 100614; c) B. Ferrigno, R. Bordett, N. Duraisamy, J. Moskow, M. R. Arul, S. Rudraiah, S. P. Nukavarapu, A. T. Vella, S. G. Kumbar, *Bioact. Mater.* **2020**, *5*, 468.
- [139] B. Tandon, A. Magaz, R. Balint, J. J. Blaker, S. H. Cartmell, *Adv. Drug Deliv. Rev.* **2018**, *129*, 148.

- [140] Z. R. Liu, X. Y. Wan, Z. L. Wang, L. L. Li, *Adv. Mater.* **2021**, *33*, e2007429.
- [141] a) Y. Zhang, M. A. Hopkins, D. J. Liptrot, H. Khanbareh, P. Groen, X. Zhou, D. Zhang, Y. Bao, K. Zhou, C. R. Bowen, *Angew. Chem. Int. Ed.* **2020**, *59*, 7808; b) B. Tandon, J. J. Blaker, S. H. Cartmell, *Acta Biomater.* **2018**, *73*, 1; c) L. Zhao, S. Y. Wong, J. Y. Sim, J. Zhou, X. Li, C. Wang, *BMEMat* **2023**, *n/a*, e12020; d) F. Zhao, C. Zhang, J. Liu, L. Liu, X. Cao, X. Chen, B. Lei, L. Shao, *Chem. Eng. J.* **2020**, *402*, 126203.
- [142] a) K. Hosoyama, M. Ahumada, K. Goel, M. Ruel, E. J. Suuronen, E. Alarcon, *Biotechnol. Adv.* **2019**, *37*, 444; b) K. Kapat, Q. T. H. Shubhra, M. Zhou, S. Leeuwenburgh, *Adv. Funct. Mater.* **2020**, *30*, 1909045.
- [143] a) D. Khare, B. Basu, A. K. J. B. Dubey, *Biomaterials* **2020**, *258*, 120280; b) D.-M. Shin, S. W. Hong, Y.-H. J. N. Hwang, *Nanomaterials* **2020**, *10*, 123.
- [144] a) P. Zhu, C. Lai, M. Cheng, Y. He, Y. Xu, J. Chen, Z. Zhou, P. Li, S. Xu, *Front. Mater.* **2022**, *8*, 611; b) Z. Wang, X. He, B. Tang, X. Chen, L. Dong, K. Cheng, W. J. B. S. Weng, *Biomater. Sci.* **2021**, *9*, 874.
- [145] X. Zhang, L. Li, J. Ouyang, L. Zhang, J. Xue, H. Zhang, W. Tao, *Nano Today* **2021**, *39*, 101196.
- [146] A. Behera, in *Advanced Materials: An Introduction to Modern Materials Science*, Springer, Cham **2022**, p. 43.
- [147] P. K. Szewczyk, A. Gradys, S. K. Kim, L. Persano, M. Marzec, A. Kryshital, T. Busolo, A. Toncelli, D. Pisignano, A. Bernasik, S. Kar-Narayan, P. Sajkiewicz, U. Stachewicz, *ACS Appl. Mater. Interfaces* **2020**, *12*, 13575.
- [148] C. Chen, Z. Bai, Y. Cao, M. Dong, K. Jiang, Y. Zhou, Y. Tao, S. Gu, J. Xu, X. Yin, W. Xu, *Compos. Sci. Technol.* **2020**, *192*, 108100.
- [149] C. Zhang, W. Liu, C. Cao, F. Zhang, Q. Tang, S. Ma, J. Zhao, L. Hu, Y. Shen, L. Chen, *Adv. Healthc. Mater.* **2018**, *7*, 1701466.
- [150] S. Yu, Y. Tai, J. Milam-Guerrero, J. Nam, N. V. Myung, *Nano Energy* **2022**, *97*, 107174.
- [151] H. Yook, J. Hwang, W. Yeo, J. Bang, J. Kim, T. Y. Kim, J.-S. Choi, J. W. Han, *Adv. Mater.* **2022**, *n/a*, 2204938.
- [152] C. Ribeiro, V. Correia, P. Martins, F. M. Gama, S. Lanceros-Mendez, *Colloids Surf., B* **2016**, *140*, 430.
- [153] Y. Dong, L. Suryani, X. Zhou, P. Muthukumar, M. Rakshit, F. Yang, F. Wen, A. M. Hassanbhai, K. Parida, D. T. Simon, *Int. J. Mol. Sci.* **2021**, *22*, 6438.
- [154] Y. Tai, S. Yang, S. Yu, A. Banerjee, N. V. Myung, J. J. N. E. Nam, *Nano Energy* **2021**, *89*, 106444.
- [155] A. Pryadko, M. A. Surmeneva, R. A. Surmenev, *Polymers* **2021**, *13*, 1738.
- [156] a) M. Mohammadipour, M. Asadolahi, Z. Mohammadipour, T. Behzad, S. Karbasi, *Int. J. Biol. Macromol.* **2023**, *230*, 123167; b) R. Sheng, J. Mu, R. V. Chernozem, Y. R. Mukhortova, M. A. Surmeneva, I. O. Pariy, T. Ludwig, S. Mathur, C. Xu, R. A. Surmenev, H. H. Liu, *ACS Appl. Mater. Interfaces* **2023**, *15*, 3731.
- [157] J. Li, X. Zhang, A. Udduttula, Z. S. Fan, J. H. Chen, A. R. Sun, P. Zhang, *Front. Bioeng. Biotechnol.* **2021**, *12*, 1249.
- [158] H. Wu, H. Dong, Z. Tang, Y. Chen, Y. Liu, M. Wang, X. Wei, N. Wang, S. Bao, D. Yu, Z. Wu, Z. Yang, X. Li, Z. Guo, L. Shi, *Biomaterials* **2023**, *293*, 121990.
- [159] a) E. Mancuso, L. Shah, S. Jindal, C. Serenelli, Z. M. Tsikriteas, H. Khanbareh, A. J. M. S. Tirella, E. C. *Mat. Sci. Eng. C-Mater.* **2021**, *126*, 112192; b) T. Pan, J. Jiang, J. Li, T. Liu, S. Yu, X. Sun, Z. Yan, S. Chen, Y. Fan, M. J. C. P. B. E. Gao, *Compos. Part B-Eng.* **2021**, *204*, 108475.
- [160] Y. Bai, X. Dai, Y. Yin, J. Wang, X. Sun, W. Liang, Y. Li, X. Deng, X. J. I. J. o. N. Zhang, *Int. J. Nanomed.* **2019**, *14*, 3015.
- [161] X. Dai, X. Yao, W. Zhang, H. Cui, Y. Ren, J. Deng, X. Zhang, *Int. J. Nanomed.* **2022**, *17*, 4339.
- [162] T. Zheng, H. Zhao, Y. Huang, C. Gao, X. Zhang, Q. Cai, X. Yang, *Ceram. Int.* **2021**, *47*, 28778.
- [163] T. Zheng, Y. Yu, Y. Pang, D. Zhang, Y. Wang, H. Zhao, X. Zhang, H. Leng, X. Yang, Q. Cai, *Composites*,

*Part B* **2022**, 234, 109734.

- [164] G. Murillo, A. Blanquer, C. Vargas-Estevez, L. Barrios, E. Ibáñez, C. Nogués, J. Esteve, *Adv. Mater.* **2017**, 29, 1605048.
- [165] P. Yu, C. Ning, Y. Zhang, G. Tan, Z. Lin, S. Liu, X. Wang, H. Yang, K. Li, X. Yi, *Theranostics* **2017**, 7, 3387.
- [166] a) C. Zhang, W. Wang, X. Hao, Y. Peng, Y. Zheng, J. Liu, Y. Kang, F. Zhao, Z. Luo, J. Guo, B. Xu, L. Shao, G. Li, *Adv. Funct. Mater.* **2021**, 31, 2007487; b) R. Chen, J. Wang, C. Liu, *Adv. Funct. Mater.* **2016**, 26, 8810.
- [167] a) J. Chen, S. Li, Y. Jiao, J. Li, Y. Li, Y.-I. Hao, Y. Zuo, *ACS Appl. Mater. Interfaces* **2021**, 13, 49542; b) K. Cai, Y. Jiao, Q. Quan, Y. Hao, J. Liu, L. Wu, *Bioact. Mater.* **2021**, 6, 4073.
- [168] V. K. Kaliannagounder, N. P. M. J. Raj, A. R. Unnithan, J. Park, S. S. Park, S.-J. Kim, C. H. Park, C. S. Kim, A. R. K. Sasikala, *Nano Energy* **2021**, 85, 105901.
- [169] B. Ma, F. Liu, Z. Li, J. Duan, Y. Kong, M. Hao, S. Ge, H. Jiang, H. Liu, *J. Mater. Chem. B* **2019**, 7, 1847.
- [170] B. Fan, Z. Guo, X. Li, S. Li, P. Gao, X. Xiao, J. Wu, C. Shen, Y. Jiao, W. Hou, *Bioact. Mater.* **2020**, 5, 1087.
- [171] R. Bagur, G. J. M. c. Hajnóczky, *Mol. Cell* **2017**, 66, 780.
- [172] S. Dong, Y. Zhang, Y. Mei, Y. Zhang, Y. Hao, B. Liang, W. Dong, R. Zou, L. Niu, *Front. Bioeng. Biotechnol.* **2022**, 10, 921284.
- [173] a) J. Xu, W. Wang, C. Clark, C. J. O. Brighton, cartilage, *Osteoarthr Cartilage* **2009**, 17, 397; b) N. More, G. J. M. h. Kapusetti, *Med. Hypotheses* **2017**, 108, 10; c) J. Jacob, N. More, K. Kalia, G. Kapusetti, *Inflammation and Regeneration* **2018**, 38, 2.
- [174] R. V. Chernozem, M. A. Surmeneva, S. N. Shkarina, K. Loza, M. Epple, M. Ulbricht, A. Cecilia, B. Krause, T. Baumbach, A. A. Abalymov, B. V. Parakhonskiy, A. G. Skirtach, R. A. Surmenev, *ACS Appl. Mater. Interfaces* **2019**, 11, 19522.
- [175] P. Khalid, M. Hussain, P. Rekha, A. Arun, *Hum. Exp. Toxicol.* **2015**, 34, 548.
- [176] I. A. Kinloch, J. Suhr, J. Lou, R. J. Young, P. M. Ajayan, *Science* **2018**, 362, 547.
- [177] a) W. Liang, X. Wu, Y. Dong, R. Shao, X. Chen, P. Zhou, F. Xu, *Biomater. Sci.* **2021**, 9, 1924; b) A. E. Pazarçeviren, Z. Evis, D. Keskin, A. Tezcaner, *Biomed. Mater.* **2019**, 14, 035018.
- [178] J. Prakash, D. Prema, K. Venkataprasanna, K. Balagangadharan, N. Selvamurugan, G. D. Venkatasubbu, *Int. J. Biol. Macromol.* **2020**, 154, 62.
- [179] H. E. Karahan, C. Wiraja, C. Xu, J. Wei, Y. Wang, L. Wang, F. Liu, Y. Chen, *Adv. Healthc. Mater.* **2018**, 7, 1701406.
- [180] D. You, K. Li, W. Guo, G. Zhao, C. Fu, *Int. J. Nanomed.* **2019**, 14, 7039.
- [181] J. Li, X. Liu, J. M. Crook, G. G. Wallace, *Mat. Sci. Eng. C-Mater.* **2020**, 107, 110312.
- [182] a) P. R. Lopes Nalesso, W. Wang, Y. Hou, L. Bagne, A. T. Pereira, J. V. Helaehil, T. A. Moretti de Andrade, G. B. Chiarotto, P. Bártolo, G. F. Caetano, *Bioprinting* **2021**, 24, e00164; b) W. Wang, J. R. P. Junior, P. R. L. Nalesso, D. Musson, J. Cornish, F. Mendonça, G. F. Caetano, P. Bártolo, *Mat. Sci. Eng. C-Mater.* **2019**, 100, 759.
- [183] a) P. Newman, A. Minett, R. Ellis-Behnke, H. J. N. N. Zreiqat, biology, medicine, *Nanomedicine (Lond)* **2013**, 9, 1139; b) S. Gholizadeh, F. Moztarzadeh, N. Haghhighipour, L. Ghazizadeh, F. Baghbani, M. A. Shokrgozar, Z. Allahyari, *Int. J. Biol. Macromol.* **2017**, 97, 365.
- [184] X. Liu, M. N. George, S. Park, A. L. Miller li, B. Gaihre, L. Li, B. E. Waletzki, A. Terzic, M. J. Yaszemski, L. Lu, *Acta Biomater.* **2020**, 111, 129.
- [185] B. D. Ulery, L. S. Nair, C. T. J. J. o. p. s. P. B. p. p. Laurencin, *J. Polym. Sci. Pol. Phys.* **2011**, 49, 832.
- [186] H. Samadian, H. Mobasheri, S. Hasanpour, R. Faridi-Majid, presented at J. Nano Res. **2017**.
- [187] H. Samadian, H. Mobasheri, S. Hasanpour, J. Ai, M. Azamie, R. Faridi-Majidi, *J. Mol. Liq.* **2020**, 298,

112021.

- [188] C. Ning, Z. Zhou, G. Tan, Y. Zhu, C. J. P. i. p. s. Mao, *Prog. Polym. Sci.* **2018**, *81*, 144.
- [189] Z. Deng, T. Hu, Q. Lei, J. He, P. X. Ma, B. J. A. a. m. Guo, *interfaces, ACS Appl. Mater. Interfaces* **2019**, *11*, 6796.
- [190] a) B. Zhu, Y. Li, F. Huang, Z. Chen, J. Xie, C. Ding, J. Li, *Biomater. Sci.* **2019**, *7*, 4730; b) W. Jing, Y. Huang, P. Wei, Q. Cai, X. Yang, W. Zhong, *J. Biomed. Mater. Res. Part A* **2019**, *107*, 1443.
- [191] M. Wu, F. Zhang, Y. Zhangyang, H. Zhang, Y. Zhao, X. Xu, M. Qin, C. Ding, J. Li, *Colloid Interface Sci. Commun.* **2021**, *43*, 100450.
- [192] S. Liu, K. Li, Q. Shen, D. Shao, S. Huang, Y. Xie, X. Zheng, *Appl. Surf. Sci.* **2021**, *545*, 148827.
- [193] Y. Huang, Z. Du, P. Wei, F. Chen, B. Guan, Z. Zhao, X. Zhang, Q. Cai, J. Mao, H. Leng, X. Yang, *Chem. Eng. J.* **2020**, *397*, 125352.
- [194] a) A. Wibowo, C. Vyas, G. Cooper, F. Qulub, R. Suratman, A. I. Mahyuddin, T. Dirgantara, P. J. M. Bartolo, *Materials (Basel)* **2020**, *13*, 512; b) L. V. Kayser, D. J. Lipomi, *Adv. Mater.* **2019**, *31*, 1806133.
- [195] a) T. Zhou, L. Yan, C. Xie, P. Li, L. Jiang, J. Fang, C. Zhao, F. Ren, K. Wang, Y. Wang, *Small* **2019**, *15*, 1805440; b) Y. Li, L. Yang, Y. Hou, Z. Zhang, M. Chen, M. Wang, J. Liu, J. Wang, Z. Zhao, C. Xie, X. Lu, *Bioact. Mater.* **2022**, *18*, 213.
- [196] A. J. Petty, R. L. Keate, B. Jiang, G. A. Ameer, J. Rivnay, *Chem. Mater.* **2020**, *32*, 4095.
- [197] M. E. Mycielska, M. B. Djamgoz, *J. Cell Sci.* **2004**, *117*, 1631.
- [198] R. Bai, J. Liu, J. Zhang, J. Shi, Z. Jin, Y. Li, X. Ding, X. Zhu, C. Yuan, B. Xiu, *J. Nanobiotechnol.* **2021**, *19*, 1.
- [199] A. W. Orr, B. P. Helmke, B. R. Blackman, M. A. Schwartz, *Dev. Cell* **2006**, *10*, 11.
- [200] a) Y. He, L. Yu, J. Liu, Y. Li, Y. Wu, Z. Huang, D. Wu, H. Wang, Z. Wu, G. Qiu, *The FASEB Journal* **2019**, *33*, 6069; b) K. Iwasa, A. H. Reddi, *Tissue Eng. Part B Rev.* **2018**, *24*, 144.
- [201] Y. Xia, J. Sun, L. Zhao, F. Zhang, X.-J. Liang, Y. Guo, M. D. Weir, M. A. Reynolds, N. Gu, H. H. Xu, *Biomaterials* **2018**, *183*, 151.
- [202] a) Z. Liu, J. Liu, X. Cui, X. Wang, L. Zhang, P. Tang, *Front. Chem.* **2020**, *8*, 124; b) V. F. Cardoso, A. Francesko, C. Ribeiro, M. Bañobre - López, P. Martins, S. Lanceros - Mendez, *Adv. Healthc. Mater.* **2018**, *7*, 1700845.
- [203] M. Filippi, B. Dasen, J. Guerrero, F. Garello, G. Isu, G. Born, M. Ehrbar, I. Martin, A. Scherberich, *Biomaterials* **2019**, *223*, 119468.
- [204] a) V. Manescu, G. Paltanea, I. Antoniac, M. Vasilescu, *Materials* **2021**, *14*, 5948; b) Y. Gao, J. Lim, S.-H. Teoh, C. Xu, *Chem. Soc. Rev.* **2015**, *44*, 6306.
- [205] S. Tong, H. Zhu, G. Bao, *Mater. Today* **2019**, *31*, 86.
- [206] K. Wu, D. Su, J. Liu, R. Saha, J. P. Wang, *Nanotechnology* **2019**, *30*, 50.
- [207] a) K. Marycz, P. Sobierajska, M. Roecken, K. Kornicka-Garbowska, M. Kępska, R. Idczak, J. M. Nedelec, R. J. Wiglusz, *J. Nanobiotechnol.* **2020**, *18*, 33; b) K. Marycz, P. Sobierajska, R. J. Wiglusz, R. Idczak, J.-M. Nedelec, A. Fal, K. Kornicka-Garbowska, *Int. J. Nanomed.* **2020**, *15*, 10127.
- [208] C. Shuai, Y. Cheng, W. Yang, P. Feng, Y. Yang, C. He, F. Qi, S. Peng, *Composites, Part B* **2020**, *192*, 107986.
- [209] H. Chen, J. Sun, Z. Wang, Y. Zhou, Z. Lou, B. Chen, P. Wang, Z. Guo, H. Tang, J. Ma, Y. Xia, N. Gu, F. Zhang, *ACS Appl. Mater. Interfaces* **2018**, *10*, 44279.
- [210] Z. Huang, Y. He, X. Chang, J. Liu, L. Yu, Y. Wu, Y. Li, J. Tian, L. Kang, D. Wu, H. Wang, Z. Wu, G. Qiu, *Adv. Healthc. Mater.* **2020**, *9*, 2000318.
- [211] S. Hao, J. Meng, Y. Zhang, J. Liu, X. Nie, F. Wu, Y. Yang, C. Wang, N. Gu, H. Xu, *Biomaterials* **2017**, *140*,

16.

- [212] D. Huang, K. Xu, X. Huang, N. Lin, Y. Ye, S. Lin, J. Zhang, J. Shao, S. Chen, M. Shi, X. Zhou, P. Lin, Y. Xue, C. Yu, X. Yu, Z. Ye, K. Cheng, *Small* **2022**, *18*, 2203680.
- [213] H. Jalili, B. Aslibeiki, A. Hajalilou, O. Musalu, L. P. Ferreira, M. M. Cruz, *Ceram. Int.* **2022**, *48*, 4886.
- [214] a) P. Martins, M. Silva, S. Lanceros-Mendez, *Nanoscale* **2015**, *7*, 9457; b) R. Brito-Pereira, D. M. Correia, C. Ribeiro, A. Francesko, I. Etxebarria, L. Pérez-Álvarez, J. L. Vilas, P. Martins, S. Lanceros-Mendez, *Composites, Part B* **2018**, *141*, 70.
- [215] a) M. Guillot-Ferriols, M. I. García-Briega, L. Tolosa, C. M. Costa, S. Lanceros-Méndez, J. L. Gómez Ribelles, G. Gallego Ferrer, *Gels* **2022**, *8*, 680; b) M. M. Fernandes, D. M. Correia, C. Ribeiro, N. Castro, V. Correia, S. Lanceros-Mendez, *ACS Appl. Mater. Interfaces* **2019**, *11*, 45265; c) W. Liu, F. Zhang, Y. Yan, C. Zhang, H. Zhao, B. C. Heng, Y. Huang, Y. Shen, J. Zhang, L. Chen, X. Wen, X. Deng, *Adv. Funct. Mater.* **2021**, *31*, 2006226.
- [216] B. Tang, X. Shen, Y. Yang, Z. Xu, J. Yi, Y. Yao, M. Cao, Y. Zhang, H. Xia, *Colloids Surf., B* **2021**, *198*, 111473.
- [217] N. Wang, Y. Xie, Z. Xi, Z. Mi, R. Deng, X. Liu, R. Kang, X. Liu, **2022**, *10*, 937803.
- [218] a) Q. Wang, B. Chen, M. Cao, J. Sun, H. Wu, P. Zhao, J. Xing, Y. Yang, X. Zhang, M. Ji, N. Gu, *Biomaterials* **2016**, *86*, 11; b) J. Zhuang, S. Lin, L. Dong, K. Cheng, W. Weng, *Acta Biomater.* **2018**, *71*, 49.
- [219] Y. Xia, Y. Guo, Z. Yang, H. Chen, K. Ren, M. D. Weir, L. C. Chow, M. A. Reynolds, F. Zhang, N. Gu, H. H. K. Xu, *Mat. Sci. Eng. C-Mater.* **2019**, *104*, 109955.
- [220] a) A. Qu, M. Sun, J.-Y. Kim, L. Xu, C. Hao, W. Ma, X. Wu, X. Liu, H. Kuang, N. A. Kotov, C. Xu, *Nat. Biomed. Eng.* **2021**, *5*, 103; b) W. Zhao, Y. Zhao, Q. Wang, T. Liu, J. Sun, R. Zhang, *Small* **2019**, *15*, e1903060; c) A. Higuchi, P.-Y. Shen, J.-K. Zhao, C.-W. Chen, Q.-D. Ling, H. Chen, H.-C. Wang, J.-T. Bing, S.-T. Hsu, *Tissue Eng. Part A* **2011**, *17*, 2593.
- [221] S. De Martino, S. Cavalli, P. A. Netti, *Adv. Healthc. Mater.* **2020**, *9*, 2000470.
- [222] W.-T. Li, Y.-C. Leu, J.-L. Wu, *Photomed. Laser Surg.* **2010**, *28*, S.
- [223] Y. Kong, J. Duan, F. Liu, L. Han, G. Li, C. Sun, Y. Sang, S. Wang, F. Yi, H. Liu, *Chem. Soc. Rev.* **2021**, *50*, 12828.
- [224] J. Lee, B. Yoo, H. Lee, G. D. Cha, H. S. Lee, Y. Cho, S. Y. Kim, H. Seo, W. Lee, D. Son, *Adv. Mater.* **2017**, *29*, 1603169.
- [225] Z. Yan, H. Qin, J. Ren, X. Qu, *Angew. Chem. Int. Ed.* **2018**, *57*, 11182.
- [226] H. Kang, K. Zhang, Q. Pan, S. Lin, D. S. H. Wong, J. Li, W. Y.-W. Lee, B. Yang, F. Han, G. Li, B. Li, L. Bian, *Adv. Funct. Mater.* **2018**, *28*, 1802642.
- [227] S. A. Leon, S. O. Asbell, H. H. Arastu, G. Edelstein, A. J. Packel, S. Sheehan, I. Daskai, G. G. Guttmann, I. Santos, *Int. J. Hyperther.* **1993**, *9*, 77.
- [228] a) S. Sayed, O. Faruq, M. Hossain, S.-B. Im, Y.-S. Kim, B.-T. Lee, *Mat. Sci. Eng. C-Mater.* **2019**, *105*, 110027; b) C. Shui, A. Scutt, *J. Bone Miner. Res.* **2001**, *16*, 731.
- [229] Z. Wan, P. Zhang, L. Lv, Y. Zhou, *Theranostics* **2020**, *10*, 11837.
- [230] S. Chen, R. Guo, Q. Liang, X. Xiao, *J. Biomat. Sci-Polym. E.* **2021**, *32*, 1598.
- [231] L. Tong, Q. Liao, Y. Zhao, H. Huang, A. Gao, W. Zhang, X. Gao, W. Wei, M. Guan, P. K. Chu, H. Wang, *Biomaterials* **2019**, *193*, 1.
- [232] a) Y. Wu, X. Zhang, B. Tan, Y. Shan, X. Zhao, J. Liao, *Biomater. Adv.* **2022**, *133*, 112641; b) Y. Li, L. Huang, G. Tai, F. Yan, L. Cai, C. Xin, S. Al Islam, *Composites, Part A* **2022**, *152*, 106672.
- [233] a) S. Dong, Y. Chen, L. Yu, K. Lin, X. Wang, *Adv. Funct. Mater.* **2020**, *30*, 1907071; b) K. Ma, C. Liao, L. Huang, R. Liang, J. Zhao, L. Zheng, W. Su, *Small* **2021**, *17*, 2104747; c) L. Ma, X. Feng, H. Liang, K.

- Wang, Y. Song, L. Tan, B. Wang, R. Luo, Z. Liao, G. Li, X. Liu, S. Wu, C. Yang, *Mater. Today* **2020**, *36*, 48.
- [234] a) C. He, L. D. Yu, H. L. Yao, Y. Chen, Y. Q. Hao, *Adv. Funct. Mater.* **2021**, *31*, 14; b) H. Xiang, Q. Yang, Y. Gao, D. Zhu, S. Pan, T. Xu, Y. Chen, *Adv. Funct. Mater.* **2020**, *30*, 1909938.
- [235] a) D. Zhu, M. Lyu, Q. Huang, M. Suo, Y. Liu, W. Jiang, Y. Duo, K. Fan, *ACS Appl. Mater. Interfaces* **2020**, *12*, 36928; b) X. Xu, X. Chen, H. Wang, X. Mei, B. Chen, R. Li, Y. Qin, *Mater. Today Adv.* **2022**, *13*, 100209.
- [236] C. Zhao, Z. Zeng, N. T. Qazvini, X. Yu, R. Zhang, S. Yan, Y. Shu, Y. Zhu, C. Duan, E. Bishop, J. Lei, W. Zhang, C. Yang, K. Wu, Y. Wu, L. An, S. Huang, X. Ji, C. Gong, C. Yuan, L. Zhang, W. Liu, B. Huang, Y. Feng, B. Zhang, Z. Dai, Y. Shen, X. Wang, W. Luo, L. Oliveira, A. Athiviraham, M. J. Lee, J. M. Wolf, G. A. Ameer, R. R. Reid, T.-C. He, W. Huang, *ACS Biomater. Sci. Eng.* **2018**, *4*, 2943.
- [237] W. Nie, X. Dai, J. S. Copus, C. Kengla, R. Xie, M. Seeds, A. Atala, C. He, *Acta Biomater.* **2022**, *153*, 573.
- [238] a) S. Dong, Y.-n. Zhang, J. Wan, R. Cui, X. Yu, G. Zhao, K. Lin, *J. Mater. Chem. B* **2020**, *8*, 368; b) B. Geng, H. Qin, W. Shen, P. Li, F. Fang, X. Li, D. Pan, L. Shen, *Chem. Eng. J.* **2020**, *383*, 123102.
- [239] X. Zhang, G. Cheng, X. Xing, J. Liu, Y. Cheng, T. Ye, Q. Wang, X. Xiao, Z. Li, H. Deng, *J. Phys. Chem. Lett.* **2019**, *10*, 4185.
- [240] J. Zhang, B. Zhang, Z. Zheng, Q. Cai, J. Wang, Q. Shu, L. Wang, *Adv. Funct. Mater.* **2022**, *32*, 2109882.
- [241] R. A. Doganov, E. C. O'farrell, S. P. Koenig, Y. Yeo, A. Ziletti, A. Carvalho, D. K. Campbell, D. F. Coker, K. Watanabe, T. Taniguchi, *Nat. Commun.* **2015**, *6*, 1.
- [242] S. Shen, R. Liu, C. Song, T. Shen, Y. Zhou, J. Guo, B. Kong, Q. Jiang, *Nano Res.* **2023**, *16*, 7383.
- [243] X. Wang, J. Shao, M. Abd El Raouf, H. Xie, H. Huang, H. Wang, P. K. Chu, X.-F. Yu, Y. Yang, A. M. AbdEl-Aal, N. H. M. Mekawy, R. J. Miron, Y. Zhang, *Biomaterials* **2018**, *179*, 164.
- [244] B. Li, F. Liu, J. Ye, X. Cai, R. Qian, K. Zhang, Y. Zheng, S. Wu, Y. Han, *Small* **2022**, *18*, 2202691.
- [245] a) W. Shao, F. Zhao, J. Xue, L. Huang, *BMEMat* **2023**, *1*, e12009; b) C. Xu, K. Pu, *Chem. Soc. Rev.* **2021**, *50*, 1111.
- [246] S. Shen, R. Liu, C. Song, T. Shen, Y. Zhou, J. Guo, B. Kong, Q. Jiang, *Nano Res.* **2023**, *16*, 7383.
- [247] H. Shan, X. Zhou, B. Tian, C. Zhou, X. Gao, C. Bai, B. Shan, Y. Zhang, S. Sun, D. Sun, Q. Fan, X. Zhou, C. Wang, J. Bai, *Biomaterials* **2022**, *284*, 121482.
- [248] Y. Xue, L. Zhang, F. Liu, Y. Zhao, J. Zhou, Y. Hou, H. Bao, L. Kong, F. Ma, Y. Han, *Adv. Healthc. Mater.* **2022**, *11*, e2200998.
- [249] a) Y. Wang, H.-M. Meng, Z. Li, *Nanoscale* **2021**, *13*, 8751; b) S. Roy, J. Roy, B. Guo, *J. Mater. Chem. B* **2023**, *11*, 2287.
- [250] a) E. Cazares-Cortes, S. Cabana, C. Boitard, E. Nehlig, N. Griffete, J. Fresnais, C. Wilhelm, A. Abou-Hassan, C. Ménager, *Adv. Drug Deliv. Rev.* **2019**, *138*, 233; b) X. Liu, Y. Zhang, Y. Wang, W. Zhu, G. Li, X. Ma, Y. Zhang, S. Chen, S. Tiwari, K. Shi, S. Zhang, H. M. Fan, Y. X. Zhao, X.-J. Liang, *Theranostics* **2020**, *10*, 3793.
- [251] L. Wang, P. Hu, H. Jiang, J. Zhao, J. Tang, D. Jiang, J. Wang, J. Shi, W. Jia, *Nano Today* **2022**, *43*, 101401.
- [252] Z. Cao, D. Wang, Y. Li, W. Xie, X. Wang, L. Tao, Y. Wei, X. Wang, L. Zhao, *Sci. China Life Sci.* **2018**, *61*, 448.
- [253] Z. Ding, G. Lu, W. Cheng, G. Xu, B. Zuo, Q. Lu, D. L. Kaplan, *ACS Biomater. Sci. Eng.* **2020**, *6*, 2357.
- [254] L. Hao, L. Li, P. Wang, Z. Wang, X. Shi, M. Guo, P. Zhang, *Nanoscale* **2019**, *11*, 23423.
- [255] P. Li, S. Zhang, K. Li, J. Wang, M. Liu, X. Gu, Y. Fan, *J. Mater. Chem. B* **2018**, *6*, 4952.
- [256] S. Hao, M. Wang, Z. Yin, Y. Jing, L. Bai, J. Su, *Mater. Today Bio* **2023**, *22*, 100741.
- [257] S. Tan, J. Y. Fang, Z. Yang, M. E. Nimni, B. Han, *Biomaterials* **2014**, *35*, 5294.
- [258] P. Jiang, Z. Mao, C. Gao, *Acta Biomater.* **2015**, *19*, 76.

- [259] L. Cui, J. Zhang, J. Zou, X. Yang, H. Guo, H. Tian, P. Zhang, Y. Wang, N. Zhang, X. Zhuang, Z. Li, J. Ding, X. Chen, *Biomaterials* **2020**, *230*, 119617.
- [260] a) O. F. Zouani, J. Kalisky, E. Ibarboure, M.-C. Durrieu, *Biomaterials* **2013**, *34*, 2157; b) L. Zhou, Y. Huang, J. Zhao, H. Yang, F. Kuai, *Life Sci.* **2020**, *262*, 118563.
- [261] a) A. Khademhosseini, R. Langer, *Nat. Protoc.* **2016**, *11*, 1775; b) M. P. Lutolf, P. M. Gilbert, H. M. Blau, *Nature* **2009**, *462*, 433.
- [262] N. B. McNamara, D. A. D. Munro, N. Bestard-Cuche, A. Uyeda, J. F. J. Bogie, A. Hoffmann, R. K. Holloway, I. Molina-Gonzalez, K. E. Askew, S. Mitchell, W. Mungall, M. Dodds, C. Dittmayer, J. Moss, J. Rose, S. Szymkowiak, L. Amann, B. W. McColl, M. Prinz, T. L. Spires-Jones, W. Stenzel, K. Horsburgh, J. J. A. Hendriks, C. Pridans, R. Muramatsu, A. Williams, J. Priller, V. E. Miron, *Nature* **2023**, *613*, 120.
- [263] R. Rubin, *Jama* **2021**, *325*, 329.
- [264] Q. Zhou, S. Y. Lyu, A. A. Bertrand, A. C. Hu, C. H. Chan, X. Y. Ren, M. J. Dewey, A. S. Tiffany, B. A. C. Harley, J. C. Lee, *Macromol. Biosci.* **2021**, *21*, e2000370.
- [265] a) L. Xiao, Y. Ma, R. Crawford, J. Mendhi, Y. Zhang, H. Lu, Q. Zhao, J. Cao, C. Wu, X. Wang, Y. Xiao, *Mater. Today* **2022**, *54*, 202; b) M. D. Park, A. Silvin, F. Ginhoux, M. Merad, *Cell* **2022**, *185*, 4259.
- [266] M. Rodrigues, N. Kosaric, C. A. Bonham, G. C. Gurtner, *Physiol. Rev.* **2019**, *99*, 665.
- [267] Y. Xiong, B.-B. Mi, Z. Lin, Y.-Q. Hu, L. Yu, K.-K. Zha, A. C. Panayi, T. Yu, L. Chen, Z.-P. Liu, A. Patel, Q. Feng, S.-H. Zhou, G.-H. Liu, *Mil. Med. Res.* **2022**, *9*, 65.
- [268] T. A. Einhorn, L. C. Gerstenfeld, *Nat. Rev. Rheumatol.* **2015**, *11*, 45.
- [269] A. G. Robling, L. F. Bonewald, *Annu. Rev. Physiol.* **2020**, *82*, 485.
- [270] Z. Qiao, M. Lian, X. Liu, X. Zhang, Y. Han, B. Ni, R. Xu, B. Yu, Q. Xu, K. Dai, *ACS Appl. Mater. Interfaces* **2022**, *14*, 31655.
- [271] C. Shuai, W. Yang, C. He, S. Peng, C. Gao, Y. Yang, F. Qi, P. Feng, *Mater. Des.* **2020**, *185*, 108275.